

PURIFICATION AND CHARACTERIZATION OF PROTEOLYTIC
ASPARTATE TRANSCARBAMOYLASE (ATCase) FROM
Burkholderia cepacia 25416 AND CONSTRUCTION
OF A *pyrB1* KNOCK- OUT MUTANT

Seongcheol Kim, B.S., M.S.

Dissertation Prepared for the Degree of
DOCTOR OF PHILOSOPHY

UNIVERSITY OF NORTH TEXAS

December 2004

APPROVED:

Gerard A. O' Donovan, Major Professor
Robert C. Benjamin, Committee Member
Mark A. Farinha, Committee Member
Debrah A. Beck, Committee Member
John Knesek, Committee Member
Arthur. J. Goven, Chair of Department of
Biological Sciences
Sandra L. Terrell, Dean of the Robert B. Toulouse
School of Graduate Studies

Kim, Seongcheol, Purification and Characterization of Proteolytic Aspartate

Transcarbamoylase (ATCase) from *Burkholderia cepacia* 25416 and Construction of a *pyrB1* Knock-out Mutant. Doctor of Philosophy (Molecular Biology), December 2004, 132 pages, 3 tables, 49 illustrations, references, 42 titles.

Burkholderia cepacia is a common soil bacterium of significance in agriculture and bioremediation. *B. cepacia* is also an opportunistic pathogen of humans causing highly communicable pulmonary infections in cystic fibrosis and immunocompromized patients. The *pyrB* gene encoding ATCase was cloned and ATCase was purified by the glutathione S-transferase gene fusion system. The ATCase in *B. cepacia* has been previously classified as a class A enzyme by Bethell and Jones. ATCase activity gels showed that *B. cepacia* contained a holoenzyme *pyrBC* complex of 550 kDa comprised of 47 kDa *pyrB* and 45 kDa *pyrC* subunits. In the course of purifying the enzyme, trimeric subunits of 140 kDa and 120 kDa were observed as well as a unique proteolysis of the enzyme. The 47 kDa ATCase subunits were cleaved to 40 kDa proteins, which still demonstrated high activity as trimers. The proteolysis site is between Ser74 and Val75 residues. To confirm this, we converted the Ser74 residue to an Ala and to an Arg by site-directed mutagenesis. After this primary sequence changed, the proteolysis of ATCase was not observed.

To further investigate the characteristics of *B. cepacia pyrB* gene, a *pyrB* knock-out (*pyrB⁻*) was constructed by *in vitro* mutagenesis. In the assay, the 550 kDa holoenzyme and 140 kDa and 120 kDa trimers disappeared and were replaced with a previously unseen 480 kDa holoenzyme *pyrB⁻* strain. The results suggest that *B. cepacia* has two genes that encode ATCase. ATC1 is constitutive and ATC2 is expressed only in the absence of ATC1 activity.

To check for the virulence of these two strains, a eukaryotic model virulence test was performed using *Caenorhabditis elegans* (*C. elegans*). The *pyrB1⁺pyrB2⁺* (wild type) *B. cepacia* killed the nematode but *pyrB1⁻pyrB2⁺* *B. cepacia* had lost its virulence against *C. elegans*. This suggests that ATC1 (*pyrB1*) is involved in virulence in *B. cepacia* and ATC2 (*pyrB2*) is not.

ACKNOWLEDGMENTS

Without the guidance of a good teacher such as Dr. O' Donovan, I would not have been able to accomplish this doctorate degree. I would sincerely like to thank him for passing the precious knowledge that he has passed onto me. I also appreciate the help and guidance from Dr. Farinha. I would like to thank all our lab members who have been very supportive throughout the years and wish them every success in their future endeavors.

The support of my family has been invaluable. I thank my mother for believing in me. I thank my father being here and protecting me in spirit from heaven while I have been in the United States. Hyunju Kim, my lovely wife, has been a constant supporter while I have been doing this program. There were times of disappointment, anger, and frustration, and there were also times of joy, excitement, and happiness. Through them all, Hyunju has always been with me to share the sorrow and happiness, and I am deeply grateful to her for that. I also want to share this happiness with my lovely children, Stephanie and Anthony. I thank you for all your support and thank you for being my inspiration.

TABLE OF CONTENTS

	Page
ACKNOWLEDGMENTS	ii
LIST OF TABLES.....	iv
LIST OF ILLUSTRATIONS.....	v
INTRODUCTION	1
MATERIALS AND METHODS	34
RESULTS AND DISCUSSION.....	78
CONCLUSIONS	116
REFERENCE LIST	117

LIST OF TABLES

	Page
1. List of strains and plasmids.....	35
2. PCR primers used in this study.....	44
3. Thrombin recognition sites	91

LIST OF ILLUSTRATIONS

		Page
1.	Biofilm formation of <i>B. cepacia</i> H111 and <i>B. cepacia</i> H111-R.....	5
2.	Quorum- sensing system of <i>B. epacia</i> H111	6
3.	Structure of salicylic acid and pyochine	8
4.	The pyrimidine biosynthetic and salvage pathway in <i>E. coli</i>	11
5.	Regulation by transcriptional attenuation of <i>E. coli</i> <i>pyrBI</i> operon	17
6.	Pyrimidine salvage pathway in <i>E. coli</i>	21
7.	Pyrimidine salvage pathway in <i>P. aeruginosa</i>	22
8.	Metabolic blocks constructed in <i>P. aeruginosa</i>	26
9.	Classes of bacterial ATCase	28
10.	Schematic diagram of plasmid pUC18	45
11.	Schematic diagram of plasmid pSKBB18	46
12.	Schematic diagram of plasmid pGEX.....	49
13.	Schematic diagram of MSC site in plasmid pGEX2T	50
14.	Schematic diagram of plasmid pSK2T	51
15.	Diagram of elution by thrombin in GST fusion system.....	56
16.	Diagram of elution by reduced glutathione in GST fusion system.....	57
17.	Scheme of mutagenesis of ATCase from <i>B. cepacia</i>	65
18.	The procedure of site-specific mutagenesis on <i>pyrB</i> gene by overlap extension	66
19.	Schematic diagram of plasmid pSKBB18A	68
20.	Schematic diagram of plasmid pSKBB18N	69
21.	Schematic diagram of plasmid pSK2TA	70
22.	Schematic diagram of plasmid pSK2TN	71

23.	Restriction map and primers of EZ::TN<KAN-1> transposon	73
24.	Schematic diagram of plasmid pSKBB18X	74
25.	Restriction of pUC18 and pUCSKBB18 by <i>EcoRI</i> and <i>BamHI</i>	79
26.	ATCase specific activity of TB2 and TB2 containing pSKBB18 plasmid.....	80
27.	Amino acid sequence alignment of <i>Burkholderia</i> spp.....	81
28.	SDS-PAGE of directly eluted ATCases by thrombin.....	84
29.	SDS-PAGE of eluted ATCases by reduced glutathione	87
30.	Expression of ATCase eluted by two-step method.....	88
31.	Proteolysis site in ATCase	89
32.	Michaelis-Menten plot for purified proteolytic ATCase	93
33.	Michaelis-Menten plot for purified uncleaved ATCase from <i>B. cepacia</i>	94
34.	First PCR from site-directed mutagenesis by overlap extension	97
35.	Second PCR for complete mutagenesis from site-directed mutagenesis by overlap extension	98
36.	Expression of purified ATCases (Ser74 to Arg74) in 10 % SDS-PAGE	99
37.	Expression of purified ATCases (Ser74 to Ala74) in 10 % SDS- PAGE.....	100
38.	Expression of purified ATCases in 8 % N-SDS-PAGE activity gel	101
39.	Proposed new class of ATCase, Class D	102
40.	ATCase specific activity of purified ATCases	103
41.	Verification of the transposon insertion in <i>pyrB</i> <i>B. cepacia</i>	106
42.	Expression of second ATCase in activity gel	107
43.	The pigment comparison of wild type and <i>pyrB</i> <i>B. cepacia</i> in PIA	108
44.	Expression of second ATCase from wild type <i>B. cepacia</i> on ATCase activity gel	109
45.	Growth curve of <i>B. cepacia</i> and <i>pyrBI</i> <i>B. cepacia</i>	112
46.	Growth curve of <i>B. cepacia</i> and <i>pyrBI</i> <i>B. cepacia</i> with uracil.....	113

47.	The picture of nematodes paralyzed by <i>B. cepacia</i>	114
48.	The picture of nematodes with <i>pyrBI</i> <i>B. cepacia</i>	114
49.	Standard paralysis assay of wild type <i>B. cepacia</i> and <i>pyrB</i> <i>B. cepacia</i>	115

INTRODUCTION

Burkholderia cepacia

Burkholderia cepacia is a common bacterium, which has a wide geographic distribution. It was been isolated from soil, pasteurized milk, contact saline solutions used to wash contact lens, rotting tree trunks, rivers, and tap water. Nosocomial infections such as septicemia, meningitis, endocarditis, pneumonia, and urinary tract infections are caused in part by *B. cepacia*. The species can be found growing in distilled water, disinfectants, aerosol polymyxin, anesthetics, detergent solutions, respirators, humidifiers, urinary catheter kits, baby lotion, and flower vases.

Clinical strains of this organism are known to have three or four replicons whereas non-clinical strains have but a single replicon. *B. cepacia* is a promising plant-growth-promoting inoculant for maize (Di Cello F et al., 1997). Also, *B. cepacia* can be a member of an indigenous bacterial consortium for the bioremediation of crude oil pollutant system (Kedzie, 1987). This is due to the strain's exceptional ability for degradation of chloroaromatic compounds and hydrocarbon complexes in soil. However, *B. cepacia* is also a multi-drug resistant and significant opportunistic human pathogen infecting cystic fibrosis (CF) patients (Govan et al., 1996). The organism is capable of pulmonary colonization in CF patient and causes a dramatic reduction in patient survival (Govan and Vanamme, 1998). Because of these two contrary aspects, it is very important to investigate the characteristics of *B. cepacia*.

B. cepacia is one of the most nutritionally versatile pseudomonads. In 1950, Burkholder reported that *Pseudomonas cepacia* was the causative agent of onion rot. This organism is capable of utilizing over 150 organic compounds for carbon and

energy (Ballard et al., 1970). This nutritional versatility is likely to be due to the organism's fluid genome (Rodley et al., 1995). *B. cepacia* produces various yellow, brown, red, and purple pigments. Unlike most pseudomonads which are oxidase positive, *B. cepacia* is oxidase variable. Several cell wall chemical differences can be seen in *B. cepacia* as compared to the other pseudomonads. For instance, the major components of the cell wall of *B. cepacia* are myristic, 3-hydroxymyristic, and 3-hydroxypalmitic acid which are not seen with other pseudomonads. Likewise, hopane, a triterpene derivative similar to sterols in size and function, is found only in the cell wall of *B. cepacia*. The organism grows slowly on agar medium and is often non-viable after 3-4 days on solid media. Other differential characteristics or distinct biochemical tests include: one to seven polar flagella, positive for lysine and ornithine decarboxylase, gelatin hydrolysis, accumulation of poly- β -hydroxybutyrate, polymyxin resistant, *ortho* cleavage of protocatechuate, and G + C content of 67.4%. Based on DNA and rRNA homology studies, *B. cepacia* was placed in RNA homology group II. The entire RNA homology group II has now been placed in a new genus, *Burkholderia*. Thus *P. cepacia* has now become *Burkholderia cepacia* (Yabuuchi et al., 1992).

This organism is highly resistance to many antibiotics. Once the organism establishes itself in the human body, it can withstand most antimicrobial treatments and continue to thrive.

Another unprecedented feature of *B. cepacia* is its genome mobility (Rodley et al., 1995). The genomes of *B. cepacia* strain ATCC 25416 contains a large number of insertion sequences (IS) which afford the organism the ability to mobilize and recruit foreign genes (Lessie et al., 1990). Moreover, these IS are involved in the

rearrangement of the genome and replicon fusion (Cheng and Lessie, 1994). The acquisition of new genetic material not only enhances nutritional diversity, but also contributes to the organism's ability to become resistant to antimicrobials. *B. cepacia* has an 8.1 megabase (Mb) genome, twice the size of the genome of the average bacterium (Cole and Saint-Girous, 1994). Atypically, *B. cepacia* strains have three large circular chromosomes and one large cryptic plasmid.

Because of its unusual genetic characteristics, the organism has the capacity to use many different substrates as carbon and energy, sources. For this reason, *B. cepacia* has become an excellent candidate for bioremediation.

However, the organism has emerged as an important pulmonary pathogen in persons with CF (Gilardi et al., 1985). Isolation of *B. cepacia* from patients having CF is associated with the rapid deterioration in pulmonary status and death (Gilligan et al., 1984). What makes this organism so serious for CF patients is its resistance to both conventional and experimental antimicrobial therapy (Gilligan et al., 1985). In *B. cepacia*, proteolytic and lipolytic activities are observed, but unlike *P. aeruginosa*, neither elastase nor toxin A is produced. Moreover, *B. cepacia* makes colonization with *P. aeruginosa* in CF lung as a biofilm. Biofilm formation in CF airway disease begins when *P. aeruginosa* cells are seeded onto the thick mucus surface by inhalation. The bacteria then penetrate the mucus and become embedded. It has been shown that CF airway mucus has a tendency to become aerobic, especially during chronic infection. As the infection progresses, the *P. aeruginosa*, growing within CF mucus, senses an oxygen gradient and this signals the cells to convert to a mucoid phenotype (Hassett et al., 2002). This phenotype is characterized by the production of the hyper-viscous substance alginate, which has been referred to as the most

significant virulence determinant in the context of CF airway disease (Hassett et al., 2002). Alginate is a linear polymer of acetylated β -D-mannuronate and its C-5 epimer, α -L-guluronate and its production contributes to the impairment of airway mucus clearance. *P. aeruginosa* produces volumes of slimy polysaccharides and lipopeptides that form the structural components of a biofilm and help to shield the bacteria from antibiotics. Thus, the clinical course of infection in CF patients is significantly worsened by the *P. aeruginosa* biofilm, and the concomitant production of alginate in airway mucus. Fig 1 showed the biofilm formation by *B. cepacia* H111 (Huber et al., 2001). When *B. cepacia* makes biofilm with *P. aeruginosa*, the patient survival is reduced severely.

Today, an extensive research exists on the numerous virulence factors produced by *P. aeruginosa*. One of the first virulence factors studied was probably also the most physically evident namely, pyocyanin. Pyocyanin is a redox-active compound capable of reducing oxygen to form super-oxide radicals and hydrogen peroxide. As a defense mechanism and competitive tool, the structure of pyocyanin allows it to readily cross the membranes of rival microorganisms, resulting in toxic oxygen intermediates that kill the competitor. In the lungs, pyocyanin has been shown to inhibit ciliary beat frequency in airway epithelial cells. This inhibition correlates with decreased cellular levels of ATP and cAMP (Denning et al., 1998). Pyocyanin has also been shown to induce rapid and overwhelming apoptosis in neutrophil populations *in vitro* (Usher et al., 2002). Many researches also investigated the correlation of virulence factors with siderophores. Siderophores are low molecular mass, high affinity, iron chelators capable of delivering iron to bacterial cells via specific receptor proteins on the cell surface (Neilands, 1982).

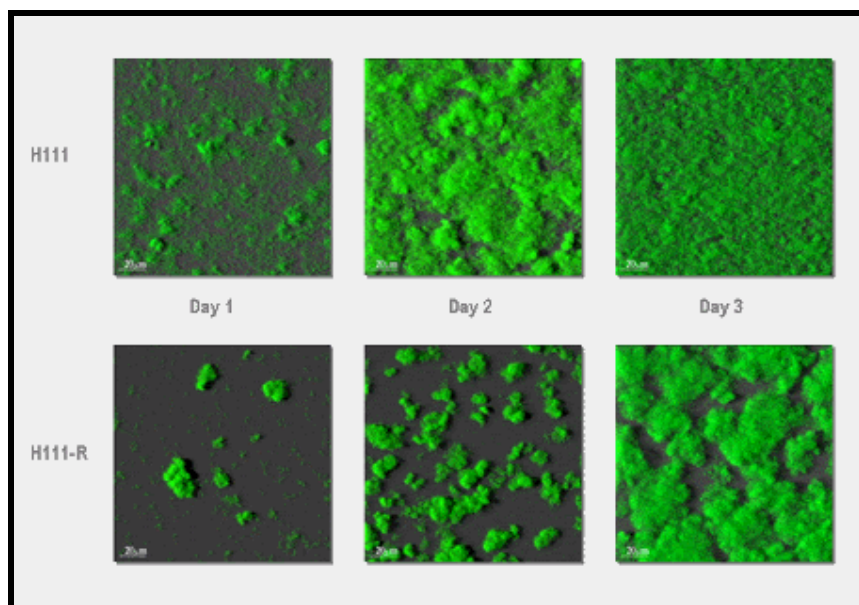


Fig 1. Biofilm formation of *B. cepacia*H111 and *B. cepacia*H111-R (used with permission)

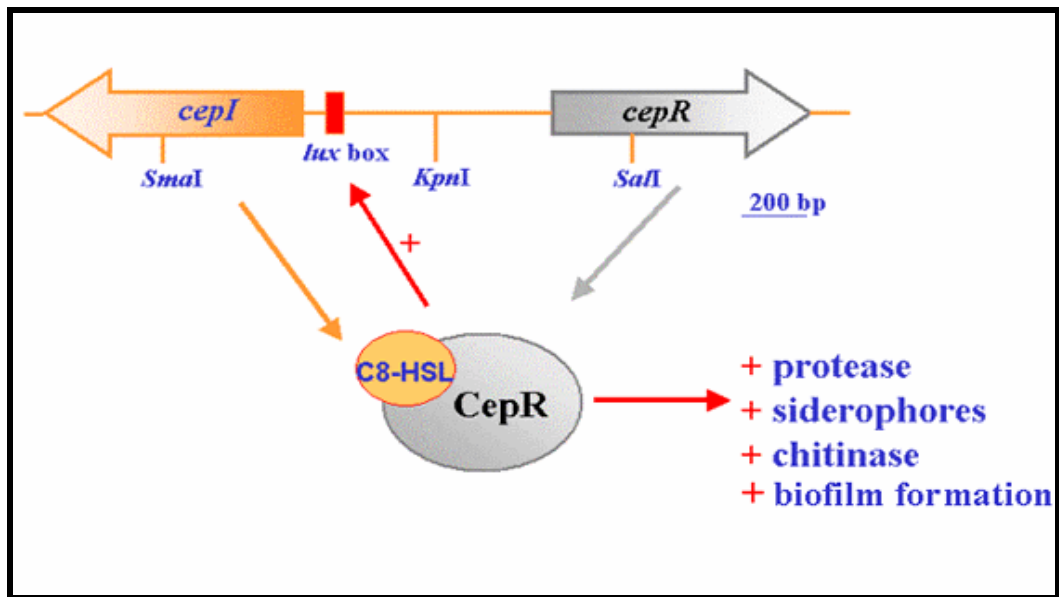


Fig 2. Quorum sensing system of *B. cepacia* H111 (used with permission from Huber)

Siderophores are produced by quorum sensing (Fig 2). Quorum sensing is the process in which bacteria monitor their own population density by sensing the level of signal molecules that are released by the microorganism. When these signal molecules reach a threshold concentration, the population density has attained a critical level or quorum, and quorum-dependent genes are expressed. *P. aeruginosa* produces two known siderophores, pyochelin and pyoverdine. The biological significance of siderophores has been demonstrated for a number of species; for example, siderophore deficient mutants of pathogenic bacteria are invariably less virulent in disease models (Ratledge & Dover, 2000; Meyer et al., 1996.). Thus, while pyoverdine itself is not a virulence factor, it is a secreted product that enables *P. aeruginosa* to survive as a pathogen. Quorum sensing regulates Biofilm production, which is mediated by hormone-like N-acyl homoserine lactones. These molecules control the production not only of biofilm matrix material but also of virulence factors such as proteases, flagellae, and fimbriae. Recent research has found that *B. cepacia* shares the same quorum-sensing molecules as *P. aeruginosa*; thus, these organisms potentially enhance each other's virulence (Huber et al., 2001). *B. cepacia* has been reported to produce four different types of siderophores; pyochelin, salicylic acid (SA), cepabactin, and ornibactins (Fig 3). It is important to study if the same relationships hold for *B. cepacia*. Because of these two contrary aspects of the organism, characterization of *B. cepacia* in virulence is very important in pathogenic research.

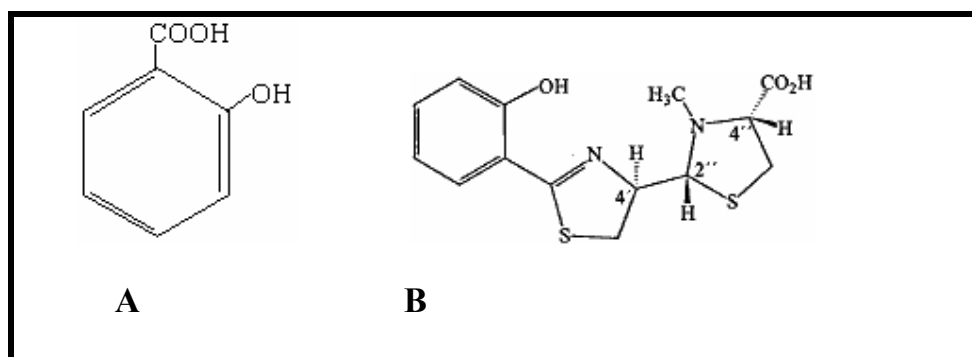


Fig 3. Structure of Salicylic acid and Pyochine

A. Salicylic acid B. Pyochine

Pyrimidine Biosynthetic Pathway in *E. coli* and *S. typhimurium*

The nucleoside triphosphates (NTPs) are the immediate precursors of both the nucleic acids and the coenzymes. The nucleotide-containing coenzymes, as well as a small fraction of the nucleic acids, i.e., the mRNAs, undergo a high rate of turnover, yielding NMPs and NDPs as products (Beck, 1995). For stable RNA and DNA synthesis, a constant supply of ribonucleoside triphosphates (rNTPs) and deoxyribonucleoside triphosphates (dNTPs) is required, which in the absence of preformed utilizable precursors must be provided through de novo biosynthesis.

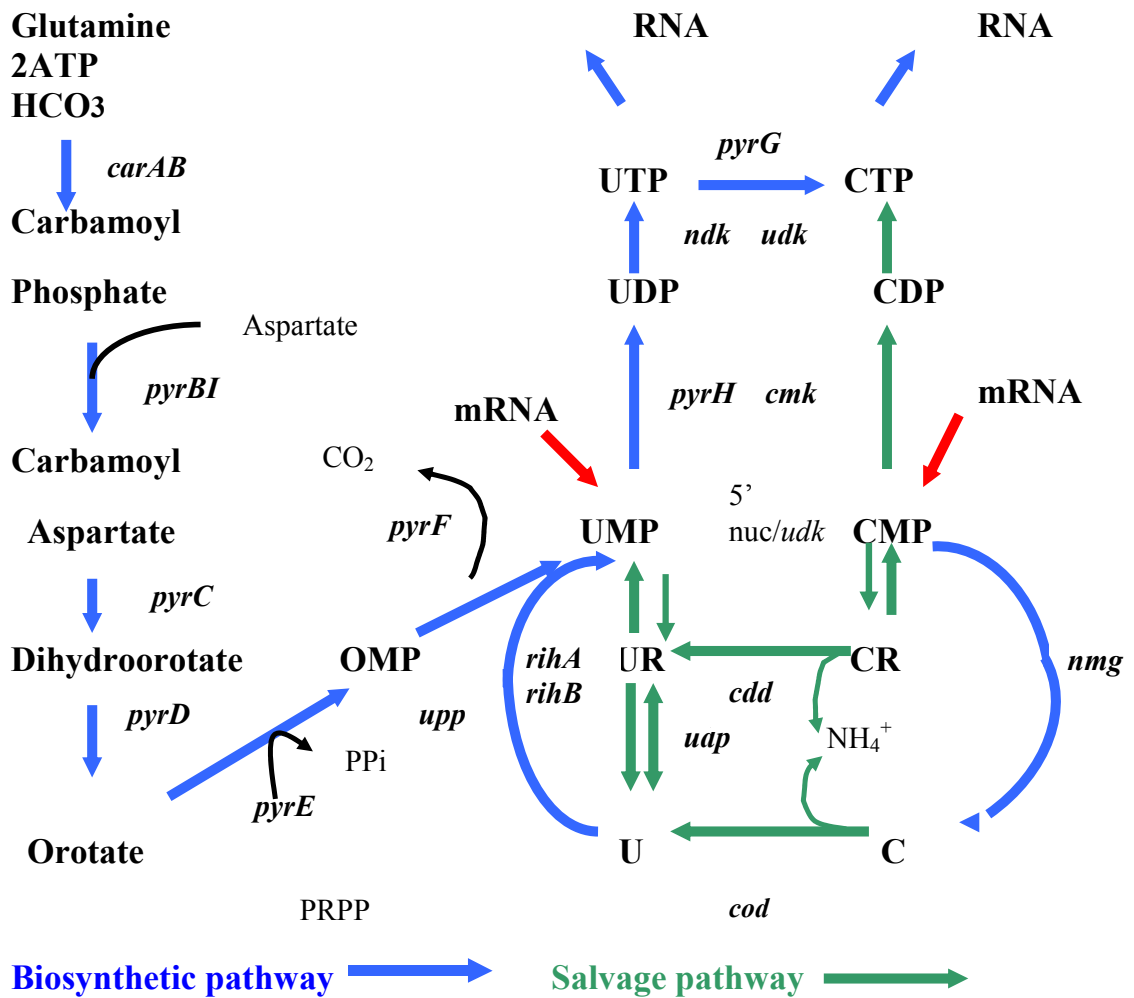
The pathway for de novo synthesis of the pyrimidine NTPs may be regarded as an unbranched sequence of enzyme reactions in which dTTP is the ultimate end product and UTP, CTP, and dCTP are obligatory intermediates (Fig 4). The product of first reaction, carbamoylphosphate, is also an intermediate, of arginine biosynthesis and constitutes the only branch point of the pathway. To provide the cells with a balanced supply of rNTPs and dNTPs for RNA and DNA synthesis, the pathway is regulated through allosteric enzymes at five strategic points (Fig 4) : (i) the first reaction of the pathway, which is the synthesis of carbamoylphosphate; (ii) the first reaction specific to pyrimidine nucleotide synthesis, which is the formation of carbamoylaspartate; (iii) the amination of UTP to form CTP; (iv) the reduction of CDP to dCTP; and (v) the conversion of dCTP to dTTP. In addition, the pathway is controlled at the level of gene expression by mechanisms regulating the synthesis of the six enzymes catalyzing the de novo synthesis of UMP and of ribonucleotide reductase, the enzyme specific for the key crossover reaction from ribonucleotides to deoxyribonucleotides. Certain intermediates of the pathway can be derived directly from preformed pyrimidine compounds present in the growth medium via the salvage

pathways, through which exogenous pyrimidine bases and nucleosides are converted to intracellular pyrimidine NMPs.

De novo Synthesis of UTP and CTP

General Features of the Pathway

The pathway responsible for UTP and CTP biosynthesis is shown in Fig. 4. It is initiated by the formation of carbamoylphosphate from glutamine, bicarbonate, and ATP, a reaction catalyzed by carbamoylphosphate synthetase (CPSase) encoded by the *carAB* operon. Aspartate carbamoyltransferase (ATCase), a multimeric enzyme encoded by the *pyrBI* operon, catalyzes the first unique reaction of pyrimidine biosynthesis, namely, the condensation of carbamoylphosphate and the amino group of aspartate to form carbamoylaspartate (ureidosuccinate). The reaction is driven by the high-energy acid anhydride bond of carbamoylphosphate. In the next two steps, the pyrimidine ring is formed through cyclization and oxidation. The first reaction is catalyzed by dihydroorotase (DHOase) (*pyrC*) and results in ring closure to yield dihydroorotate. Dihydroorotate dehydrogenase (DHOdehase) (*pyrD*), which is membrane bound and linked to the electron transport system, carries out the oxidation of dihydroorotate to orotate. The first pyrimidine nucleotide is formed by the transfer of ribose 5-phosphate from α -D-5-phosphoribosyl-1-pyrophosphate (PRPP) to orotate, forming orotidine 5'-monophosphate (OMP), which is subsequently decarboxylated to UMP. The reactions are catalyzed by orotate phosphoribosyltransferase (OPRTase) (*pyrE*) and OMP decarboxylase (OMPdecase)



Biosynthetic pathway		Salvage pathway	
Genes	Enzymes	Genes	Enzymes
<i>carAB</i>	Carbamoylphosphate synthetase	<i>cdd</i>	Cytidine deaminase
<i>pyrB</i>	Aspartate transcarbamoylase	<i>cmk</i>	Cytidine 5'-monophosphate kinase
<i>pyrC</i>	Dihydroorotase	<i>cod</i>	Cytosine deaminase
<i>pyrD</i>	Dihydroorotate dehydrogenase	<i>nmg</i>	Nucleoside monophosphate glycosylase
<i>pyrE</i>	Orotate phosphoribosyltransferase	<i>upp</i>	Uracil phosphoribosyltransferase
<i>pyrG</i>	Cytidine 5'-triphosphate synthetase	<i>udk</i>	Uridine kinase
<i>pyrH</i>	Uridine 5'-monophosphate kinase	<i>udp</i>	Uridine phosphorylase
<i>ndk</i>	Nucleotide diphosphokinase	<i>rihA</i>	Ribonucleoside hydrolase A
		<i>rihB</i>	Ribonucleoside hydrolase B

Fig 4. The pyrimidine biosynthetic and salvage pathway in *E. coli*

(*pyrF*), respectively. The generation of UTP involves phosphorylation of UMP to UDP and then to UTP by the sequential action of UMP kinase (*pyrH*) and NDP kinase (NDK) (*ndk*). Finally, UTP is animated to CTP by CTP synthetase (*pyrG*). The enzyme uses glutamine as the preferred amino group donor and ATP to energize the reaction. Although CMP is not an obligatory intermediate in de novo CTP synthesis, *E. coli* and *S. typhimurium* each has a CMP kinase (*cmk*) distinct from UMP kinase; the enzyme also uses dCMP as substrate. Presumably, the physiological function of this enzyme is to rephosphorylate the CMP produced by the turnover of mRNA and CDP-diacyl-glycerols.

Properties of the Enzymes in E. coli and S. typhimurium

CPSase (*carAB*). CPSase (EC 6.3.5.5) is an allosteric enzyme that catalyzes the synthesis of carbamoylphosphate from bicarbonate and glutamine at the expense of two molecules of ATP. One ATP is required for the formation of the reaction intermediate, carboxyphosphate, and the other is required for a kinase reaction in which enzyme-bound carbamate becomes phosphorylated (Anderson and Meister, 1965). The enzyme also catalyzes carbamoylphosphate synthesis with ammonia replacing glutamine, but the affinity for ammonia is much lower than that for glutamine. CPSase is feedback regulated in accordance with its metabolic role. If the supply of carbamoylphosphate becomes limiting for arginine synthesis, ornithine accumulates and antagonizes the inhibition by UMP. In the presence of excess arginine, ornithine is not produced, and the enzyme is controlled solely by UMP. The physiological importance of this control is illustrated by the observation that

mutations rendering CPSase hypersensitive to inhibition by UMP induce a uracil sensitivity phenotype (Pierard et al., 1965).

ATCase (*pyrB*). ATCase catalyzes the first step of pyrimidine nucleotide biosynthesis whereby carbamoylphosphate is reacted with L-aspartate to form N-carbamoyl-L-aspartate and Pi. This enzyme will be discussed in more detail later in this dissertation.

DHOase (*pyrC*). DHOase catalyzes the cyclization of N-carbamoyl-L-aspartate, the product of the ATCase reaction, to L-dihydroorotate. The reaction is readily reversible. DHOase is a metallo-enzyme and has been reported to contain one tightly bound essential zinc ion per subunit (Washabaugh and Collins, 1984) in addition to two weakly bound structural zinc ions per subunit which are not essential for activity (Washabaugh and Collins, 1986). Comparison of the amino acid sequences of DHOase from various species reveals that two conserved histidine-containing regions are likely to be involved in active-site zinc binding.

DHOdehase (*pyrD*). The only redox reaction in de novo UMP biosynthesis is the oxidation of dihydroorotate to orotate, a reaction catalyzed by the membrane-bound DHOdehase. The amino acid sequences of a number of DHOdehases contain a highly conserved region that resembles the cofactor binding site of flavoproteins (Nagy et al., 1992).

OPRTase (*pyrE*). The nucleotide-forming step in the pathway consists of the Mg^{2+} -dependent formation of OMP and PPi from orotate and PRPP, a reaction catalyzed by OPRTase. The sole function of Mg^{2+} in the reaction is formation of a monomagnesium complex with the PPi group of PRPP, Mg^{2+} -PRPP, which is the actual ribosyl donor in the reaction (Bhatia and Grubmeyer, 1993). The reaction is

accompanied by anomeric inversion at C-1 of the ribosyl group to give a β -N glycosyl. Amino acid sequence alignments of a number of OPRTases revealed a conserved sequence also found in a number of other phosphoribosyltransferases and in PRPP synthetase and inferred to be the PRPP binding site (Hove-Jensen et al., 1986).

OMPdecase (*pyrF*). The final reaction of de novo pyrimidine nucleotide biosynthesis is catalyzed by OMPdecase (EC 4.1.1.23), whereby OMP is decarboxylated to yield UMP, the parent compound for all other pyrimidine nucleotide. The decarboxylation proceeds in the absence of a coenzyme requirement and the reaction may occur via a noncovalent zwitterionic intermediate. Alignments of the amino acid sequences revealed four conserved sequences.

UMP kinase (*pyrH*). UMP kinase catalyzes the next step in pyrimidine synthesis which is the phosphorylation of UMP to UDP. UMP kinase is one of the regulation points in the pyrimidine pathway and is allosterically regulated by the positive regulator, GTP and a negative regulator UTP (Serina et al., 1995)

CTP synthetase (*pyrG*). In the last step in pyrimidine ribonucleotide biosynthesis, CTP synthetase catalyzes the formation of CTP from UTP, ATP, and glutamine. This step is also stimulated by GTP. The reaction mechanism involves the initial glutamylation of a specific cysteine residue on the enzyme, with the liberation of ammonia. The ammonia immediately reacts with UTP, and in a series of steps that probably involves a phosphorylated amido derivative of UTP (Van der Saal et al., 1985), CTP is formed at the expense of one ATP.

Genetic Regulation of the Pathway in E. coli and S. typhimurium

Expression of the genes and small operons encoding the first six enzymes of the pathway is regulated in a complex manner by the intracellular nucleotide pools, involving both pyrimidine and purine nucleotides and, for the *carAB* operon, arginine. The nucleotide effectors responsible for the regulation were identified largely through the use of mutant strains that allowed manipulation of individual nucleotide pools in vivo (Jensen, 1989). Expression of the genes is regulated noncoordinately, with some genes responding to changes in the UTP pool and others responding to fluctuations in the CTP pool. However, mutants exhibiting a simultaneous increase in the expression of several *pyr* genes have been characterized. In most cases, this phenotype was caused by mutations in genes encoding enzymes involved in nucleotide interconversion, resulting in altered effector nucleotide pools. These include *pyrH* mutants defective in UMP kinase (Ingraham and Neuhard, 1972). In mutants in which altered *pyr* gene regulation did not result from disturbed nucleotide pools, the mutations were localized in *rpoBC*, implying a direct involvement of RNA polymerase in the regulation of *pyr* gene expression (Jensen et al., 1982). Superimposed on the nucleotide control, a twofold repression of *carAB*, *pyrC*, and *pyrD* expression is mediated by purine bases. This control requires a functional purine repressor, which is encoded by *purR*. In the presence of one of the corepressors, guanine or hypoxanthine, PurR binds to a purine operator sequence located in the promoter regions of these genes (Choi and Zalkin, 1990).

Expression of *pyrBI* and *pyrE* of *E. coli* is regulated at the transcriptional level, and the synthesis of ATCase and OPRTase is repressed when the intracellular UTP pool is increased and derepressed when it is lowered (Jensen, 1989). An

inverse correlation between synthesis and the size of the GTP pool has also been observed (Jensen, 1979). For *E. coli* and *S. typhimurium*, the DNA upstream of the start of the *pyrB* (Michael et al., 1987) and *pyrE* (Neuhard and Nygaard, 1985) genes is very similar and contains a rho-independent transcriptional terminator sequence (attenuator). Another region of dyad symmetry (transcriptional pause site), followed by a sequence encoding a uridylate-rich cluster in the transcript, precedes the attenuator. The leader regions of the mRNAs are open reading frames; for *pyrBI*, the leader encodes a short polypeptide of 44 (*E. coli*) or 33 (*S. typhimurium*) amino acids, whereas for *pyrE*, the leader is the *rph* mRNA that codes for the RNase PH polypeptide. The essential features of attenuation control require that transcription terminate at the attenuator in the absence of closely coupled translation and that termination be prevented if transcription and translation are coupled. Tight coupling between the transcribing RNA polymerase and the first ribosome translating the leader mRNA is required for transcription through the attenuator. When the UTP concentration is high, transcription and translation are effectively uncoupled, facilitating termination at the attenuator. When the UTP concentration is low, however, this polarity is relieved by the reduced rate of elongation by RNA polymerase through the uridylate-rich pause region, which allows for coupling with the more rapidly progressing lead ribosome (Fig 5a, 5b, 5c). Direct evidence for

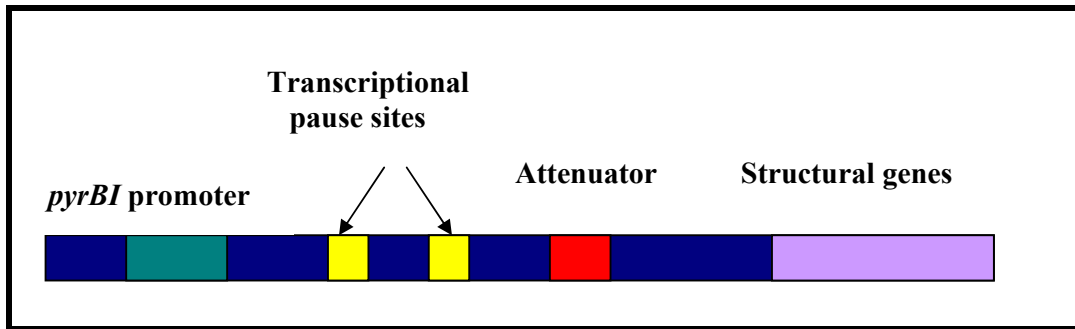


Fig 5a. Promoter regulatory region

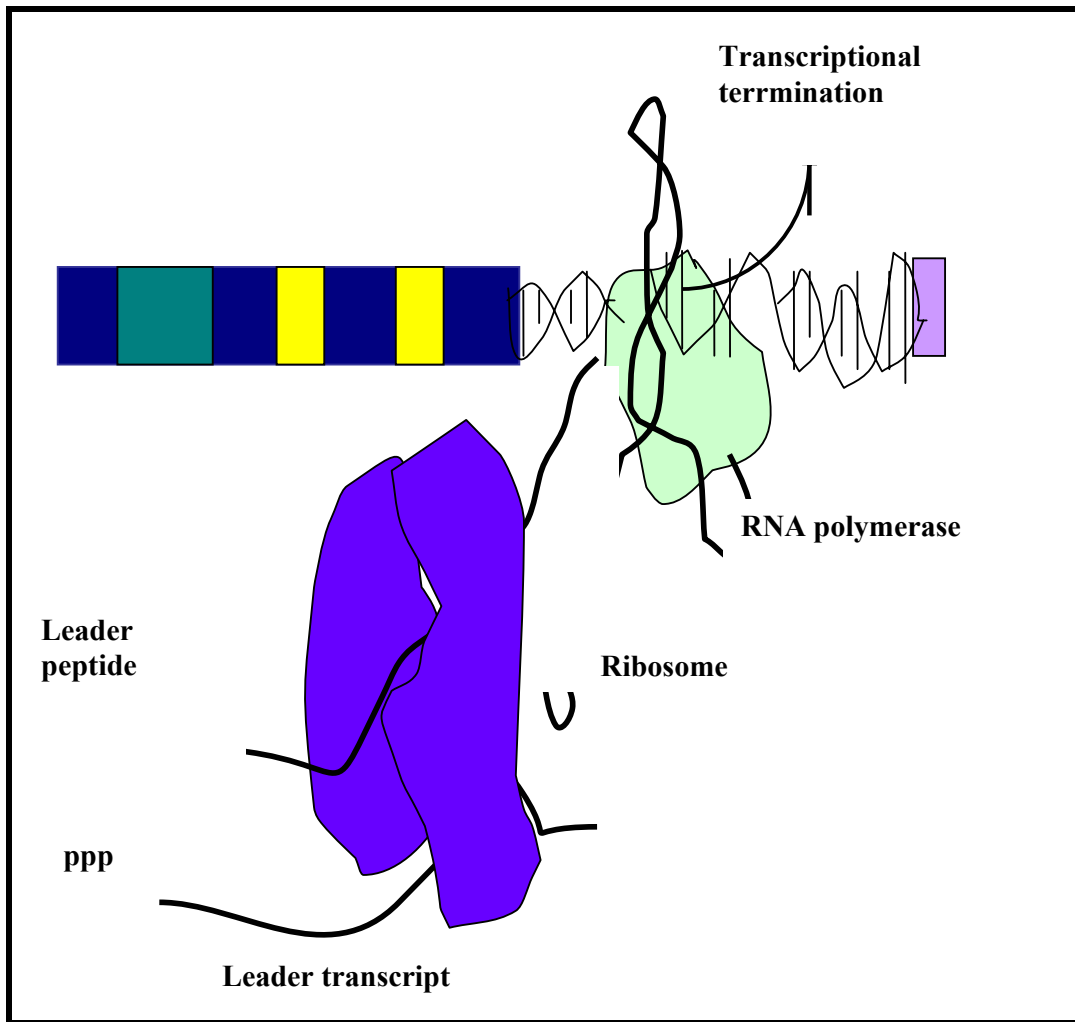


Fig 5b. High UTP-no or weak transcriptional pausing

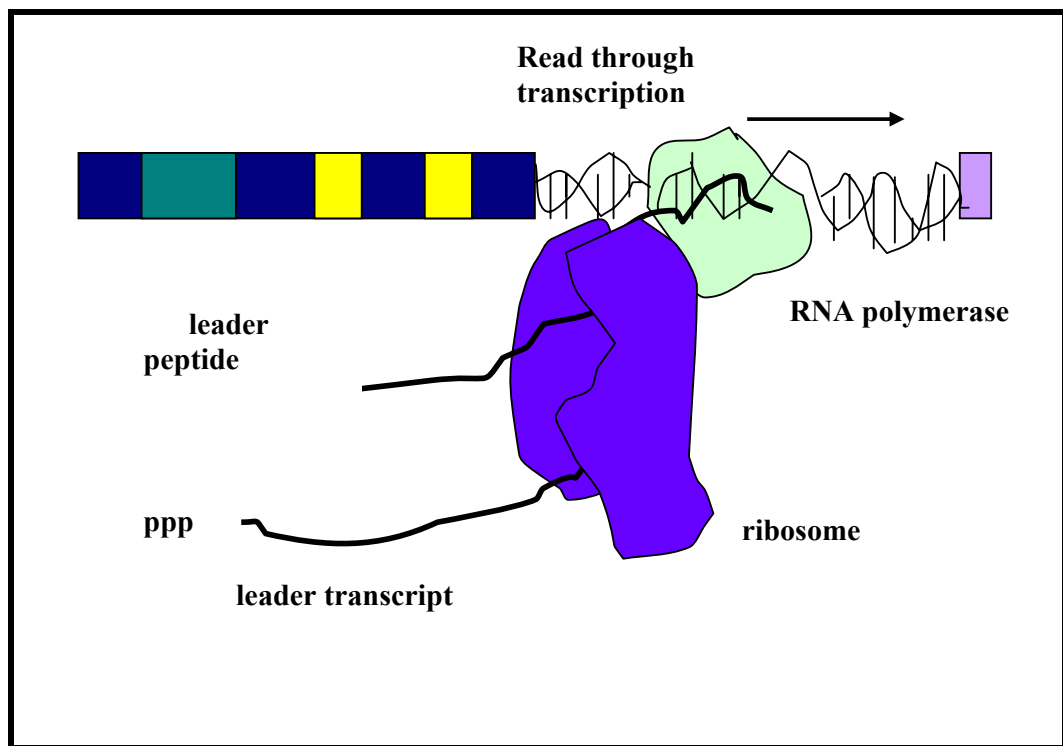


Fig 5c. Low UTP-strong transcriptional pausing

involvement of the attenuator in regulation was obtained by showing that chromosomal mutations leading to elevated expression can result from base substitutions in the attenuator region that reduce the stability of the putative hairpin structure of the transcript (Neuhard and Kelln, 1988). Furthermore, plasmid constructs deleted for the attenuator region have elevated expression and reduced repressibility (Barilla and Kelln, 1992). The necessity of translation of the leader region for expression and UTP-mediated regulation has been demonstrated for both *pyrBI* (Clemmensen et al., 1985) and *pyrE* (Bonekamp et al., 1984). Translation through the attenuator is, however, not a prerequisite for preventing transcriptional termination (Michaels et al., 1987), for *pyrBI*, the ribosome must translate to within 14 to 16 nucleotides of the attenuator-encoded leader mRNA hairpin to inhibit transcriptional termination efficiently (Roland et al., 1988).

Salvage Pathway

The pyrimidine salvage pathways of *E. coli* and *S. typhimurim* serve three physiological functions. The first is assimilation of exogenous free bases and nucleosides; the nucleosides are predominantly metabolized to free bases before being used for nucleotide synthesis. The second function is making the pentose moieties of exogenous nucleosides available as a source of carbon and energy (Neuhard and Kelln, 1988) and the amino groups of cytosine compounds available as a nitrogen source. The third function is reutilizing free bases and nucleosides produced intracellularly from nucleotide turnover. Significant amounts of ribonucleotides are degraded during normal growth, and the reutilization of these free bases and

nucleosides requires salvage enzymes (Hammer-Jespersen and Munch-Peterson, 1973).

Pyrimidine ribo- and deoxyribonucleotides serve as the sole pyrimidine sources in both *E. coli* and *S. typhimurium* (Lichtenstein et al., 1960). Their utilization is dependent on a number of periplasmic phosphatases that hydrolyze nucleotides to nucleosides (Neuhard, 1983). The nucleosides are subsequently taken up via specific transport systems located in the cytoplasmic membrane. In addition, specific outer membrane pore-forming proteins are required for passage of the nucleotides into the periplasmic space (Beacham et al., 1977).

Beck (1995) has studied the pyrimidine salvage pathway in 44 prototrophic bacteria and 11 auxotrophs, which were selected because of specific mutations that they contained in biosynthetic and salvage pathways (O' Donovan and Shanley, 1995). This study was conducted using High Performance Liquid Chromatography and offered much insight into the salvage pathways of a wide range of microorganisms. The prototype organism used was *E. coli* and the researcher discovered eight more variations of the salvage pathways in other organisms. Through this study, many groups emerged which differed in the enzymes that were responsible for salvaging pyrimidines. Figures (6) and (7) show the enzymes involved in the salvaging of pyrimidine nucleotides in *E. coli* and *P. aeruginosa* respectively.

The following is a general list of all the compounds in the pyrimidine salvage pathway and how they are utilized in an organism. Some organisms have two pathways by which to produce UMP from uracil (U). The first pathway is the catalysis of uracil by the enzyme uracil phosphoribosyltransferase (Upp). One

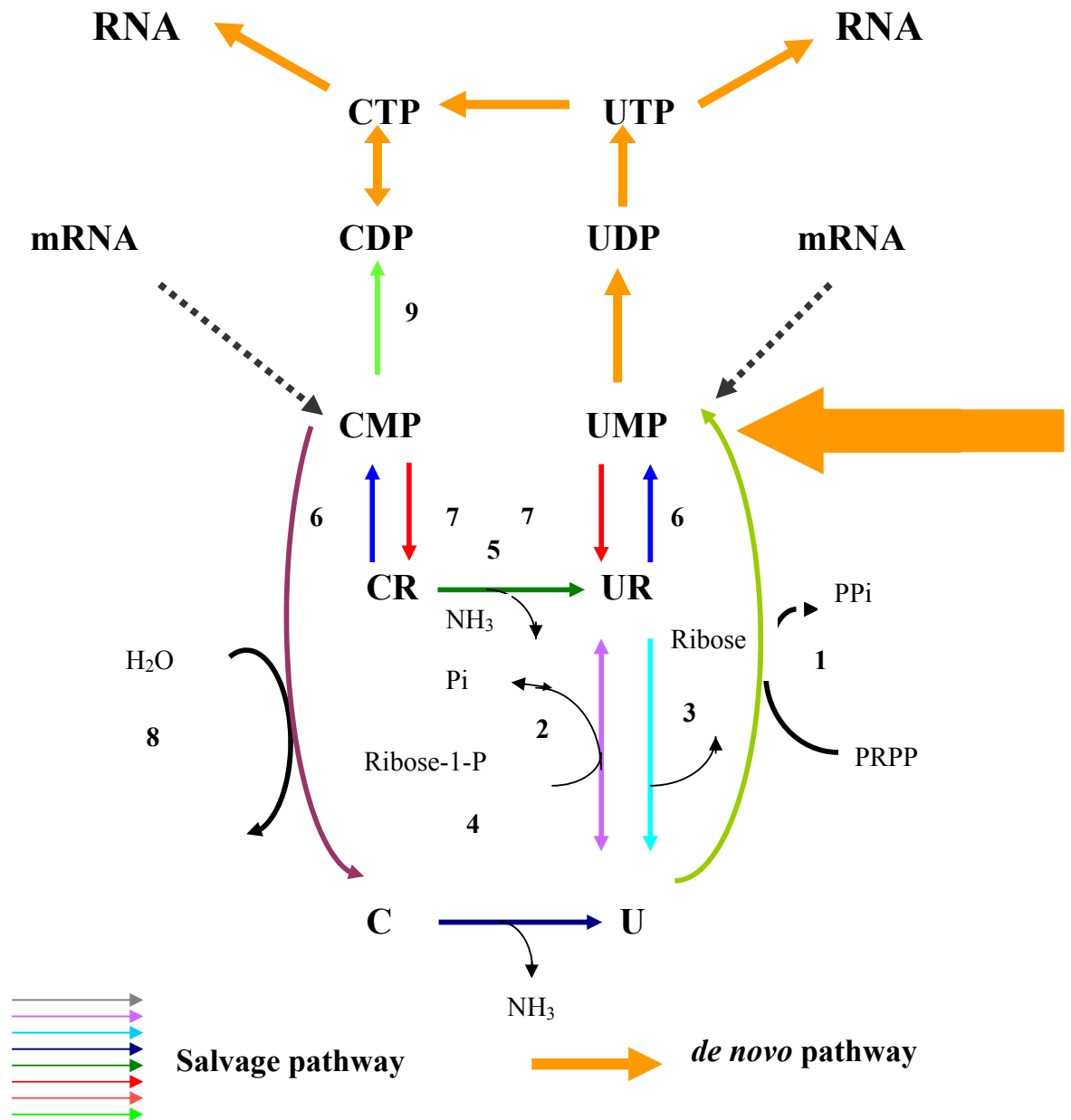


Fig 6. Pyrimidine salvage pathway in *Escherichia coli*.

1. uracil phosphoribosyltransferase (Upp), 2. uridine phosphorylase (Udp),
3. ribonucleoside hydrolase A & B (Rih), 4. cytosine deaminase (Cod),
5. cytidine deaminase (Cdd), 6. uridine kinase (Udk), 7. 5'-nucleotidase,
8. CMP glycosylase, 9. CMP kinase (Cmk)

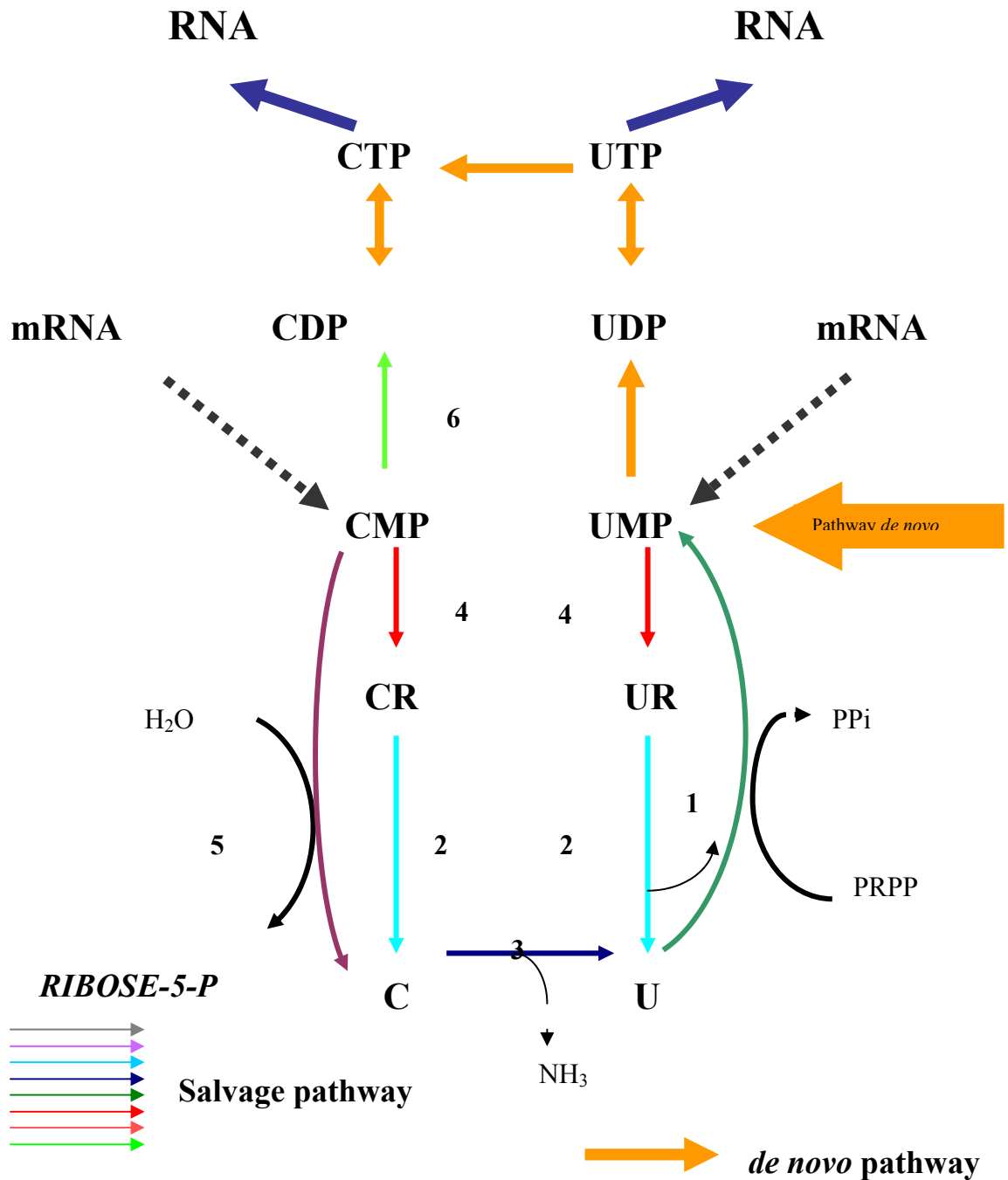


Fig 7. Pyrimidine salvage pathway in *P. aeruginosa*.

1. Uracil phosphoribosyltransferase (Upp),
2. Ribonucleoside hydrolase A & B (Rih),
3. Cytosine deaminase,
4. 5'-nucleotidase,
5. CMP glycosylase (Cmg),
6. CMP kinase (Cmk)

molecule of PRPP is utilized in this reaction (Anderson et al., 1992). The second pathway for the formation of UMP can be produced by the enzyme uridine phosphorylase (Udp) when a high amount of ribose-1-phosphate is present. Uridine then can be converted to UMP by the enzyme uridine kinase (Udk). GTP donates its γ -phosphate for this reaction (Neuhard and Nygaard, 1987). Cytosine deaminase (CodA) catalyzes the deamination of cytosine to uracil in an irreversible reaction (West et al., 1982). Uridine is a substrate for at least four different salvage enzymes. Uridine phosphorylase (Udp), uridine kinase (Udk), ribonucleoside hydrolase A and B (Rih) and uridine hydrolase. In *E. coli* only the first three of the enzymes have been found (Beck, 1995). Cytidine in enteric bacteria is phosphorylated to CMP by uridine (cytidine) kinase. When cytidine is available to *E. coli* much of it is converted to uridine by cytidine deaminase (cdd) and also by hydrolytic cleavage (Beck 1995). In *Pseudomonas* cytidine has also been shown to be a substrate for ribonucleoside hydrolase (Terada et al., 1967; Beck, 1995).

The salvaging of pyrimidines is important when one considers that some organisms do not have a pyrimidine biosynthetic pathway. If a mutation were to occur in the biosynthetic pathway (making a pyrimidine auxotroph) the salvage pathway would in effect take over and continue to make the cell survive. Breakdown products of mRNA (the 5' mononucleotides UMP and CMP) can be toxic to the cell and therefore are removed very quickly (O' Donovan, 1978). If they are allowed to accumulate, they will undoubtedly cause bacterial cell death. A mutation that affected the process of mRNA degradation in a cell would have the result of self-destruction. The cell would die because of the buildup of the toxic 5' monophosphates (O' Donovan and Shanley 1995).

Regulation of Pyrimidine Enzymes in P. aeruginosa.

As in *Escherichia coli* the pyrimidine biosynthetic pathway shares in the production of UTP and CTP for RNA with the pyrimidine salvage pathway. While salvage pathways are essential in providing a balance of RNA synthesis in prototrophs, they are obligately required to satisfy pyrimidine requirements in auxotrophs. Salvage pathways also return mRNA degraded monomers, the 5' monophosphates, to their triphosphate levels for RNA resynthesis. A portion of the 5' monophosphates (CMP) is further degraded to cytosine, which is subsequently deaminated to uracil for the conversion to UMP.

Pseudomonas aeruginosa lacks the salvage enzyme uridine (cytidine) kinase and therefore cannot convert uridine to UMP and cytidine to CMP. Thus, a pyrimidine auxotroph (Pyr⁻) in a *upp*⁻ background cannot grow when fed exogenous uracil. In the absence of uridine (cytidine) kinase it is impossible to study the regulation of the pyrimidine enzymes in *P. aeruginosa* (Fig 7).

Various authors have shown that in *E. coli* and *S. typhimurium* the expression of aspartate transcarbamoylase (*pyrBI*), orotate phosphoribosyltransferase (*pyrE*) and orotidine-5'-monophosphate decarboxylase (*pyrF*) is under negative control by a uridine nucleotide.

A cytidine nucleotide has been shown to exert control on carbamoylphosphate synthetase (*carAB*), dihydroorotase (*pyrC*) and dihydroorotate dehydrogenase (*pyrD*) (O' Donovan et al., 1989; Smith et al., 1980; Schwartz and Neuhard, 1975). In the above organisms with ~50% G + C, it has been observed that a uridine compound was the

primary repressing metabolite for the expression of *pyrB* gene. It is thought that a cytidine compound may be the primary repressing metabolite in organisms, which have a higher G + C composition such as *P. aeruginosa*.

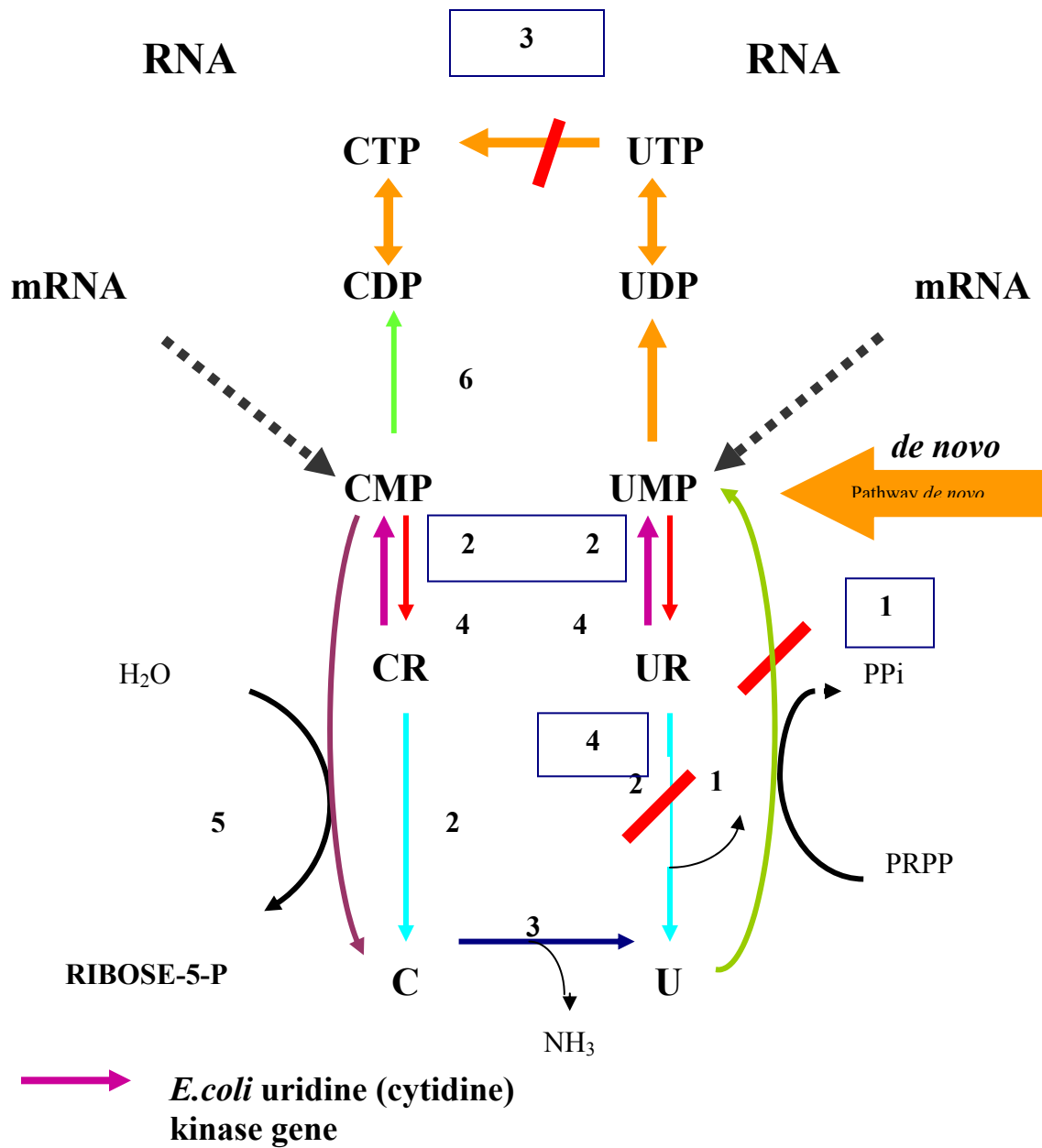


Fig 8. Red lines show the metabolic blocks that were created in *P. aeruginosa* so that uridine and cytidine could be fed to increase the nucleotide pools. The uridine (cytidine) kinase gene from *E. coli* was expressed in *P. aeruginosa*. Numbers in boxes represent the order in which the blocks were created.

Aspartate Transcarbamoylase

Aspartate transcarbamoylase (EC 2.1.3.2) catalyzes the first reaction unique to pyrimidine biosynthesis (Figure 2), namely the condensation of aspartate and carbamoylphosphate to yield carbamoylaspartate and inorganic phosphate. Aspartate transcarbamoylase exists as either a single monofunctional enzyme in bacteria or as part of a multienzyme complex in higher organisms. In mammals, the third biosynthetic enzyme dihydroorotase (DHOase) is fused to a carbamoylphosphate synthetase (CPSase) - aspartate transcarbamoylase (ATCase) protein to form a multienzyme complex referred to as CAD (Beck and Ingraham, 1971). In higher organisms the enzymes for pyrimidine biosynthesis de novo tend to be multifunctional proteins that are thought to have arisen by through gene fusion (Donahue and Turnbough, 1990). In some higher organisms such as *Saccharomyces cerevisiae*, the first two enzymes of pyrimidine biosynthesis are fused to form a CPSase-ATCase complex with an inactive DHOase in between (Kimsey and Kaiser, 1992). Interestingly, the molecular mass of the CPSase-ATCase complex of *S. cerevisiae* is similar to the molecular mass seen in CAD which has three functional proteins. Upon sequence analysis, it was shown that *S. cerevisiae* contains a region of homology between CPSase and ATCase that is similar to known DHOases. However, this open-reading frame did not encode an active DHOase (Kimsey and Kaiser, 1992).

Bacterial ATCases have been divided into three classes depending on their molecular mass, subunit composition, and allosteric properties (Anderson et al., 1992).

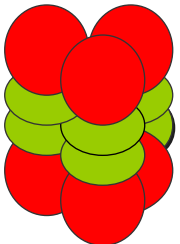
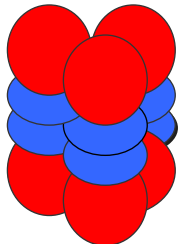
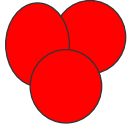





Class	Class A (480 kDa)	Class B (300 kDa)	Class C (100 kDa)
Structure			
Subunit Structure	PyrB catalytic 34 kDa  PyrC' active or inactive 45 kDa 	PyrB catalytic 34 kDa  PyrI regulatory 17 kDa 	PyrB catalytic 34 kDa 
Representative organism	<i>Pseudomonas putida</i> <i>P. aeruginosa</i> <i>Burkholderia cepacia</i>	<i>Escherichia coli</i> <i>Salmonella typhimurium</i> <i>Serratia marcescens</i> <i>Neisseria meningitidis</i> <i>Proteus vulgaris</i> <i>Pyrococcus abyssi</i>	<i>Bacillus subtilis</i> <i>Bacillus cauldolyticus</i> <i>Streptococcus pyogenes</i>

Fig 9. Classes of bacterial ATCase

Schematic representations of the three bacterial ATCase classes are shown in Figure (9). Class C ATCases have the smallest molecular mass of 100 kDa and are composed of three identical monomer of 34 kDa. The class C ATCases exhibit Michaelis-Menten kinetics for both substrates, aspartate and carbamoylphosphate, and are not regulated by nucleotide effectors such as ATP, CTP, or UTP (Anderson, 1983). Gram positive bacteria such as *Bacillus subtilis* (Anderson, 1983), *Enterococcus faecalis* (Barilla and Kelln, 1992), and *Staphylococcus epidermidis* (Eliasson et al., 1992), have trimeric ATCase of 100 kDa with polypeptide subunit monomer of 34 kDa. The studies from Shepherdson's laboratory have shown that some Gram negative bacteria such as *Xanthomonas campestris*, *Stenotrophomonas maltophilia*, and *Lysobacter enzymogenes* also have trimeric ATCases with molecular masses of 100 kDa with a polypeptide monomer of 34 kDa (Anderson, 1983). The catalytic trimer of *E. coli* is also classified as class C ATCase. In all organisms listed in the class C ATCases, the catalytic activity is associated with a polypeptide of 34 kDa, which forms a trimeric structure.

Class B ATCases, which have molecular masses of approximately 310 kDa, are found in the enteric bacteria with the *E. coli* ATCase being the best studied (Bothwell and Schachman, 1980). The holoenzyme of *E. coli* has a molecular mass of 310 kDa and is composed of two different proteins: a catalytic polypeptide encoded by *pyrB* and a regulatory polypeptide encoded by *pyrI* (Jordan et al., 1994). Six identical polypeptide chains form two trimeric catalytic subunits and six identical polypeptide chains form three dimeric regulatory subunits with dodecameric architecture of 2c3:3r2. The catalytic polypeptide has a monomer of 34 kDa contains two domains. A carbamoylphosphate

binding region is found in the polar domain (amino terminus) and an aspartate binding region is located in the equatorial domain (carboxyl terminus). Likewise, the regulatory polypeptide with a monomer of 17 kDa (Lu et al., 1993) has two domains, the effector binding sites for ATP and CTP are housed at the amino terminus while the carboxyl terminus contains the zinc binding sites. Six zinc molecules stabilize the regulatory dimer and promote the association of regulatory and catalytic subunits (Lu et al., 1992). A schematic representation of the quaternary structure of the class B ATCase is shown in Figure 4 (England et al., 1994). The ATCase holoenzyme in *E. coli* exhibits sigmoidal kinetics with both aspartate and carbamoylphosphate when initial velocity is plotted as a function of substrate concentration (Anderson et al., 1992). When velocity-substrate plots are carried out using the catalytic subunits only, a hyperbolic or Michaelis-Menten kinetic curve is observed using either substrate. Michaelis-Menten kinetics are observed also if the assay temperature were lowered to 4°C in the presence or absence of CTP (Herve et al., 1989) or if the native enzyme were treated with 0.1 mM urea or assayed at pH 8.0 (Lu et al., 1992).

Yates and Pardee (1956) showed that in *E. coli*, ATCase is feedback inhibited by CTP and activated by ATP. Yet, the inhibition of ATCase by CTP can be overcome by increasing aspartate concentrations to saturating levels of 25 mM or greater. ATP decreases the K_m of ATCase for aspartate whereas, CTP increases the K_m . UTP by itself does not inhibit the activity of ATCase, but in concert with CTP, a synergistic inhibition is seen which is not seen when UTP or CTP is used separately (Machida and Kuninaka, 1969).

The regulatory and catalytic subunits of class B ATCases can be dissociated by treating the holoenzyme with heat or mercurial compounds such as ρ -hydroxymercuribenzoate or neohydrin (Bouvier et al., 1984). The catalytic trimer remains enzymatically active, but there is a loss of nucleotide effector response. Moreover, the separated catalytic trimer appears to be four times more enzymatically active than the holoenzyme (Drabikowska et al., 1990). These active dissociated subunits can be reassembled to form holoenzyme with no loss of catalytic or regulatory activity when incubated in β -mercaptoethanol or dithiothreitol (Bouvier et al., 1984).

Class A ATCases have the largest molecular mass of between and 500 kDa and are mostly found in the pseudomonads (Abdelal et al., 1976). The first class A ATCase was purified from *P. fluorescens* (Abdelal et al., 1976) and was thought to be composed of two identical subunits of monomer of 180 kDa. The class A ATCases were considered to be dimers until Bergh and Evans (PNAS) showed that the *P. fluorescens* ATCase enzyme was actually composed of two polypeptide chains with molecular masses of 34 kDa and 45 kDa. The 34 kDa chain, encoded by *pyrB*, contains both the active site for ATCase and the nucleotide effector binding sites. The 34 kDa polypeptide is the same size as the catalytic counterparts found in other bacterial, fungal (Kimsey and Kaiser, 1992), and CAD (Chalier et al., 1988) aspartate transcarbamoylases. This 34 kDa polypeptide is universal in ATCases studied thus far. Bergh and Evans (PNAS) concluded that catalytic and regulatory domains were both located on the 34 kDa polypeptide using affinity labelling with an analog of the allosteric effector ATP. The 45 kDa chain is encoded by *pyrC'* and produces an inactive DHOase-like polypeptide. It has been designated *pyrC'*

because of the striking sequence homology to known dihydroorotases, yet lacks DHOase activity, by virtue of its missing five essential histidine residues (Karibian, 1978). In *P. putida* and *P. aeruginosa*, there is a four base pair overlap between the *pyrB* and *pyrC*, which insures that each polypeptide will be produced in equimolar amounts (Mathews et al, 1990). Therefore, *Pseudomonas* ATCases are active only as dodecameric holoenzymes comprised of six *pyrB*-encoded (34kDa) polypeptides complexed with six *pyrC'*-encoded polypeptide chains (45kDa) which give 480 kDa molecular mass. *B. cepacia* ATCase was defined as a Class A ATCase. ATCase of *B. cepacia* forms a significantly larger holoenzyme (550 kDa). It also forms a much smaller, active form of trimeric subunits at 140 kDa; this is unusual for class A enzyme. At the present time, the 45 kDa chain is thought to be needed to maintain dodecameric architectural integrity. The class A ATCases exhibit Michaelis-Menten saturation curves with both aspartate and carbamoylphosphate when initial velocity is plotted as a function of substrate concentration, both *P. aeruginosa* and *P. putida* inhibition is seen with nucleotide effectors ATP, CTP, and UTP, but the amount of inhibition varies considerably for the two pseudomonad species (Brabson and Switzer, 1975).

In this dissertation, research explored the characterization of ATCase from *B. cepacia*. The uncleaved ATCases and atypical auto-proteolysis ATCases of *B. cepacia* were purified and assayed to investigate the nature of ATCase. Moreover, the mutagenesis at the auto-proteolysis site in *B. cepacia* ATCase was obtained to investigate further and new class of ATCase, namely Class D, will be proposed to accommodate the unique *B. cepacia* and *B. cepacia*-like ATCases.

In addition, the second ATCase from *B. cepacia* was discovered by construction of *pyrB* knocked out *B. cepacia*, and using *in vivo* virulent test, the relationship between pyrimidine metabolism and siderophores production was inspected.

MATERIALS AND METHODS

Bacterial Strains, Plasmids, Media and Growth Conditions

The bacterial strains and plasmids used in this study are listed in Table 1. *E. coli* strains were grown in Luria-Bertani (LB) enriched medium (Miller, 1992), and *E. coli* minimal medium (Ecm) (Miller, 1992) with the addition of arginine, uracil or both at a concentration of 50 µg/ml. Ecm contains per liter: 10.5 g of K₂HPO₄, 4.5 g of KH₂PO₄, 1.0 g of (NH₄)₂SO₄, and, 0.5 g of Na₃-citrate. After autoclaving, sterile solutions 10 mL of 20 % glucose (w/v) (0.2 % final), 1 mL of 1M MgSO₄ (1 mM final) and 5mL of 0.337 % thiamine (w/v) (0.0015 % final) (Miller, 1972) were added. *B. cepacia* and *P. aeruginosa* were cultivated in *Pseudomonas* minimal medium (Psm) (Ornston and Stanier, 1966) which contains per liter: 25 mL of 0.5 M Na₂HPO₄, 25 mL of 0.5 M 1 KH₂PO₄, 10 mL of 10 % (NH₄)₂SO₄ and 10 mL of concentrated base in 930 mL of distilled, deionized H₂O (ddH₂O). 0.2 % glucose was added to the medium as carbon and energy source. The concentrated base contains per liter: 14.6 g of KOH, 20 g of nitroacetic acid, 28.9 g of MgSO₄ anhydrous, 6.67 g of CaCl₂•7 H₂O, 18.5 g of (NH₄⁺)₆Mo₇O₂₄ • 7H₂O, 0.198 g of FeSO₄•7H₂O, and 100 mL of Metals 44. It is important to add the next chemical after dissolving the previously added chemical to prevent any precipitation. The pH was adjusted to 6.8. Metals 44 consists of the following components: 2.5 g EDTA, 10.95 g of ZnSO₄ • 7 H₂O, 5.0 g of FeSO₄• 7 H₂O, 1.54 g of MnSO₄•H₂O, 0.392 g of CuSO₄ • 5 H₂O, 0.251 g of CuSO₄ anhydrous, 0.25 g of Co(NO₃)₂ • 6 H₂O or 0.177 g of Na₂B₄O₇ • 10 H₂O (Borax). *Pseudomonas* Isolation

Strain or Plasmid	Genotype or relevant property	Source or reference
Strain		
<i>B. cepacia</i> 25416	Wild type	ATCC
<i>B. cepacia</i> SKB1	<i>B. cepacia pyrBI</i> ⁻	This study
PAO1	<i>P. aeruginosa</i> wild type	ATCC
<i>E. coli</i>		
BL21	<i>E. coli</i> B, F ⁻ , <i>ompT</i> , <i>hsdS</i> , <i>gal</i> , <i>dcm</i> and used for GST system	Amersham
DH5 α	<i>recA1</i> , <i>hsdR17</i> , <i>endA1</i> <i>supE44</i> , <i>relA1</i> , <i>gyrA96</i> , Δ (<i>argF-lacZYA</i>)U169	BRL, 1986
HB101	F ⁻ , <i>thi-1</i> , <i>hsdS20</i> , <i>recA13</i> , <i>ara-14</i> , <i>leuB6</i> , <i>lacY1</i> , <i>galK2</i> , <i>rpsL20</i>	Promega
JM109	<i>recA1</i> , <i>endA1</i> , <i>gyrA96</i> , <i>thi</i> , <i>hsdR17</i> , <i>supE44</i> , <i>relA1</i> , [<i>F'</i> , <i>lacIqZ</i> Δ M15]	Promega
TB2	Δ <i>pyrBI</i> , <i>arg I</i> , <i>argF</i>	
Plasmids		
pUC18	pMB1 origin, high copy <i>E. coli</i> shuttle vector, Amp ^r	Bio-rad
pSKBB18	pUC18 with 1.29 kb insert of <i>B. cepacia pyrB</i>	This study
pSKBB18X	pSKBB18 with 1.5kb insert of mini-transposon in <i>pyrB</i>	This study
pSKBB18A	pSKBB18 with mutagenized <i>B. cepacia pyrB</i> (Ser74 to Ala74)	This study
pSKBB18N	pSKBB18 with mutagenized <i>B. cepacia pyrB</i> (Ser74 to Arg74)	This study
pGEX2T	GST gene fusion vector, <i>tac</i> promoter, <i>lac I</i> ^r , Amp ^r	Amersham
pSK2T	pGEX2T with 1.29 kb insert of <i>B. cepacia pyrB</i>	This study
pSK2TA	pGEX2T with mutagenized <i>B. cepacia pyrB</i> (Ser74 to Ala74)	This study
pSK2TN	pGEX2T with mutagenized <i>B. cepacia pyrB</i> (Ser74 to Arg74)	This study

Table 1. List of strains and plasmids.

Agar (PIA) supplied by Difco, was also used as a selective medium for transconjugate in Tri-parental mating experiment.

Preparation of Cell Extracts

Cell extracts of *E.coli*, *P. aeruginosa*, *B. cepacia* and its ATCase mutant were prepared from 50 mL cultures. Cells which reached the mid to late exponential phase ($OD_{600} = 0.6$ to 1.4) of growth were collected by centrifugation at $6,000 \times g$ for 10 minutes in $4^{\circ}C$. The cells were resuspended in 1 mL of ATCase breaking buffer (2 mM β -mercaptoethanol, 20 μ M $ZnSO_4$, 50 mM Tris-HCl, pH 8.0, and 20 % glycerol). The suspensions were disrupted ultrasonically using a Branson Cell Disrupter 200 for three times of cycle of 1 minute breaking and 1 minute rest in 50 mL conical tubes that were submerged in an ethanol-ice water slurry to prevent the over-heating of the samples. The broken cell suspensions were transferred to 1.5 mL centrifuge tubes and then centrifuged at $10,000 \times g$ for 20 minutes in $4^{\circ}C$. The cell extract from the supernatant was then dialyzed in 150 volumes of ATCase breaking buffer for 18 to 24 hours and then transferred to fresh microcentrifuge tubes for storage at $-20^{\circ}C$ until assayed.

Preparation of Chemical Competent Cells

For the transformation of *E.coli*, cells were made chemically competent by the calcium chloride method of Mandel and Higa, 1970, with slight modification. A 50ml LB broth was inoculated by 0.5 mL of overnight cell culture and incubated at $37^{\circ}C$ for 2-4 hours until the culture reached the OD_{600} of about 0.5. The culture was stored in ice for

20 minutes. Then cells were transferred to a 50 mL polypropylene conical tube and centrifuged at 5,000 x g for 20 minutes in 4°C. The supernatant was removed and the pellet was resuspended with 20 mL of ice-cold 0.1M CaCl₂ stored in ice for 20 minutes. The mixture was centrifuged at 3,000 x g for 15 minutes. After discarding the supernatant, the pellet was gently mixed with 700 µL of 0.1M CaCl₂ and stored at 4°C overnight. The next day, 300 µL of ice-cold 50% glycerol was added and mixed. Then cell mixture was dispensed as 0.2 mL aliquots into pre-chilled 1.5 mL a. Eppendorf tubes and stored in -80 °C until being used.

Transformation of Plasmid by Heat Shock Method

For transformations, the competent cells were removed from the -80 °C and allowed to thaw on ice. When thawed, plasmid DNA was added, usually between 40 - 500 ng in a volume of 3-10 µL. The plasmid DNA/cell mixture was incubated on ice for 20-30 minutes, and then “heat shocked” by incubation in a 42 °C water bath for 2 minutes and “cold shocked” by incubation in ice for 2 minutes. Next, 800 µL of cold LB was added to each transformation tube and the cells were incubated at 37°C shaker for 1 hour. 100 µL of incubated cell mixtures with plasmid were plated on to selective medium with appropriate antibiotics. Then the rest of cells were centrifuged at 10,000 x g for 30 seconds and the pellet was resuspended with 100 µL of LB. This suspension was plated on the same selective medium with same antibiotics and labeled as “spindown” and both plates were incubated at 37°C overnight. If minimal medium plates were to be used, the cells were washed 3 times with the same minimal medium or 10 mM MgSO₄

solution prior to plating, in order to avoid carry-over of the rich nutrients of the LB medium.

Extraction of Chromosomal DNA from *B. cepacia*

Chromosomal DNA of *B. cepacia* was extracted using the modified method described by Berns & Thomas Jr., (1965). A culture of *B. cepacia* was grown in 5 mL of *Pseudomonas* minimal medium supplemented with 0.2 % glucose overnight. A 1% inoculum was used to initiate the growth. Then 3 mL of cells were harvested by centrifugation at 14,000 x g for 1 minute in 4°C. The pellet was washed by resuspending with saline solution or phosphate-buffered saline (PBS) solution. The resuspended cell was harvested at 14,000 x g for 1 minute and the supernatant was discarded. 250 µL of 0.1M BaCl₂, 10mM of Tris (pH 8.0), and 10mM of EDTA were added and resuspended with the cell pellet. After 25µl of 10% SDS was added, the resuspended solution was incubated at 65°C for 10 minutes. Then 25µL of proteinase K (5mg/ml) was added and incubated at 37°C for 30 minutes. The solution was extracted with equal volume of phenol equilibrated with 50 mM Tris-HCl pH 8.0 and 1 mM EDTA. The solution was re-extracted with equal volume of phenol:chloroform mixture. Next, phenol contamination was removed by extracting with equal volume of isoamyl alcohol:chloroform mixture. To precipitate the chromosomal DNA, 100 µL of 7.5 M ammonium acetate and 750 µL of cold ethanol were added and gently mixed. After freezing in -80°C for 30 minutes, then the pellet was spun down at 14,000 x g for 5 minutes in 4°C. Then the supernatant was removed and the tube was inverted and dried. After all the ethanol was evaporated,

the chromosomal DNA was resuspended with dd-H₂O and 1 μL of RNase A and incubated at 65°C for 10 minutes to destroy DNase activity. The purity and quantity of DNA was read at 280 nm and 260 nm respectively in as Shimadzu 500 UV spectrophotometer. A DNA concentration of 1.2 μg/μL was recovered using the above preparation.

Rapid Extraction of DNA from an Agarose Gel

Sephaglas Bandprep Kit (Pharmacia Biotech) was used for the rapid extraction of DNA from an agarose gel. First, the slice of agarose containing the DNA band was excised by using clean razor blade and transferred to the weighted 1.5 mL microcentrifuge tube. Then 250 μL (based on 250 mg of gel amount) of gel solubilizer was added and vigorously mixed by vortexing. The tube was incubated at 60°C for at least 10 minutes. 10 μL of well-mixed Sephaglas BP was added to the dissolved gel slice tube and incubated at room temperature for 5 minutes. The dissolved gel was centrifuged for 30 seconds at 14,000 x g and the supernatant was discarded very carefully. Then 80 μL of washing buffer was added and the Sephaglas pellet was washed by pipetting. The suspension was centrifuged for 30 seconds at 14,000 x g for 30 seconds. This washing step was repeated twice more, then the Sephaglas pellet tube was inverted to be dried. After completely dried, 10 μL of dd-H₂O was added to dissolve the DNA for 1 minute at room temperature. Then tube was centrifuged at 14,000 x g for 2 minutes and the supernatant, which contained the eluted DNA, was transferred to the clean centrifuge tube and stored at -20 °C until being used.

The purity and the concentration of extracted DNA were checked by the absorbance at A_{260} and A_{280} .

The Extraction of Plasmid DNA from *E. coli*

After transformation, the plasmids were extracted by Minipreps Plasmid Purification kit from Bio-rad Company. The 1.5 mL of overnight culture were transferred to centrifuge tube and harvested at 14,000 x g for 1 minute. After removal of the supernatant, another 1.5 mL of culture were transferred and centrifuged and the supernatant were removed by aspirating or pipetting. Next, 200 μ L of the Cell Resuspension Solution were added and resuspended with cell pellet. This step is very important to maximize the recovery of plasmid. The pellet has to be resuspended completely. Then 250 μ L of the Cell Lysis Solution was added and the tube was gently inverted about 10 times. 250 μ L of the Neutralization Solution was added and the tube was gently inverted about 10 times again. Then the tube was centrifuged at 14,000 x g for 5 minutes. While waiting for the centrifugation, a spin filter was inserted into 2 mL wash tube. Then cleared lysate (supernatant) from centrifugation was transferred to a spin filter. 200 μ L of thoroughly suspended matrix was added to a spin filter, which contained cell lysate, and mixed by pipetting up and down. This tube was spun down by pulse at maximum speed, and the filtrate was discarded and the filter was replaced in the same tube. Then 500 μ L of the washing buffer was added and centrifuged at 14,000 x g for 20 seconds. The filtrate was removed and another 500 μ L of the washing buffer was added. After centrifugation at 14, 000 x g for 2 minutes, the spin filter was inserted into

new collection tube and 100 μL of dd- H_2O was added and incubated at room temperature for 1 minute. The plasmids were purified in the filtrate after centrifugation at 14,000 x g for 1 minute and stored at $-20\text{ }^\circ\text{C}$ until being used.

Polymerase Chain Reaction (PCR)

To amplify and clone the *pyrB* and mutagenized *pyrB* gene, PCR was performed. The PCR reaction contained the following in a 50 μL reaction volume: 2 μL of template DNA (about 1 μg), 1 μL of forward and reverse primer (about 0.03 nmol each), 2 μL of 10 mM dNTP, 5 μL of polymerase buffer. The final volume to 50 μL was adjusted by the amount of dd- H_2O . The polymerase was added last. In the normal cloning procedure, Vent polymerase was used and in the mutagenesis procedure, Pfu polymerase was used. The PCR reaction cycle was performed in Programmable Thermal Controller from MJ. Research, INC. The template DNA was denatured at 95°C for 5 minutes and the reaction entered the 30 cycles of following condition: 5 minute of denaturation at 95°C , 30 seconds of annealing at 5°C below of lower melting point primer, and 90 seconds of polymerization. After finishing 30 cycles, the reaction had 5 minutes extension of polymerization to complete the reaction. Then amplified DNA was stored in -20°C until being used. Before cloning, these DNAs were run on electrophoresis. Then cleaned DNA was extracted by Sephaglas Bandprep Kit (Phamacia Biotech) as mentioned earlier.

Cloning of the *pyrB* Gene from *B. cepacia* into Vector pUC18

In order to study the structure and the enzyme kinetics, the ATCases of *B. cepacia* were intended to be purified. As a first step of purification, the *pyrB* gene encoding ATCase from *B. cepacia* was cloned into vector pUC18 (Fig 10). The chromosomal DNA of *B. cepacia* was achieved by the modified method described by Berns & Thomas Jr.. The *pyrB* gene was amplified by standard polymerase chain reaction (PCR). The primers of PCR were designed based on the sequence (Table 2), which was accomplished by Dr. M.A. Farinha. To the end of forward primer (PYRB-F), *Bam*HI site was added, and the end of reverse primer (PYRB-R), *Eco*RI site was added. For the PCR of *pyrB* gene of *B. cepacia*, 63°C of annealing temperature was used for these primers. The 1.3 kb amplified *pyrB* gene was cleaned and purified by agarose gel using the Sephaglas Bandprep Kit (Pharmacia Biotech). This gene and the pUC18 plasmid were restricted by *Eco*RI and *Bam*HI enzyme and purified by above mentioned method. Then the *pyrB* gene was ligated to the pUC18 plasmid as amount ratio of 3 to 1 and the resulting plasmid, pSKBB18 (Fig 11), was 4.1kb in size and ampicillin (Amp) resistant. Sequencing was performed by Lonestar Laboratory in Houston, Texas. Sequence was analyzed using PC-gene software and homology was searched through the on-line NCBI-BLAST facility.

Primer	Sequence (5' – 3')	Relevant property	Restriction site
PYRB-F	TTT <u>GGATCC</u> ACCGTTC CCC CAGCAAGCCTTCCTC	Outer primer used to amplify <i>pyrB</i> gene for cloning into pUC18 (1300 bp)	<i>Bam</i> HI
PYRB-R	TTT <u>GAATTC</u> AAATCGACGCCGTGAAACACCGC	Inner primer used to amplify <i>pyrB</i> gene for cloning into pUC18 (1300 bp)	<i>Eco</i> RI
PYRBA-F1	TTT <u>GGATCC</u> ACCGTTC CCC CAGCAAGCCTTCCTC	Outer primer used to amplify the first fragment of mutagenized <i>pyrB</i> gene (Ser74 to Ala74) in site-directed mutagenesis by overlap extension (220 bp)	<i>Bam</i> HI
PYRBA-R1	GTTATCTACGGCTTGCGTATA	Inner primer used to amplify the first fragment of mutagenized <i>pyrB</i> gene (Ser74 to Ala74) in site-directed mutagenesis by overlap extension (220 bp)	N/A
PYRBA-F2	TATACGCAAGCCGAAGATAACCAAGGG	Outer primer used to amplify the second fragment of mutagenized <i>pyrB</i> gene (Ser74 to Ala74) in site-directed mutagenesis by overlap extension (1,180 bp)	N/A
PYRBA-R2	TTT <u>GAATTC</u> AAATCGACGCCGTGAAACACCGC	Inner primer used to amplify the second fragment of mutagenized <i>pyrB</i> gene (Ser74 to Ala74) in site-directed mutagenesis by overlap extension (1,180 bp)	<i>Eco</i> RI
PYRBN-F1	TTT <u>GGATCC</u> ACCGTTC CCC CAGCAAGCCTTCCTC	Outer primer used to amplify the first fragment of mutagenized <i>pyrB</i> gene (Ser74 to Arg74) in site-directed mutagenesis by overlap extension (220 bp)	<i>Bam</i> HI
PYRBN-R1	TTGGTTATCTACTCTTTGCGTATA	Inner primer used to amplify the first fragment of mutagenized <i>pyrB</i> gene (Ser74 to Arg74) in site-directed mutagenesis by overlap extension (220 bp)	N/A
PYRBN-F2	TATACGCAAAGAGTAGATAACCAAGGG	Outer primer used to amplify the second fragment of mutagenized <i>pyrB</i> gene (Ser74 to Arg74) in site-directed mutagenesis by overlap extension (1,180 bp)	N/A
PYRBN-R2	TTT <u>GAATTC</u> AAATCGACGCCGTGAAACACCGC	Inner primer used to amplify the second fragment of mutagenized <i>pyrB</i> gene (Ser74 to Arg74) in site-directed mutagenesis by overlap extension (1,180 bp)	<i>Eco</i> RI

Table 2. PCR primers used in this study. Primers were purchased from IDT. Incorporated restriction sites are underlined.

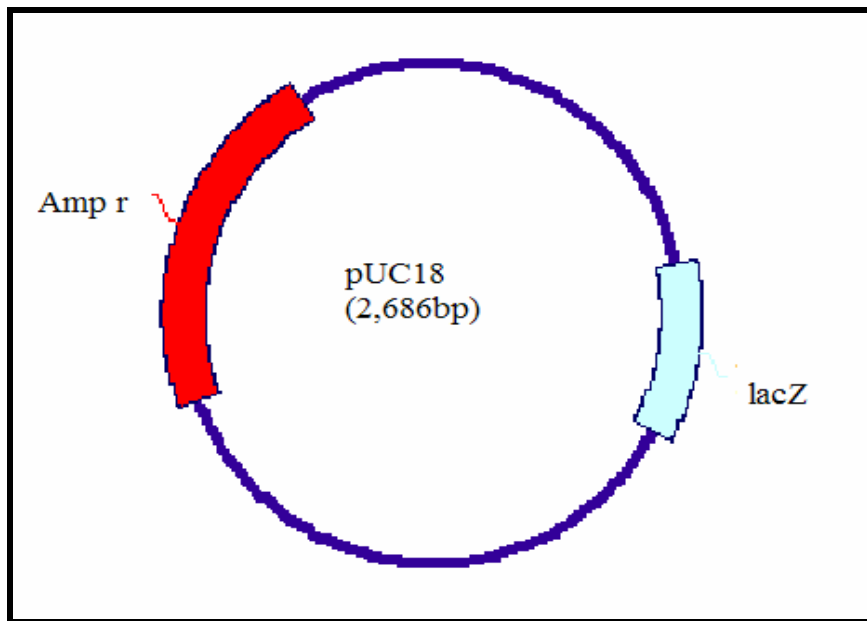


Fig 10. pUC18 vector plasmid.

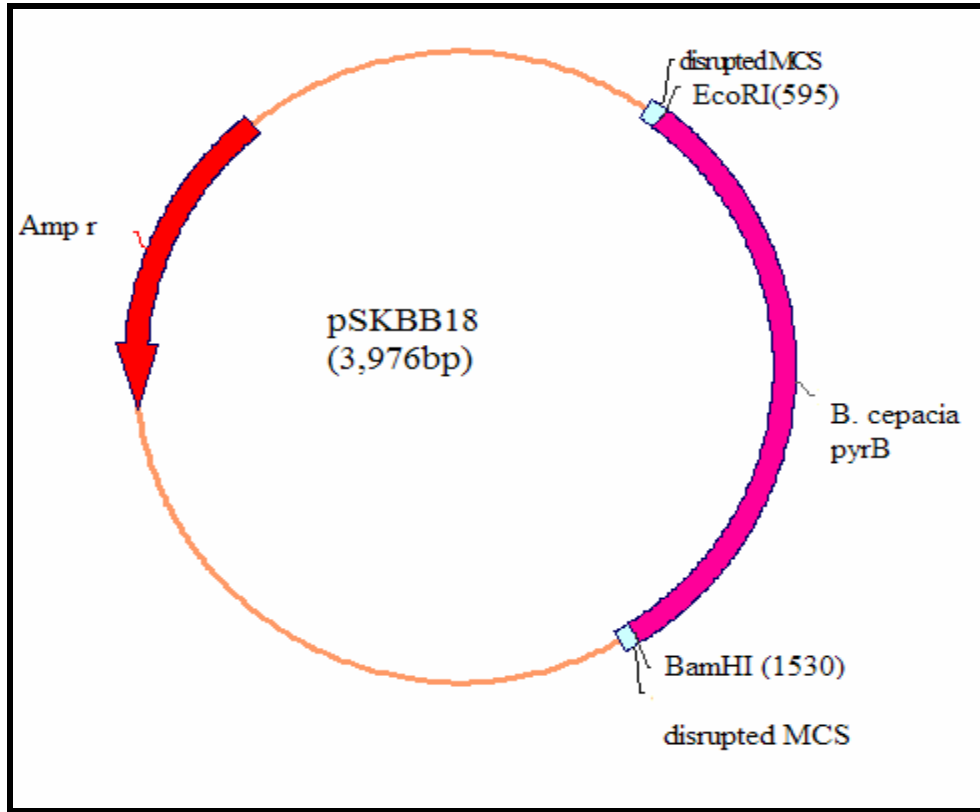


Fig 11. pSKBB18 contains the *pyrB* gene from *B. cepacia* on plasmid pUC18.

Complementation Test of *pyrB* Gene in TB2 Cell

To check the expression of *pyrB* gene, the complementation test was performed with TB2 cell. As shown in Table 1, the TB2 cell is an ATCase deficient *E. coli*. TB2 was made competent cell and the pSKBB18 plasmid was transformed into TB2 cell by heat shock. The transformants were plated on LB plate containing Amp (100 µg/mL) and incubated at 37°C overnight. The next day, the emerging colonies were patched on to a LB plate containing 100 µg/mL of Amp again and incubated at 37°C overnight. Colonies on plate were patched onto Ecmm plate containing 0.2% glucose and 50 µg/mL of uracil, and onto Ecmm plate containing 0.2% glucose without uracil. Colonies that grew on Ecmm plates without uracil were selected because these cells contained the *pyrB* gene of *B. cepacia* and grew in Ecmm without uracil by the expression of *pyrB* gene and thus complementating. This TB2 cell designated as TB2SKBB18 was inoculated into 50 mL Ecmm broth and incubated at 37 °C and the cell extracts were prepared as before. The expression of ATCase was confirmed by the ATCase activity gel and conventional activity assay.

Purification of ATCase

Purification of ATCase was carried out by the glutathione S-transferase (GST) gene fusion system. The GST gene fusion system is an integrated system for the expression, purification and detection of fusion proteins produced in *E. coli*. The pGEX2T plasmid vector (4.8kb) (Fig 12, 13) is designed for inducible, high level

intracellular expression of genes as fusions with *Schistosoma japonicum* GST in this system. GST occurs naturally as a 26 kDa protein that can be expressed in *E. coli* with full enzymatic activity. Fusion proteins are easily purified from bacterial lysates by affinity chromatography using Glutathione Sepharose 4B. Cleavage of the desired protein from GST is achieved using site-specific protease whose recognition sequence is located immediately upstream from the multiple cloning site on the pGEX plasmid. The pGEX2T vector plasmid has a *tac* promoter for chemically inducible and high level expression. It contains an internal *lacI* gene for use in any *E. coli* host. In addition, this plasmid has very mild elution conditions for release of fusion proteins from the affinity matrix, thus minimizing effects on antigenicity and functional activity.

Subcloning of the *pyrB* Gene of *B. cepacia* in pSKBB18 into pGEX2T Plasmid

The first digestion of *B. cepacia pyrB* gene from pSKBB18 restricted by *EcoRI* and *BamHI* enzyme was purified by agarose gel and released a 1.3 kb size of *pyrB* gene. The pGEX2T plasmid was also restricted by *EcoRI* and *BamHI* enzyme and purified by agarose gel. Then 1.3 kb of the *pyrB* gene was ligated to the pGEX2T as amount ratio of 3 to 1 and the resulting plasmid, pSK2T (Fig 14), was 6.1 kb and Amp resistant. Next 20 ng of pSK2T was transformed into a protease deficient *E. coli* BL21 host cell. In the GST Gene Fusion System, *E. coli* BL21 is the recommended host cell strain. The transformant *E. coli* BL21 was selected on LB plate with Amp (100 µg/mL) and cultivated overnight in LB broth with Amp (100 µg/mL) and stored at -80°C with 12 % sterile glycerol until being used.

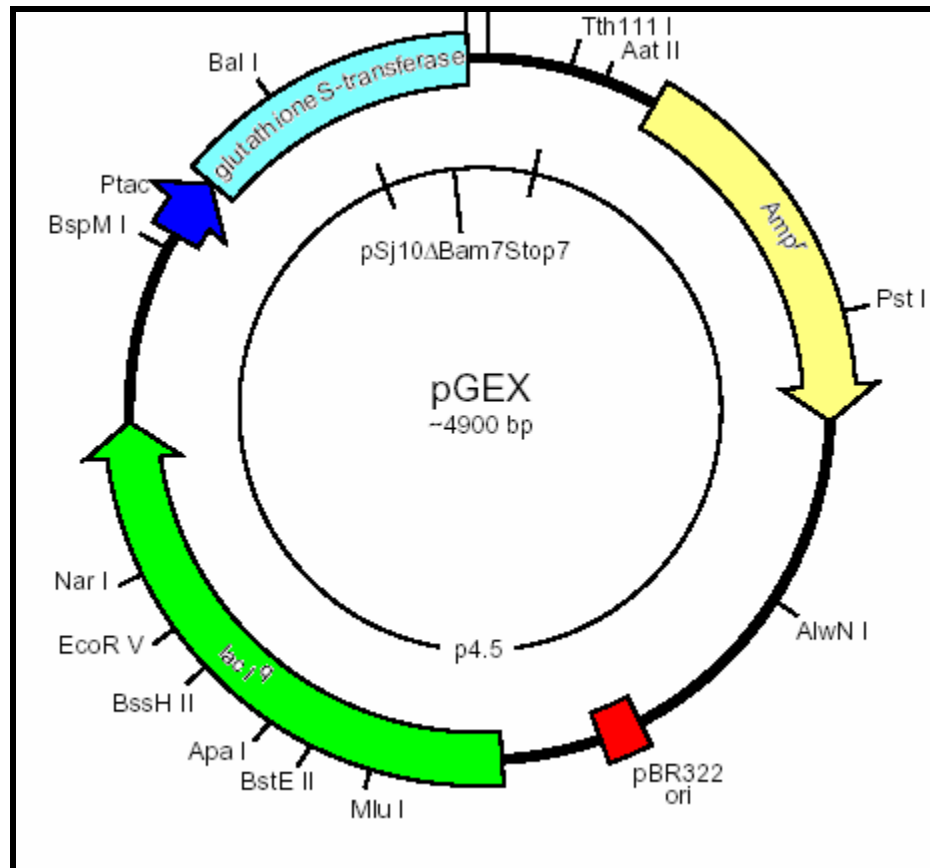


Fig 12. pGEX plasmid

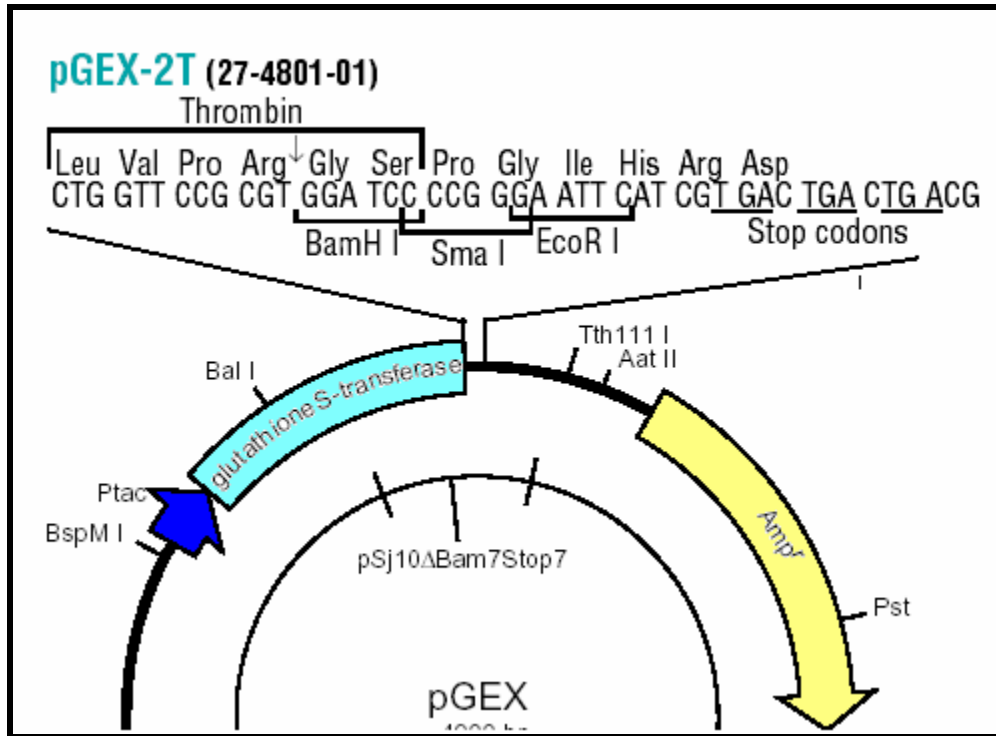


Fig 13. MSC site in pGEX2T plasmid

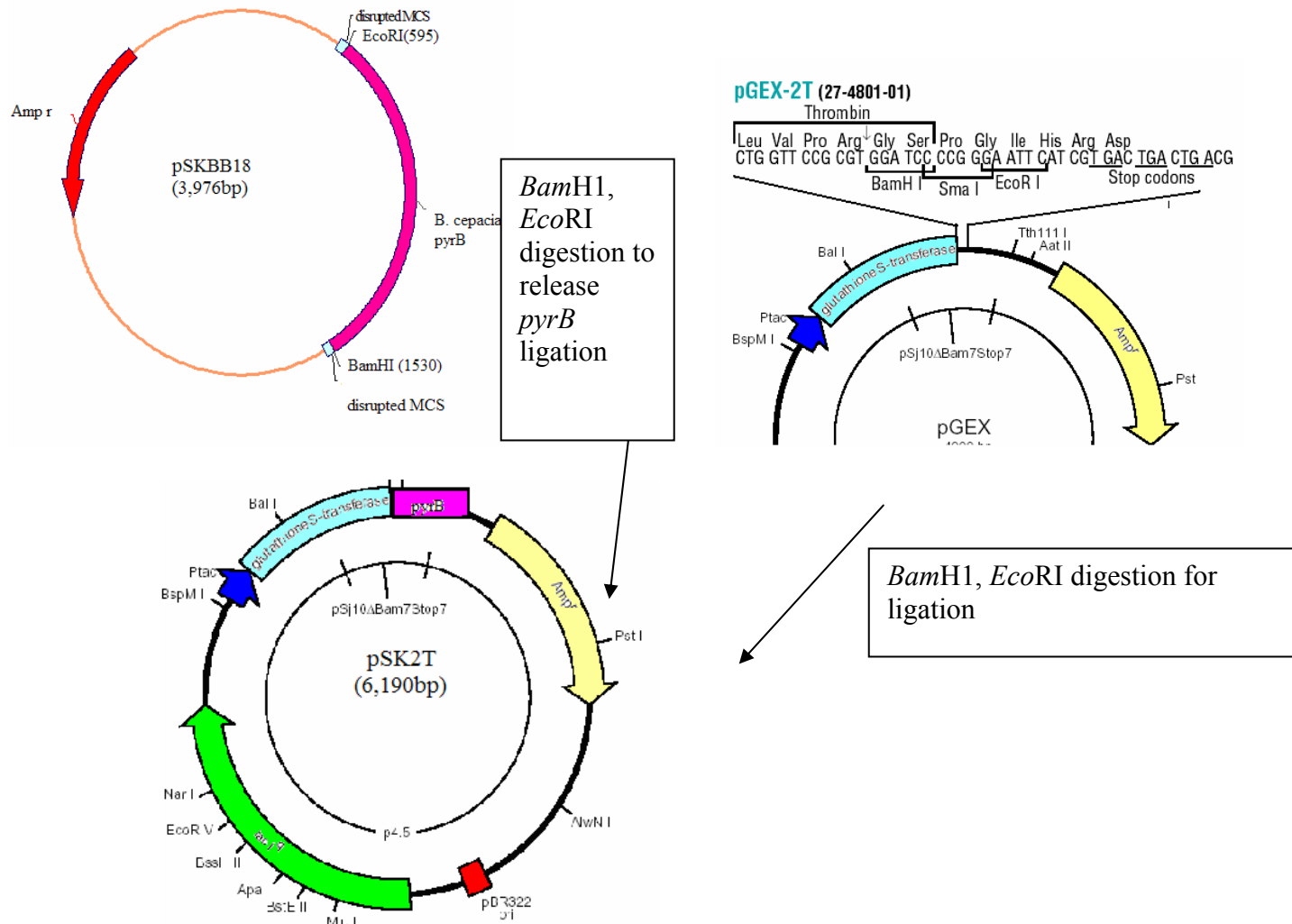


Fig 14. Construction of pSK2T plasmid containing GST and *B. cepacia pyrB* fusion gene

Purification of ATCase Enzyme by GST Gene Fusion System

A 200 μ L of *E. coli* BL21 containing pSK2T was inoculated in 20 mL LB broth with Amp (100 μ g/mL) and cultivated overnight. The next day, this overnight culture was transferred in 2 L LB broth with Amp (100 μ g/mL) and incubated at 37°C shaker for 4 hours until the culture reached the OD₆₀₀ of about 0.8. In order to induce the overexpression, 0.5mM (final concentration) of isopropyl- β -D-thiogalactoside (IPTG) was added and the cells were incubated for 3 hours on a 37°C shaker. Then the cells were harvested using a 500 mL centrifugal bucket at 6,000 x g for 15 minutes in 4°C. After removing the supernatant, the cell pellet was resuspended with 50 mL cold PBS buffer, pH 7.3. To prevent the excessive viscosity when cells were broken, 37.5 μ g/mL (final concentration) of DNase were added to the resuspension solution. Then cells were broken by means of a French pressure cell at 2000 psi. To maximize the solubility of protein, 0.1 % (final concentration) Triton X-100 was added. In addition, 5 mM DTT was added to increase the binding of some fusion proteins to the Glutathione Sepharose 4B resin. To prevent a partial degradation by serine protease, 1 mM of phenylmethylsulfonyl fluoride (PMSF) was also added. This mixture was stirred gently at 4°C overnight. The following day, the mixture was transferred to the clean 50 mL centrifuge tube and the cell debris was removed at 15,000 x g for 30 minutes. Then the clear supernatant was transferred to a 50 mL conical tube and used for protein purification. This supernatant lysate had to be used on the same day, otherwise precipitant was formed. The glutathione sepharose beads were stored at 20% ethanol. Before being used, they had to be washed with 1X PBS buffer. A 1.33 mL of bead slurry

(1 mL bed volume) was transferred to a 15 mL conical tube. This bead slurry was centrifuged at 1,750 x g for 5 minutes in 4°C. After removing the supernatant, then the beads were washed with 10 mL ice cold 1X PBS and centrifuged as above. This step was repeated twice and the beads were transferred to 50 mL conical tube.

After the beads were ready, prepared cell lysates were transferred to the washed beads and incubated with rocker at room temperature for 1 hour, then centrifuged at the same condition as above. The supernatant was carefully transferred to the fresh tube, labeled as “Flow thru”, and stored at -20 °C to be checked. Then the beads were washed with 10 mL of 1X PBS gently and centrifuged at the same condition as above. This step was repeated 3 times and each supernatant was transferred to the new tube and labeled as “Wash 1, 2, 3, and 4” in order. After this step, the bead- bound fusion proteins were ready to be eluted.

The fusion proteins were eluted in two different ways; by thrombin (Fig 15) or by reduced glutathione (Fig 16). The ATCase was eluted from the fusion protein directly by thrombin. The thrombin cut the fusion site between GST and ATCase. Thrombin was provided in lyophilized form. The thrombin solution was prepared by adding 500 µL of cold 1X PBS buffer. 50 µL of thrombin (50U) solution were mixed with 950 µL of cold 1X PBS buffer and added to the beads. This mixture was incubated in rocker for 2~16 hours at room temperature and centrifuged as above. The supernatant was carefully transferred to new tube and labeled as “Elute 1”. This step was repeated once and the eluted protein was labeled as “Elute 2”. After eluted, all protein was immediately stored at -80°C with glycerol.

The fusion proteins were also eluted by reduced glutathione. The reduced glutathione cut the binding site of GST to the bead then the fusion proteins (GST-ATCase) were eluted. The ice cold 5 mL of 10 mM reduced glutathione was added to the bead and incubated in rocker at room temperature for 15 minutes. Then this mixture was centrifuged at the same condition as above and the supernatant was carefully transferred to new tube and labeled as “RE 1”. This step was repeated 3 times and the tube was labeled as “RE 2, 3, and 4” in order. Before being cut by the thrombin, 10 μ L of each elute was run on 10% SDS-PAGE to check the presence of fusion protein. The SDS-PAGE was done by the previously mentioned method. Then fusion proteins were pooled together and dialyzed by 300X volume of 1X PBS buffer at 4 °C overnight. The dialyzed fusion proteins were transferred to the new 15 mL conical tube and 50U of thrombin were added to cut the fusion part of GST and ATCase. This tube was incubated at room temperature in rocker for 2 to 16 hours. The next day, thrombin-cut protein was stored in glycerol at -80°C until being used.

Purification of ATCase by Anion Exchange Column Chromatography

The purified ATCases from direct cut by thrombin contained thrombin in eluted tube. The purified ATCases from two- step cut by reduced glutathione and thrombin also contained thrombin, thrombin, and reduced glutathione. To further purify, ATCases were isolated by anion exchange column chromatography again. The eluted ATCase enzymes from GST fusion system were dialyzed in 300X volume of 1X PBS buffer at 4°C overnight. 1 mL of dialyzed ATCase was loaded onto a 1 mL DEAE Sepharose column

(Pharmacia) and washed three times with 1 mL of ATCase buiffer each time. Then the ATCases were eluted using linear gradient from 0 mM NaCl to 1000 mM NaCl with 1 mL collection three times for each gradient. The ATCase contained fractions were detected by 10 % SDS-PAGE. After detection, the ATCase containing fractions were collected and dialyzed 300X volume of 1X PBS buffer at 4°C overnight and stored at -80°C until being used for assay. The protein concentration of ATCase was determined by Bradford assay using lysozyme as standard.

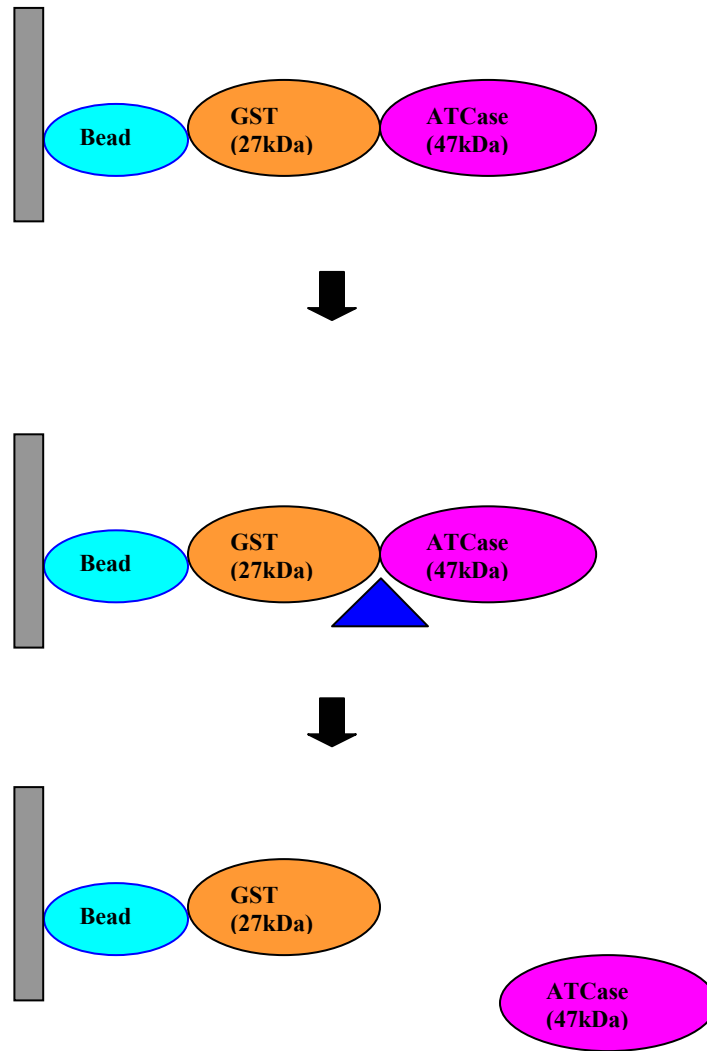


Fig 15. Elution method 1: Elution by thrombin

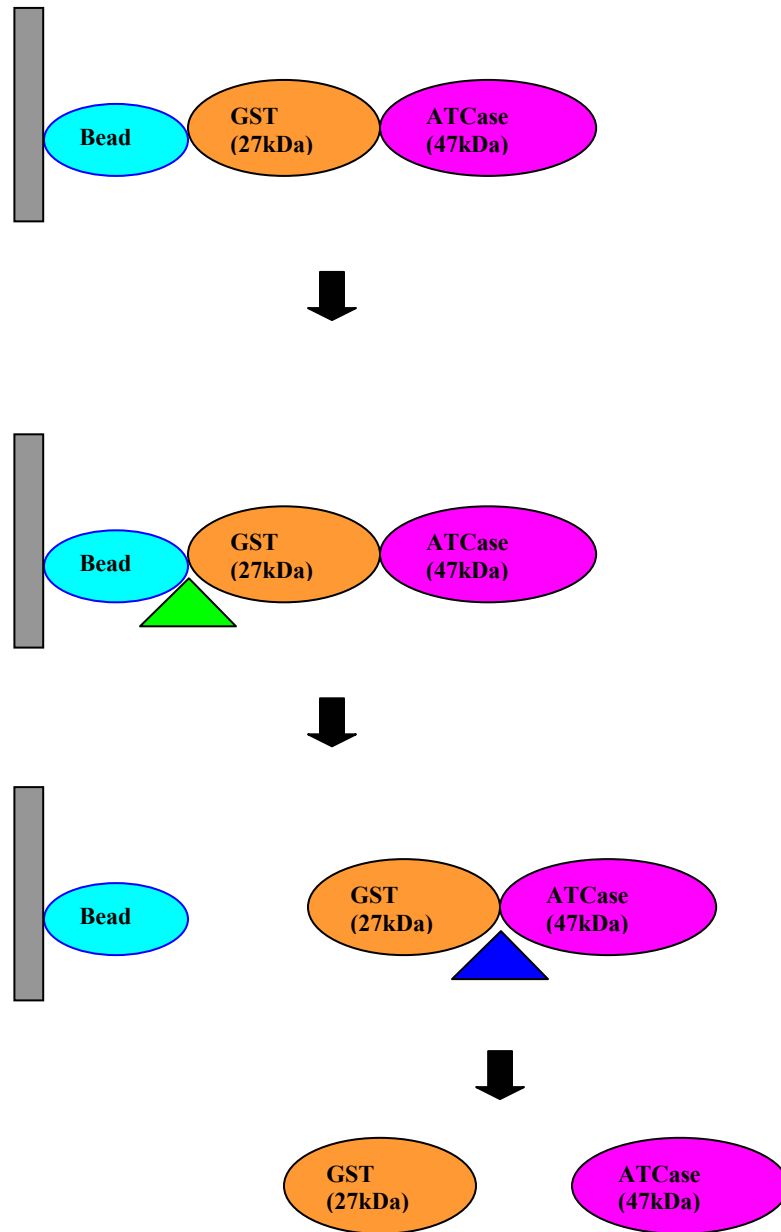


Fig 16. Elution method 2: Elution by reduced glutathione and thrombin

Sodium Dodecyl Sulfate Polyacrylamide Gel Electrophoresis (SDS-PAGE)

SDS is an anionic detergent, which denatures proteins by binding or wrapping around the protein backbone. The method denatures the protein into its individual subunits and thus separates them based on their molecular weight. SDS binds specifically to proteins and confers a negative charge on them. It is necessary to reduce the disulfide bridges in proteins so that they would adopt a random coil configuration. This allows for the proteins to be separated based on molecular weight. Therefore separation of proteins using SDS-PAGE is determined by molecular weight rather than its intrinsic electrical charge. A 10% SDS polyacrylamide separating gel with a 4% stacking gel was used to analyze the samples. The apparatus used to conduct the electrophoresis was the Mini-Protean II™ chamber (Bio-Rad). The gel was prepared by first pouring a 10% separating gel, which contained 1.67 mL of the stock solution of acrylamide (30% w/v acrylamide and 0.8 % w/v bis-acrylamide in ddH₂O), 1.25 mL of Buffer B (1.5 M Tris-HCl, pH 8.8, 0.4% w/v SDS in ddH₂O), 2.08 mL of ddH₂O, and 50 μL of 10% ammonium persulfate . The gel began to polymerize with the addition of 5 μL of N, N, N' N' - tetramethylethylenediamine (TEMED). The mixture was gently inverted and poured into the assembled apparatus using a pasteur pipet. A space of 2 cm was left at the top to pour the stacking gel. The gel was overlaid with *n* - butanol as before. The gel was allowed to polymerize for approximately 20 minutes after which the stacking gel was prepared. The stacking gel contained 0.27 mL of Solution A, 0.4 mL of buffer C (0.5 M Tris, pH 6.8, 0.4% w/v SDS) and 0.92 mL ddH₂O, ammonium persulfate (0.01 g) and 5 μL of TEMED. A 10 well comb was inserted and the gel was allowed to polymerize for

15 minutes. The gel was placed into the apparatus and the tank filled up with denaturing gel running buffer (25 mM Tris, 192 mM glycine and 0.1% SDS w/v, pH 8.3). The sample was mixed at a ratio of 4:1 with the gel loading dye (60 mM Tris-HCl, pH 6.8, 25% glycerol v/v, 2% SDS w/v, 14.4 mM β -mercaptoethanol, 0.1% Bromophenol Blue) in a sterile microfuge tube. The samples and the standards were boiled for 5 minutes and cooled on ice. The samples and the pre-stained low range SDS standards were loaded onto the gel and electrophoresed for 90 minutes at 100 V. The proteins were stained with Coomassie Blue staining solution (45% methanol v/v, 10% acetic acid v/v, 0.1% Coomassie Brilliant Blue R-250 w/v in ddH₂O) for 10 minutes with gentle rocking. The gel was destained with a solution of 10% methanol v/v and 10% glacial acetic acid v/v in ddH₂O for 3 hours.

N-terminal Sequencing of the Purified ATCase Enzyme

20 μ L (100 μ g) of purified ATCase was run on 10 % SDS-PAGE and subsequently electrotransferred onto PVDF membrane for 2 hours in cold chamber. The PVDF membrane was stained for 3 minutes with coomassie brilliant blue without acetic acid, destained with a destaining solution without acetic acid, and gently dried. After being sealed in a plastic bag, this membrane was sent to the UC Davis Protein Structure Laboratory for N-terminal amino acid sequence determination by automated Edman degradation.

Aspartate Transcarbamoylase (ATCase) Assay

ATCase activity was measured by quantifying the amount of carbamoylaspartate (CAA) produced in 20 min at 30°C. This was accomplished using the method of Gerhart and Pardee (1962), with modification, using the color development procedure of Prescott and Jones (1969). This assay was performed using a micro titer plate. The assay mixture contained the following in a 100 μ L reaction volume: 4 μ L of Tri-buffer pH 9.5 (51mM diethanolamine, 51 mM N-ethylmorpholine and 100 mM MES, adjust pH to 9.5; Ellis & Morrison, 1982), 10 mM potassium aspartate (pH 9.5), 2 mM dilitium carbamoylphosphate and cell extract or purified enzyme, usually 3 to 10 μ L. The final volume was adjusted to 100 μ L with dd-H₂O. Assay wells containing all components, except for carbamoylphosphate, were prepared in advance and pre-incubated at 30°C for 5 minutes. The reaction was initiated by the addition of carbamoylphosphate and incubated at 30°C for 30 minutes. Then the reaction was stopped by the addition of 100 μ L of stop reaction buffer (Prescott & Jones, 1969). The micro titer plate was in a 65°C heating block under fluorescent light for one hour. The plates were taped to prevent loss of volume due to evaporation. The stop reaction buffer was made by two parts of 5 mg/mL antipyrine in 50 % sulfuric acid (v/v) mixed with one part of 8 mg/ mL of 2, 3-butanedione monoxime in 5 % acetic acid (v/v). This mixture has to be made just prior to use and kept on ice. Then the micro titer plate was allowed to cool in the dark for 10 to 15 minutes and the assay was read at A₄₅₀ by Kinetic Micro Plate reader from Molecular Device Company. The amount of CAA produced was determined using a CAA standard

curve. The standard curve was prepared using the same buffering system and known concentrations of CAA ranging from 0 to 1.0 mM.

Non-denaturing Polyacrylamide Aspartate Transcarbamoylase Activity Gels

A nondenaturing polyacrylamide gel with 4 % stacking gel and an 8 % separating gel was used. The gel was prepared by first pouring the separation gel, which contained 1.33 mL of the stock solution of acrylamide (30% w/v acrylamide and 1 % w/v bis-acrylamide in ddH₂O), 1.25 mL of Buffer B (1.5 M Tris-HCl, pH 8.8), and 2.41 mL of ddH₂O. Ammonium persulfate (0.01g) was added to the mixture. The gel was polymerized with the addition of 5 µl of N, N, N' N' - tetramethylethylenediamine (TEMED). The mixture was gently inverted and poured into the assembled Bio-Rad mini protean II apparatus. A space of 2 cm was left at the top to pour the stacking gel. The gel was overlaid with *N*-butanol to exclude oxygen, which inhibits the polymerization. The *N*-butanol also helped to flatten the top of separating gel. This set was allowed to polymerize for approximately 30 minutes after which the stacking gel was prepared. The stacking gel contained 0.27 mL of acrylamide, 0.4 ml of buffer C (0.5 M Tris, pH 6.8) and 0.92 mL ddH₂O, ammonium persulfate (0.01g) and 5µL of TEMED. A 10 well comb was inserted and the gel was allowed to polymerize. 20 µL of sample was mixed with 5µL of 5X loading buffer (312.5 mM Tris, 50% v/v glycerol, and 0.05% w/v bromophenol blue in ddH₂O). The samples were loaded onto the gel. The chamber was filled with gel running buffer (25 mM Tris, 192 mM glycine in ddH₂O) and electrophoresis was carried out 100 V for 1 hour 40 minutes at room temperature.

Activity Stain of the ATCase in Non-denaturing Polyacrylamide Gels

The gels were stained specifically for ATCase activity by the method described by Bothwell (1975) as modified by Kedzie (1987). The principle of this method is that when ATCase catalyses the reaction between carbamoylphosphate and aspartate to produce carbamoylaspartate, an inorganic phosphate is generated. This phosphate group reacts with lead nitrate to form a white precipitate. A modified version of the above method by Kedzie (1987) was performed. The gels were placed in 250 mL of cold histidine buffer (50mM, pH 7.0) for 10 minutes. Then freshly made 5 mL of 1 M aspartate and 10 ml of 0.1 M carbamoylphosphate was added and the gels were incubated at room temperature for 5 minutes on a rocking shaker. The reactants were removed by rinsing the gel in 100-200 mL of cold ddH₂O for three times. Lead nitrate at a concentration of 3mM was added to another 250 mL of histidine buffer, pH 7.0, which was then poured onto the gel. After 10 minutes, the lead nitrate was removed by washing three times in cold ddH₂O. ATCase activity was observed at the site of lead phosphate precipitation. The gel was left overnight at 4 °C to increase the visibility of the bands, and then stained with 3% sodium sulfide for 3 minutes and washed three times with ddH₂O to convert the white lead nitrate to black lead sulfide. The gels were soaked in 10% glycerol and dried to preserve them.

Enzyme Kinetics of ATCase of *B. cepacia*

The purified ATCases were assayed for ATCase activity by measuring the amount of carbamoylaspartate (CAA) produced at 20 minutes at 37°C. The method used was the

color reaction described by Prescott & Jones, 1969. ATCase assays were performed to determine the V_{max} , and K_M . A tribuffer system (0.05 M MES, 0.1 M diethanolamine, and 0.051 M N-ethymorpholine) was used. The assay was conducted at pH 9.5 in a microtiter plate. Aspartate was varied from a final concentration of 0.5 mM to 6 mM and carbamoylphosphate was kept at a concentration of 5 mM. The total volume of the assay was 200 μ L. A blank control containing all ingredients minus the enzyme was used. This reading was then subtracted from the final reading for the experimental reaction. The assay reaction plate was preincubated at 37°C for 2 to 3 minutes. The reaction was initiated with the addition of carbamoylphosphate. At 20 minutes the reaction was stopped with the addition of 100 μ L of stop mix (2 parts antipyrine (5 mg/mL) in 50% sulfuric acid and 1 part monoxime (8 mg/ml) in 5% acetic acid). After the addition of the stop mix clear tape was applied to the top of the wells to prevent the evaporation of the reaction mixture. The color was developed at 60°C in a waterbath. The assay was read at 450 nm in a kinetic microplate reader from Molecular Devices. Velocity-substrate curves were generated by plotting the specific activity of the enzyme (μ mol CAA/min/ μ g of protein). The protein concentration was measured by the method described by Bradford (1976) with lysozyme as the standard. The μ mol produced was calculated by generating a CAA standard curve.

Site-specific Mutagenesis on *pyrB* Gene by Overlap Extension

To confirm the atypical site-specific proteolysis between Ser74 and Val75 residues, site-directed mutagenesis by overlap extension was performed. Two

mutagenesis experiments were carried out. The one converted the amino acid sequence from Ser74 to Arg74, and the other one converted Ser74 to Ala74. This mutagenesis was performed by the method of Aiyar from site-specific mutation by overlap extension (Fig 18). Two sets of forward and reverse primer were used in this method (Table 2). Two steps of PCR were used. In order to convert Ser74 to Arg74, the forward primer (PYRBN-F1) was designed at start codon of *B. cepacia pyrB* gene and the reverse primer (PYRBN-R1) was designed from the auto-proteolysis site with changed sequence. For the second set, the forward primer (PYRBN-F2) was designed from the auto-proteolysis site with changed sequence and the reverse primer (PYRBN-R2) was designed at the stop codon of *B. cepacia pyrB* gene. The reverse primer of first set and forward primer of second set were overlapped with changed base at proteolysis site of *pyrB* gene and produced the site specific mutagenesis. In order to convert Ser74 to Ala74, two sets of primers also used. The first set had primers of PYRBA-F1 and PYRBA-R1, and the second set had primers of PYRBA-F2 and PYRA-R2. The first step of PCR with two sets of primers was performed separately using *B. cepacia* chromosomal DNA as template. The conditions of PCR were the same as the previously mentioned method except the annealing temperature and the polymerase. The first set of PCR had annealing temperature at 63°C but the second set of PCR had annealing temperature at 55°C.

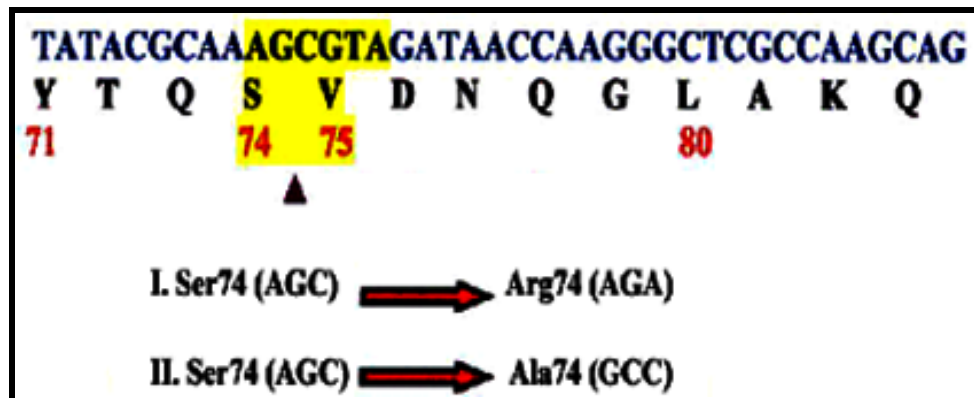


Fig 17. Scheme of mutagenesis of ATCase from *B. cepacia*

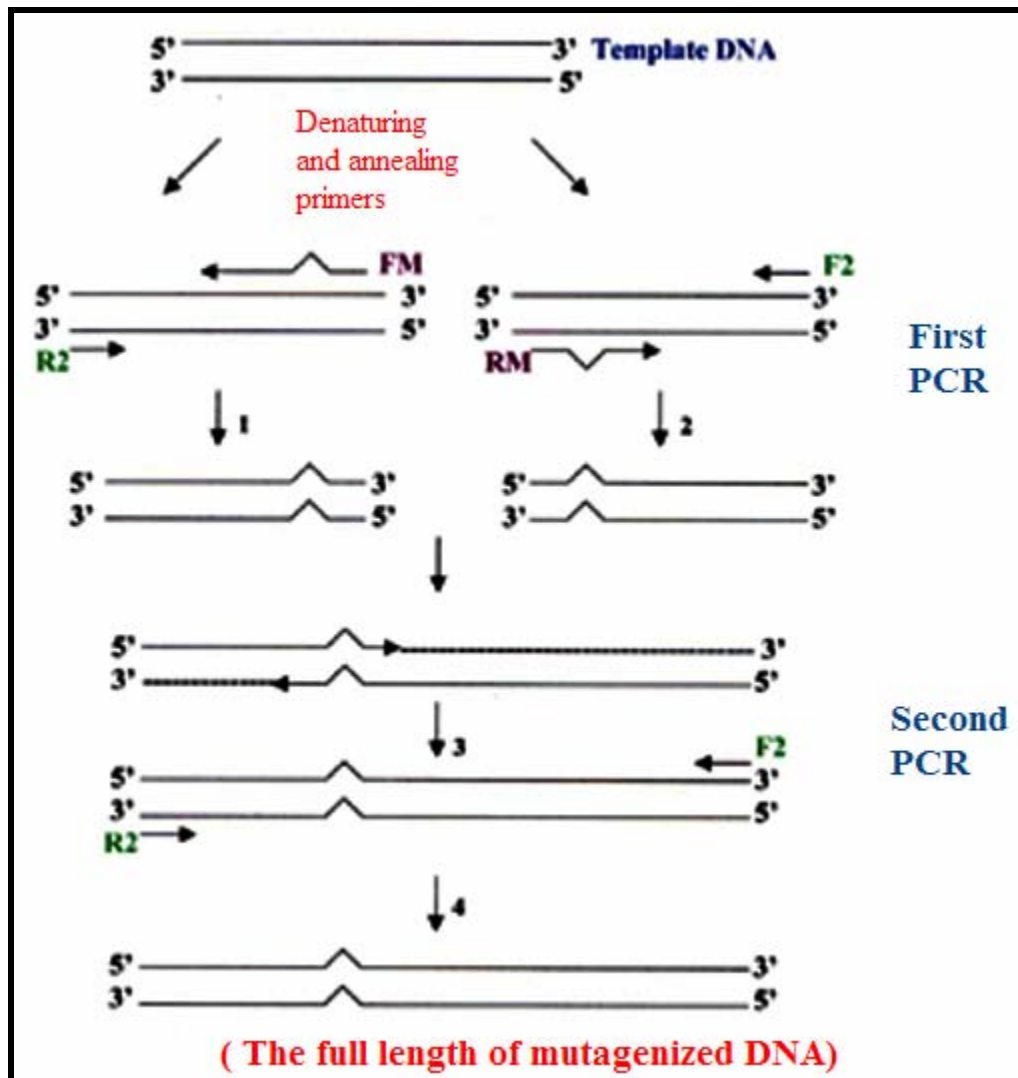


Fig 18. The procedure of Site-specific Mutagenesis on *pyrB* gene by Overlap Extension

Instead of using Vent polymerase, Pfu polymerase was used to have more precise polymerization. The expecting sizes from the first step of PCR were 220 bp from the first set and 1.28 kb from the second set.

To complete the site-directed mutagenesis, second step PCR was used. In this step, primers of PYRN-F1 and PYRN-R2 were used for Ser74 to Arg74, and primers of PYRA-F1 and PYRA-R2 were used for Ser74 Ala74. The PCR products from the first step PCR were used as template DNA and annealing temperature was set as 63°C. The expecting size from the second PCR was 1.3 kb of which had a site specific mutagenesis DNA. These PCR products were restricted by *Bam*HI and *Eco*RI enzyme, and purified by agarose gel, then ligated to the pUC18 plasmid. The pUC18 contained mutagenized *pyrB* (Ser74 to Ala74) was designated as pSKBB18A (Fig 19) and the pUC18 contained mutagenized *pyrB* (Ser74 to Arg74) was designated as pSKBB18N (Fig 20). The sequences of mutagenized *pyrB* were confirmed by Lonestar Laboratory in Houston.

The mutagenized *pyrB* were also excised from these plasmids by *Bam*HI and *Eco*RI enzyme and subcloned to the pGEX2T. The pGEX2T contained mutagenized *pyrB* (Ser74 to Ala74) was designated as pSK2TA (Fig 21) and the pGEX2T contained mutagenized *pyrB* (Ser74 to Arg74) was designated as pSK2TN (Fig 22).

Purification of Site-specific Mutagenized ATCase of *B. cepacia*

The procedure of the purification of site specific mutagenized ATCase from pSK2TA and pSK2TN followed the same procedure of pSK2T.

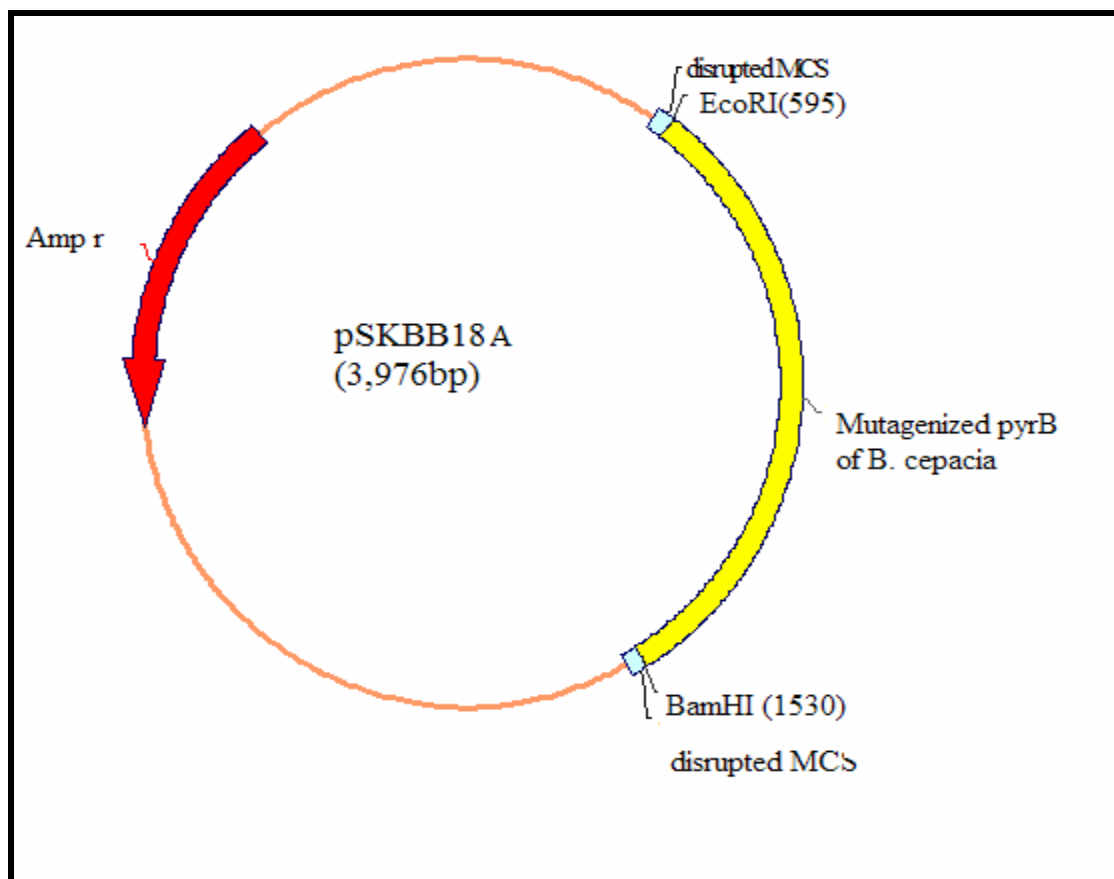


Fig 19. pSKBB18A contains the mutagenized *pyrB* (Ser74 to Ala74) from *B. cepacia* on plasmid pUC18

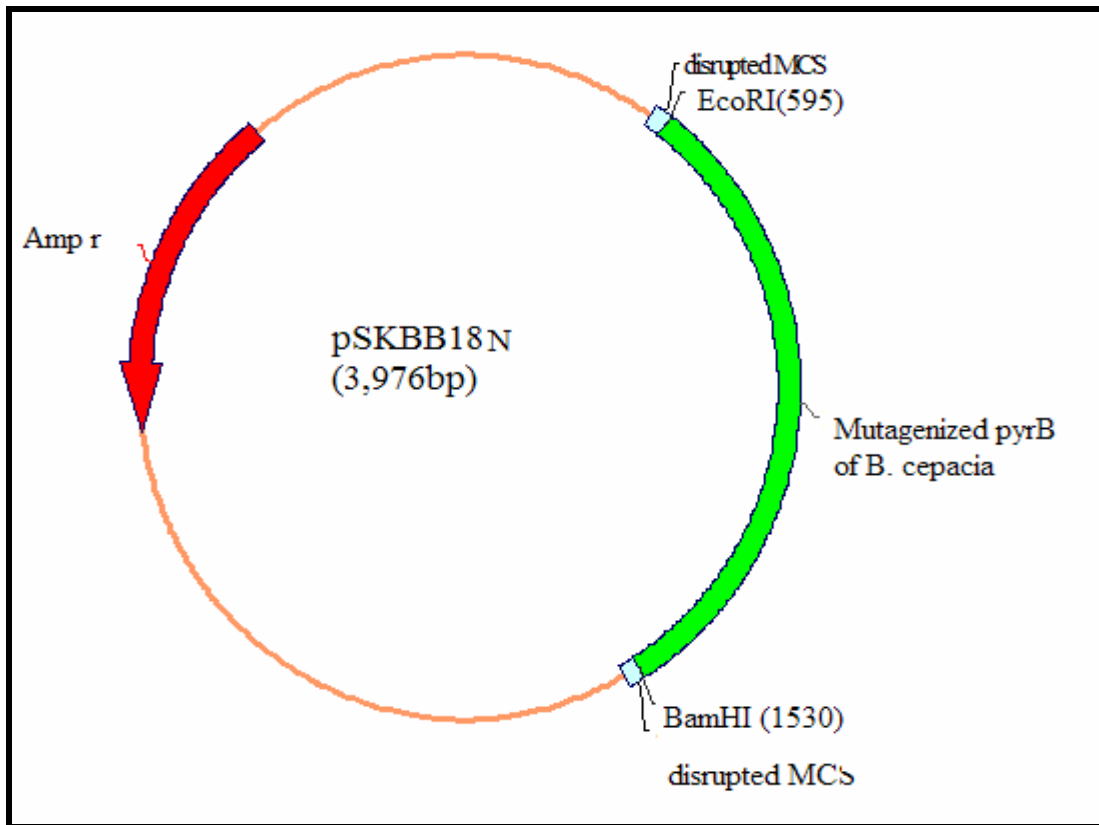


Fig 20. pSKBB18N contains the mutagenized *pyrB* (Ser74 to Arg74) from *B. cepacia* on plasmid pUC18.

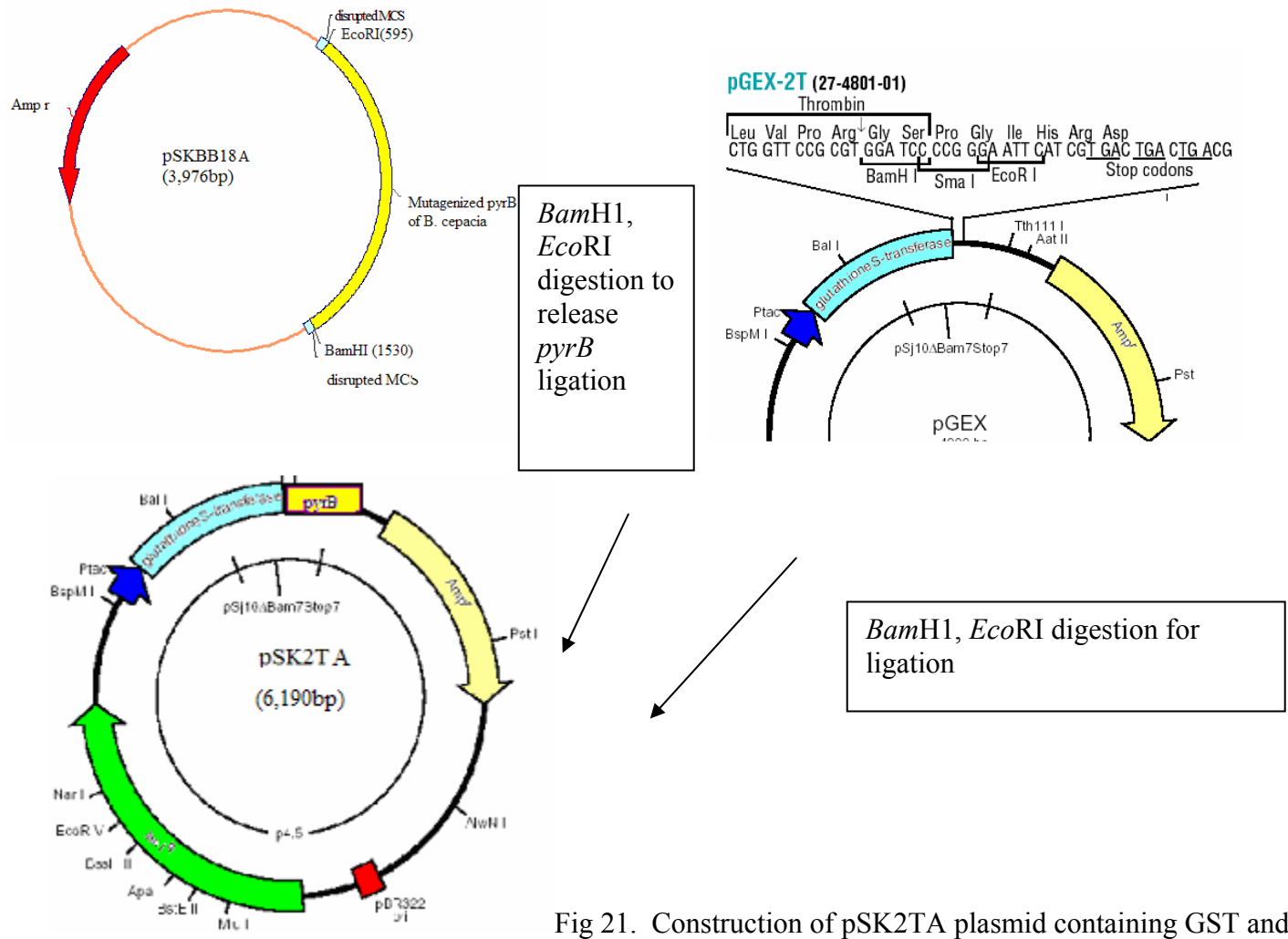


Fig 21. Construction of pSK2TA plasmid containing GST and mutagenized *B. cepacia* pyrB (Ser74 to Ala74) fusion gene

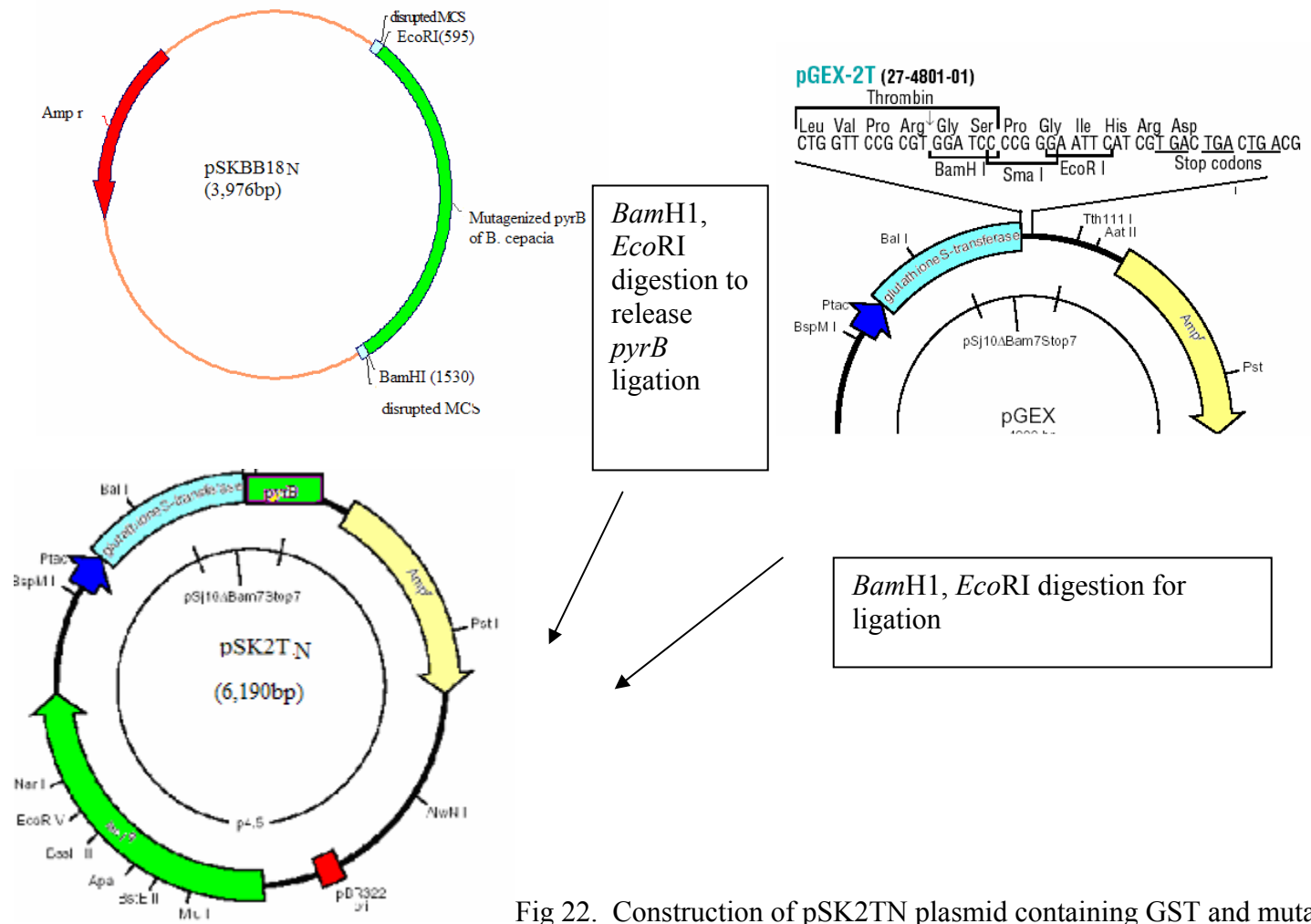


Fig 22. Construction of pSK2TN plasmid containing GST and mutagenized *B. cepacia* pyrB (Ser74 to Arg74) fusion gene

Construction of the *pyrBI*⁻ Gene

The *pyrBI* knocked out (*pyrBI*⁻) strain was constructed by EZ::TN <KAN-1>Tnp Transposome Kit (Fig 23) purchased from Epicentre Technologies. In the reaction, following materials were added: 1 µg of pSKBB18, 2 µL EZ::TN <KAN-1>Tnp Transposome, 1 µL of EZ:TN 10X buffer, 5µL of dd-H₂O, and 1 µL of EZ:TN transposase. This mixture was incubated at 37°C for 2 hours and 1 µL of stop solution was added. After mixed, this solution was incubated at 70°C for 10 minutes. Then 5 µL of the transposition reaction was transformed into chemically competent *E. coli* DH5α by heat shock. Transformants were screened by plating on LB medium containing kanamycin (50 µg/mL). The plasmids of transformants were purified by Minipreps Plasmid Purification kit from Bio-rad Company and pooled together. Then 10 µL of pooled plasmid were transformed into chemically competent TB2 cell by heat shock and plated on LB plate containing kanamycin (50 µg/mL). The next day, colonies on the plate were patched on Ecmm plate containing arginine (50 µg/mL) and LB plate containing kanamycin (50 µg/mL). The colonies appeared on both plates were selected and inoculated on 5 mL LB containing kanamycin (50 µg/mL). After cultured at 37°C overnight, the plasmids were purified by Minipreps Plasmid Purification kit from Bio-Rad Company. Then possible plasmids with *pyrB* gene inserted by transposon were screened and selected by double digestion of *Bam*HI and *Eco*RI and the insertion mutation was confirmed by sequencing (Lonestar Laboratory in Houston). This plasmid was designated as pSKBBX18 (Fig 24).

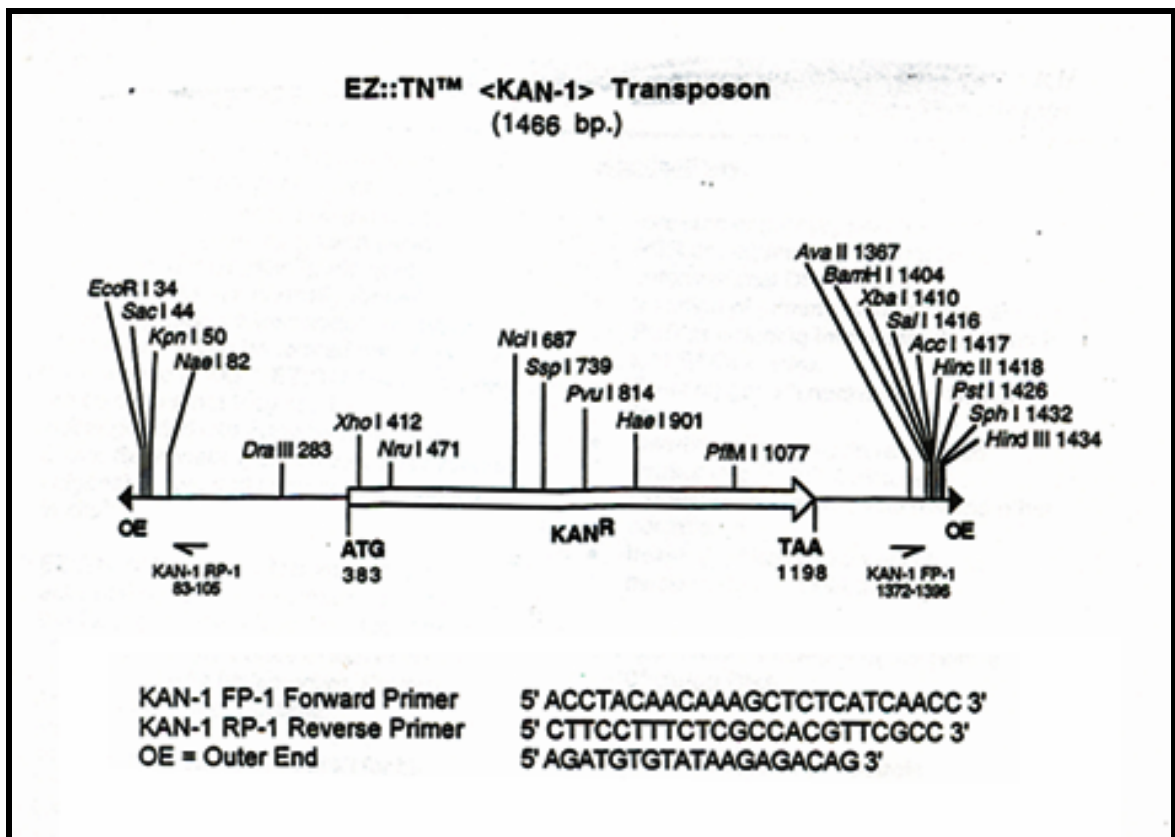


Fig 23. Restriction map and primers of EZ::TN<KAN-1> Transposon (used with permission from Epicentre)

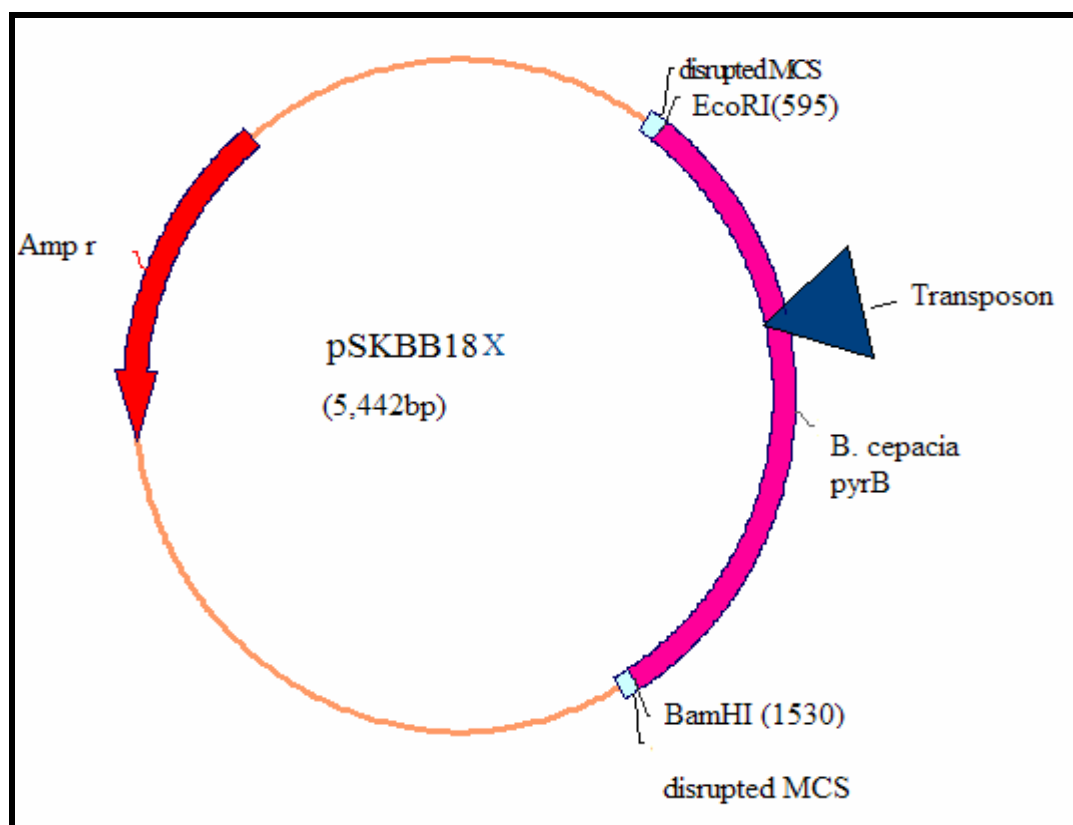


Fig 24. pSKBB18X contains the transposon at the *pyrB* region in pSKBB18 plasmid

Construction of *pyrBI* *B. cepacia*

Recombination of *pyrBI* gene of *B. cepacia* with *pyrB* gene was achieved by Tri-parental mating method (Van Haute). 3 µl of pSKBBX18 was transformed to chemically competent JM109 *E. coli* by heat shock. Then the transformed JM109 was selected by LB plate containing kanamycin (50 µg/mL). In tri-parental mating, 500 µL overnight-cultured *B. cepacia* at 42°C were mixed with 500 µL of overnight-cultured *E. coli* HB101 and 500 µL of overnight-cultured *E. coli* JM109 containing pSKBBX18. The mixed cells were washed 3 times with sterile phosphate buffered saline (pH 7.3) and transferred to a 15 mL tube, which contained 5 mL of 10 mM MgSO₄, and gently mixed. Then this cell mixture was transferred to a 5 mL sterile syringe, which had a Nalgene filter unit containing a 0.45 µm filter. The solution was forced through the filter unit. The apparatus was disassembled and the filter was removed with sterile forceps and placed on an LB agar plate bacteria side up. The plate was incubated at 37°C for 16 to 18 hours. Sterile forceps were used to remove the filter from the LB plate and it was placed into a tube containing 10 mL of 10 mM MgSO₄. The bacteria were resuspended in the solution and serial dilutions of 10⁻¹, 10⁻², 10⁻³, 10⁻⁴ were made. The serial dilution of 10⁻³ was plated on PIA plates and incubated at 37°C overnight. PIA plates select against *E. coli* strains. Colonies appearing on the plates were replica-plated on 2 plates. Plate 1 was Psmm without supplemented of uracil and Plate 2 was Psmm supplemented with 50 µg/mL uracil and kanamycin (500 µg/mL). Recombinants were selected and their chromosomal DNA was isolated by the earlier mentioned method. By using the same forward and reverse primer for wild type *pyrB* gene, PCR reaction was performed. The

pyrB of *B. cepacia* was knocked out by transposon insertion and confirmed by PCR product which has a shift-up fragment compared with the PCR product of wild type *pyrB* gene. The cell lysates of PyrB⁻ *B. cepacia* and wild type *B. cepacia* were used in assay for ATCase activity. The ATCase assay was performed as described earlier.

Growth Curves Studies

Growth curves of PyrB⁻ and wild type *B. cepacia* were initiated by first inoculating a 5 ml starter culture of the appropriate medium, the same as that to be used in the growth curve study, and incubating overnight. This overnight culture (15 – 20 hours) was used to inoculate 50 mL of medium in a 125 mL Erlenmeyer flask. The bacteria were diluted 1:1000 (0.5 ml inocula for a 50 ml culture) and the OD₆₀₀ measured and recorded for time point zero. The cultures were incubated at 37°C with shaking at 250 rpm. At the indicated time point, 1 mL of each culture was aseptically removed and the OD₆₀₀ recorded.

Virulent Test of PyrB1⁻ *B. cepacia* *in vivo*: Standard Paralysis Assay

Wild type and PyrB1⁻ *B. cepacia* are grown overnight in brain heart infusion (BHI) broth and then diluted 100-fold into separate tubes of fresh BHI broth. BHI agar plates are spread with 400 µL each of the dilution and then incubated at 37C° for 24 hours to form a lawn of bacteria. GFP strains of *Caenorhabditis elegans* (*C. elegans*) (PD4970, DP132, CB 2553, and PD 4251) that are not starved/starved are transferred with a wire pick from the *E. coli* OP50 plates as L4s and placed onto the lawns of wild

type and mutant *B. cepacia*. The plates are then incubated at room temperature (21-23°C), and the nematodes are examined every hour at 25X magnification for the first 12 hours; worms are scored as paralyzed upon the degradation of the GFP protein, which can be examined using Nomarski microscopy (Darby et al., 1999).

RESULTS AND DISCUSSION

Cloning of *B. cepacia pyrB*

From this research, 1.29 kb of *B. cepacia pyrB* was cloned in to the pUC18 plasmid vector (Fig 25). Cell extracts from *E. coli* TB2 cells with no ATCase activity containing pSKBB18 were assayed for ATCase (Fig 26). *E. coli* TB2 cells containing pSKBB18 had ATCase activity at 0.24 nm CAA/min/mg protein. This result showed that in *E. coli* cells, the *B. cepacia pyrB* gene complemented the *E.coli pyrB* auxotroph and expressed ATCase activity. Alignment of amino acid sequences with other *Burkholderia* spp. was also accomplished (Fig 27a, 27b). *B. cepacia* 25416, *B. cepacia* R18194, *B. pseudomallei*, *B. fungorum*, and *Bordetella pertussis*(*B. pertussis*) were used for this purpose. *B. cepacia* R18194 (99% identity), *B. pseudomallei* (92% identity), and *B. fungorum* (89% identity) all had very close homology to *B. cepacia* 25416. In addition, *B. pertussis* has 77% identity to *B. cepacia* 25416. The alignment of amino acid sequences also revealed many conserved regions.

Purification of *B. cepacia* ATCase

The cloned ATCase from *B. cepacia* ATCC25416 was purified by the Glutathione S-Transferase Gene Fusion System. Two strategies were used to purify the cloned *B. cepacia* ATCase from the GST fusion system. One sample was cleaved by thrombin. The other one was eluted from a Glutathione Sepharose 4B column by using reduced glutathione first and then cleavage by thrombin. Based on the known sequence of the *pyrB* gene the expected size of the subunit was 47 kDa.

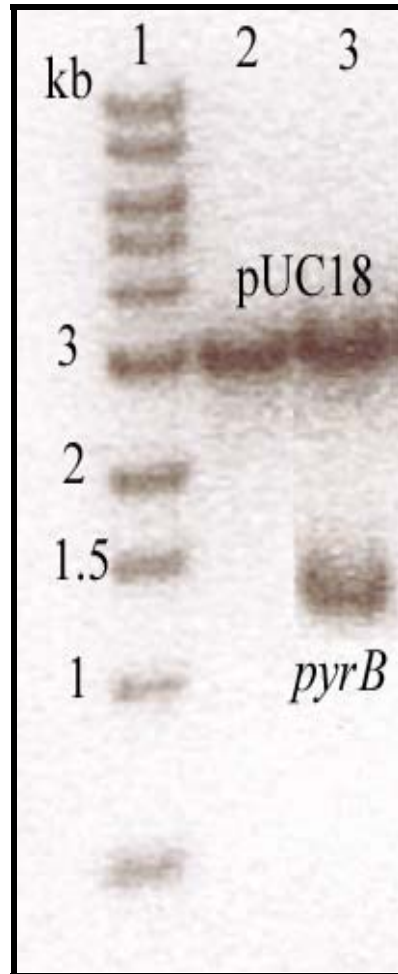


Fig 25. Double restriction of pUC18 and pSKBB18 containing *B. cepacia pyrB* gene in pUC18 by *Bam*HI and *Eco*RI. 1% agarose gel was used.

1. 1 kb ladder, 2. pUC18, 3. pSKBB18

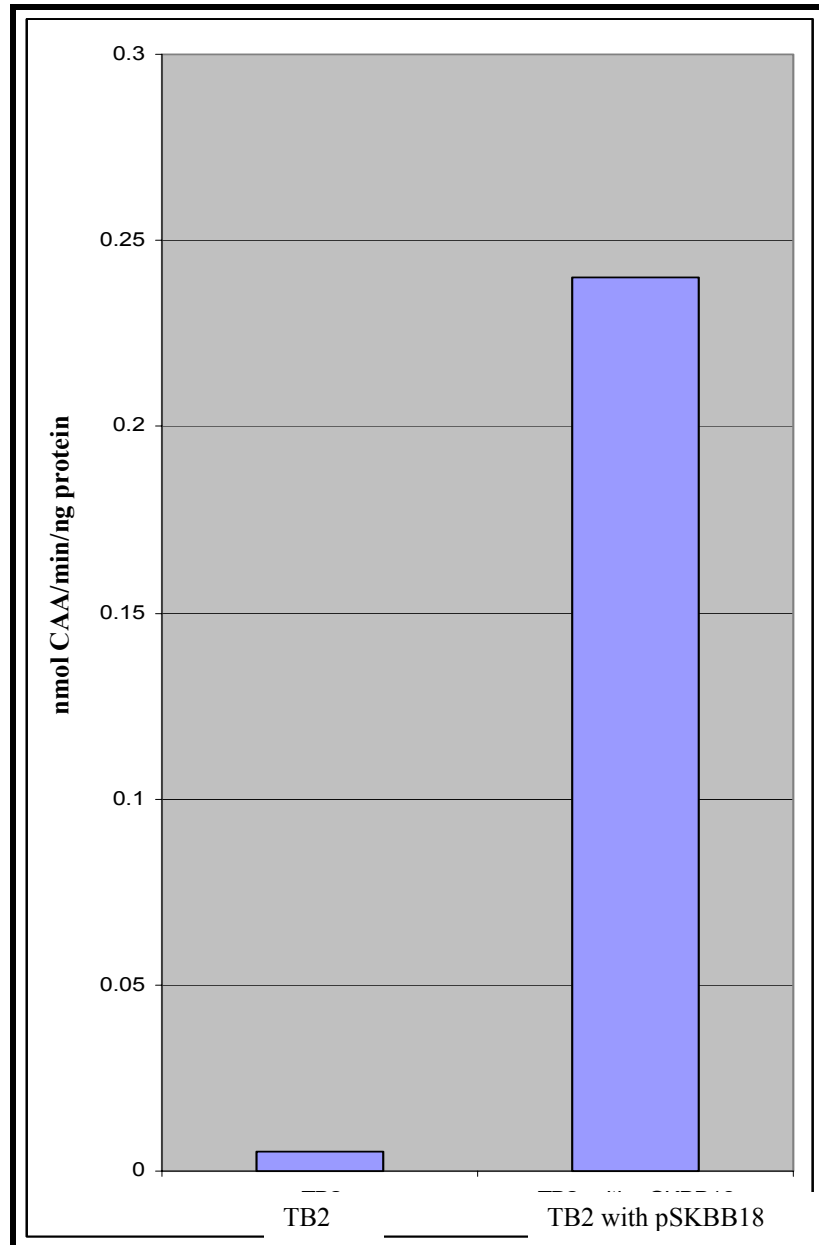


Fig 26. ATCase specific activity of TB2 and TB2 containing pSKBB18 plasmid.

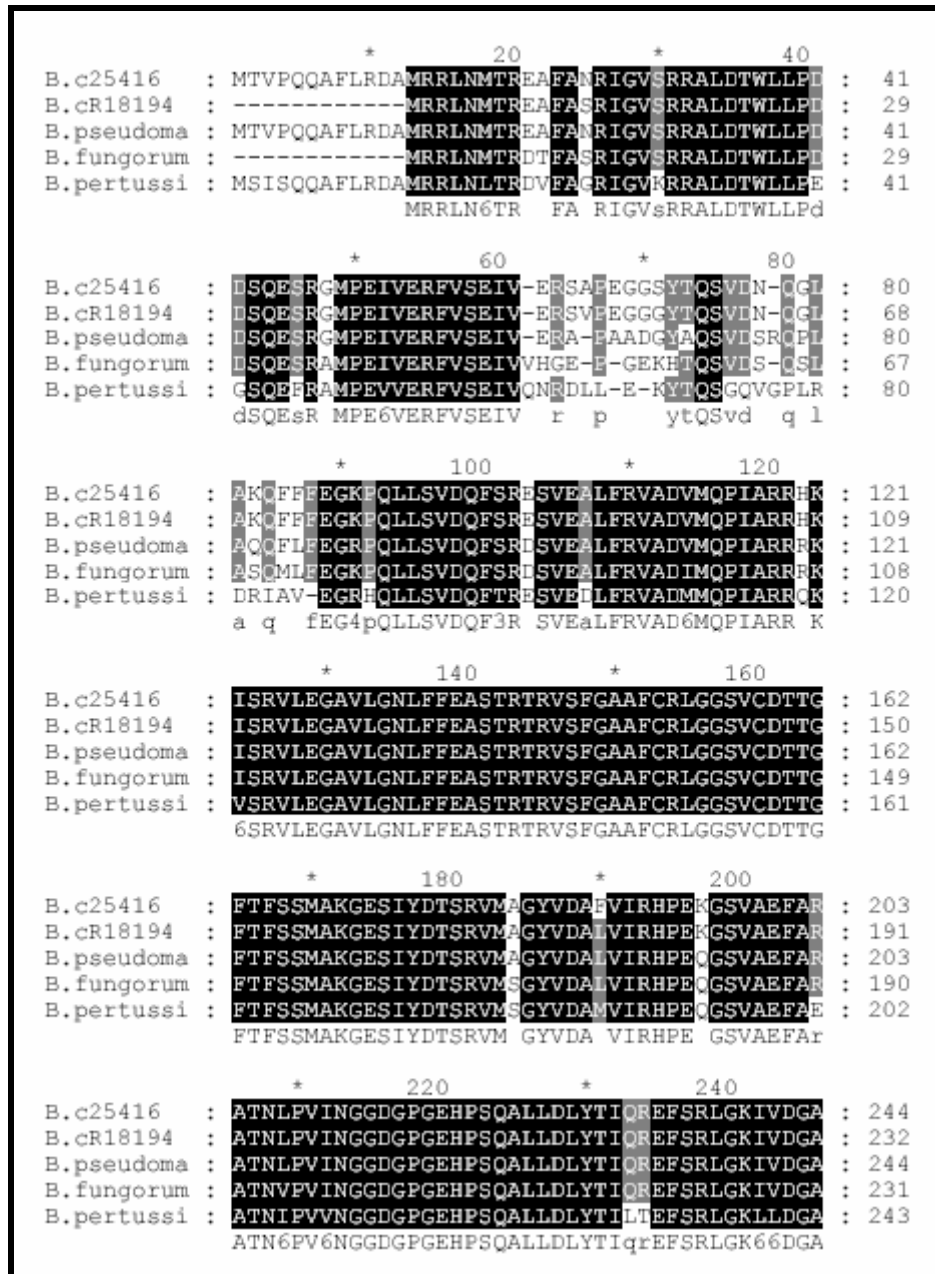


Fig 27a, 27b. Amino acids sequences alignment with *B. cepacia* 25416 (B.c25416), *B. cepacia* R18194 (B.cR18194), *B. pseudomallei* (B.pseudoma), *B. fungorum*, and *Bordetella pertussis*(B.pertussi)


```

      *           260           *           280
B.c25416 : HIALVGDLDKYGRTVHSLVKLLALYRGLKFTLVSPETLEMPA : 285
B.cR18194 : HIALVGDLDKYGRTVHSLVKLLALYRGLKFTLVSPETLEMPA : 273
B.pseudoma : CIALVGDLDKYGRTVHSLVKLLALYRGLKFTLVSPETLEMPA : 285
B.fungorum : HIALVGDLDKYGRTVHSLVKLLALYRGLKFTLVSPETLEMPA : 272
B.pertussi : HIAMVGDLDKYGRTVHSLIKLLALYKGVKFTLISEQCLEMPG : 284
      hIA6VGDLDKYGRTVHSL6KLLALY4G6KFTL6SPp LEMP

      *           300           *           320
B.c25416 : YIVICQATNGHVIECITDLAAGLRGADVVYATRIQKERFTD : 326
B.cR18194 : YIVICQATNGHVIECITDLAAGLRGADVVYATRIQKERFTD : 314
B.pseudoma : YIVICQATNGHVIECITDLAAGLRGADVVYATRIQKERFTD : 326
B.fungorum : YIIEQATSRNDEVIECIHDLSTGLRGADVVYATRIQKERFTD : 313
B.pertussi : YIVEQASRNCNVIECIKSTLEGLAGADVIYATRVQKEREFAN : 325
      YI6 Q1 NghV6E2t dLa GL GADV6YATR6QKERFT1

      *           340           *           360
B.c25416 : ESF-EGYTPDFQINQALVDTVCKPDTLIMHPLPRDSRPGAN : 366
B.cR18194 : ESF-EGYTPDFQINQALVDTVCKPDTLIMHPLPRDSRPGAN : 354
B.pseudoma : ESF-EGYTPDFQINQALVDTVCKPDTLIMHPLPRDSRPGAN : 366
B.fungorum : ESF-EGYTPDFQINQALVDSVCGVDTLIMHPLPRDSRPGAN : 353
B.pertussi : EEACEGYTADFQVSRAIIDAYCGPDTIVMHPLPRDSRPGSN : 366
      Esf EGYTpDFQ6nqA 6D C pDT66MHPLPRDSRPGaN

      *           380           *           400           *
B.c25416 : DLSVDLNRDERLAIFRQTDNGIPVRMAIFAVLLGVENLVQH : 407
B.cR18194 : DLSVDLNRDERLAIFRQTDNGIPVRMAIFAVLLGVENLVQH : 395
B.pseudoma : DLSTDLNRDERLAIFRQTDNGIPVRMAIFAVLLGVEHLVQH : 407
B.fungorum : DLSVDLNHDSRLAIFRQTDNGIPVRMAIFAVLLGVERLVQH : 394
B.pertussi : DLSTDLNHDERLAIFRQTDNGIPIRMAIFAVLLGVEGLVQH : 407
      DLS DLN DpRLAIFRQTDNGIP6RMAIFAVLLGVE LVQH

      420           *           440           *
B.c25416 : SMRDATWRPFAYLGFEDAVFHGVI----- : 431
B.cR18194 : SMRDATWRPFAYLGFEDAVFHGVI----- : 419
B.pseudoma : SMRDATWRPFPTYLGFEDAVFHGID----- : 431
B.fungorum : SMRDATWRPFVYLGFEDAVFHGID----- : 418
B.pertussi : SMRDATWOHFSHIGFEDSVFHGLD----- : 431
      SMRdatWrpP y6GP DaVFHG6D

```

Fig 27b. Amino acids sequences alignment

When the fusion proteins were cut by thrombin, only ATCases were eluted and collected. To check the efficiency of over expression and the size of the monomer of ATCases, purified ATCases were run on 10% SDS-PAGE (Fig 29). The expected size of the fusion or overexpression protein was 76 kDa because the monomer size of ATCase was 47 kDa and the GST size 26 kDa. The overexpressed 76 kDa fusion protein was seen in Fig 28, lane 2. However, in addition to the 47 kDa subunit, a 40 kDa polypeptide was also detected in eluted samples (Fig 28, lane 3). This unexpected result was also observed from the Chitin Binding Domain Affinity Chromatography (Clone Tech; Data not shown). To isolate the 40 kDa polypeptide, samples eluted from the Glutathione Sepharose 4B column were then loaded onto another Glutathione Sepharose 4B column. The pure 40 kDa polypeptide was found in the flow-through and did not bind to the column. To check the activity of ATCases, the purified 47 kDa and 40 kDa polypeptides were run on non-denaturing ATCase activity gel and stained with 3% sodium sulfide. In the gel, two active fragments appeared. These two fragments came from trimers of 47 kDa and 40 kDa. The two trimer sizes were a 140 kDa (47×3) and a 120 kDa (40×3) (Fig 38). Each gave high ATCase activity when assayed for ATCase assay was used (Fig 40).

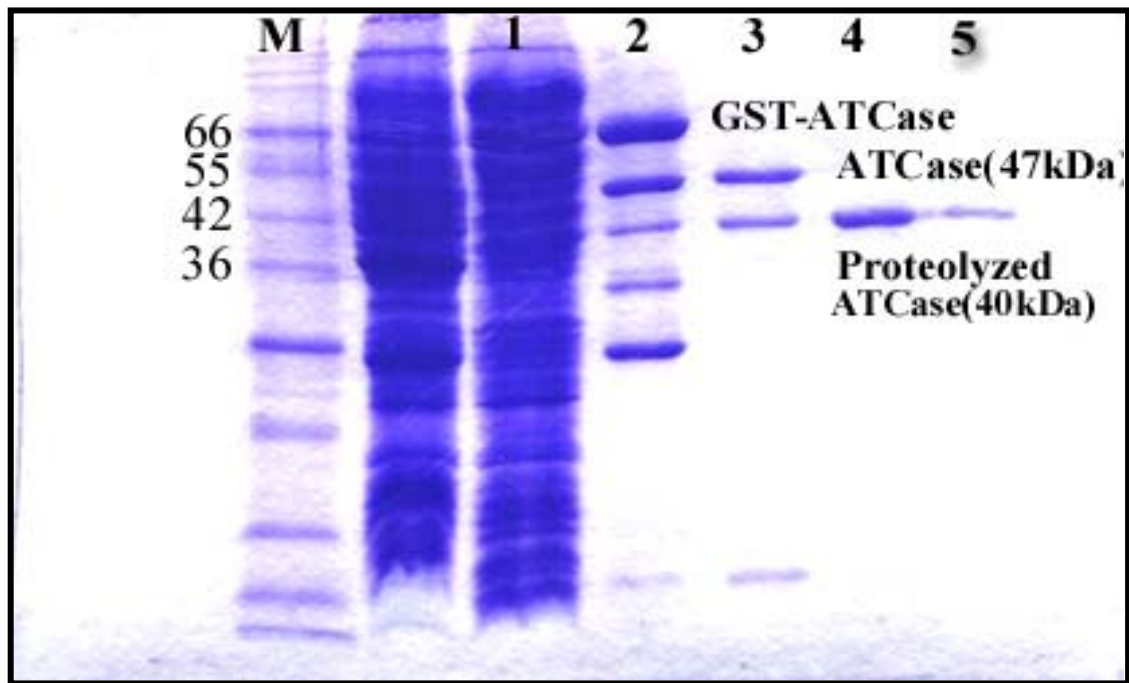


Fig 28. Direct eluting ATCase by Thrombin. Each sample was run on

10 % SDS-PAGE.

M. Molecular weight marker, 1. Cell extract,

2. Bead after binding, 3. 1st elute (E1)

4. 2nd elute (E2), 5. 3rd elute (E3)

ATCases were also eluted using reduced glutathione. Reduced glutathione cut the binding site of GST to the bead and samples were eluted as fusion protein of GST with ATCase activity (Fig 29). When the fusion proteins were cut by thrombin, ATCases were purified at the unexpected size of 40 kDa again (Fig 30, lane 1, 2). These ATCases were also run on ATCase activity gel and assayed for ATCase conventional way. The same result was seen as in the previous elution method (Fig 40). The likelihoods of thrombin and serine protease incision were excluded because there is no thrombin recognition site (Table 3) in the ATCase polypeptide. Moreover, the enzyme purification was performed with and without phenylmethylsulfonyl fluoride (PMSF;serine protease inhibitor) with no change in the results

Previously, ATCase activity gels have shown that *B. cepacia* ATCase contained an active holoenzyme (*pyrBC*) complex of 550 kDa comprised of 47 kDa *pyrB* and 38 kDa *pyrC* subunits, and two active smaller trimer complexes of 140 kDa and 120 kDa. These two smaller trimer complexes had the same sizes as the active trimers of the cloned uncleaved (3 X 47 kDa) and cleaved (3 X 40 kDa) ATCases. This suggests that the trimers from the uncleaved 47 kDa and the proteolytic 40 kDa ATCase subunits are present in the *B. cepacia* cell.

To characterize the atypical proteolyzed in *B. cepacia* ATCase, purified auto-proteolytic ATCases were sent for N-terminal sequencing. N-terminal sequencing showed that there was auto-proteolysis between Ser74 and Val75 residues downstream from the initial Met start codon. There was another Ser94-Val95

downstream from the Ser74 but there was no cleavage at this downstream site (Fig 31). Therefore, we conclude that there is an invariant Ser residue at Ser74 and a site specific proteolysis in *B. cepacia* ATCase.

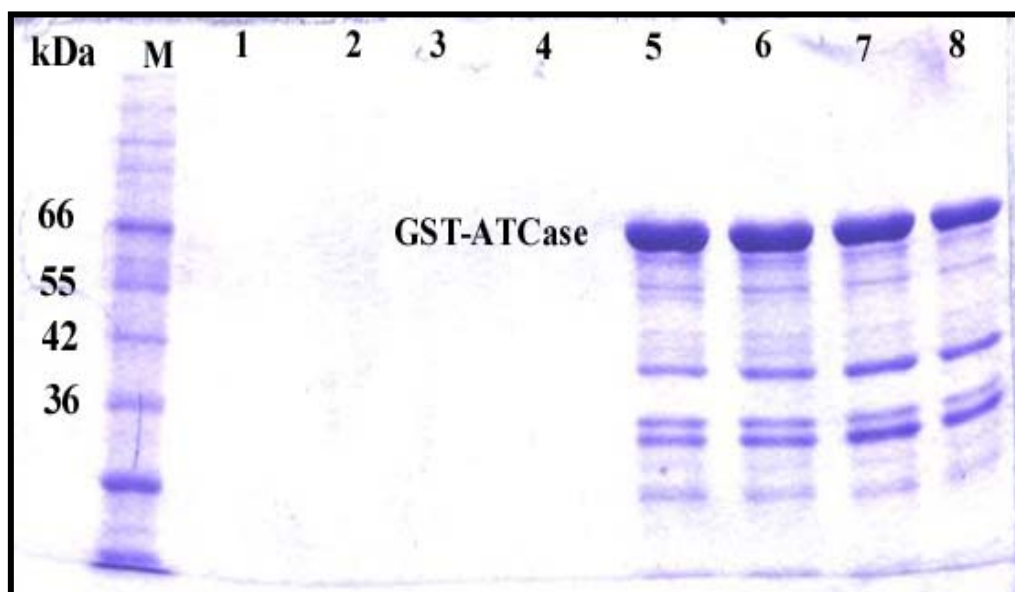


Fig 29. Expression of fusion protein in 10 % SDS-PAGE.

M: Molecular weight marker,

1, 2, 3, 4: sample from washing , 5. E1, 6. E2, 7. E3, 8. E4

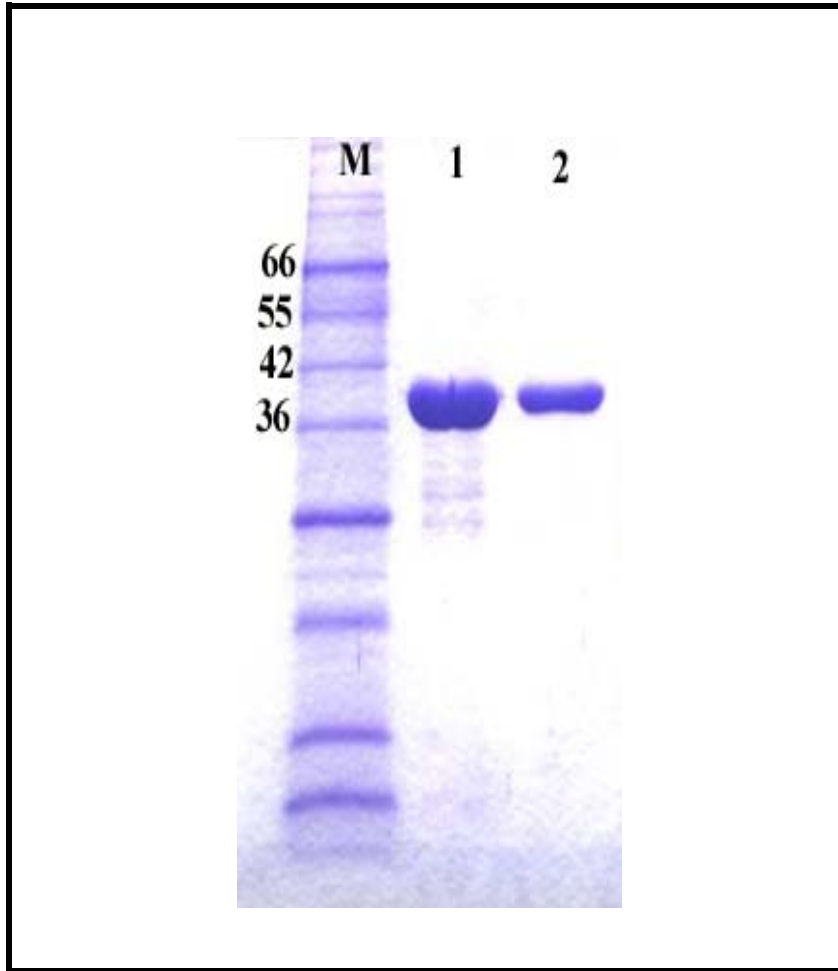


Fig 30. Expression of ATCase in 10% SDS-PAGE. This ATCase was obtained by thrombin cut after elution by reduced glutathione.

M. Molecular weight marker, 1. E1, 2. E4

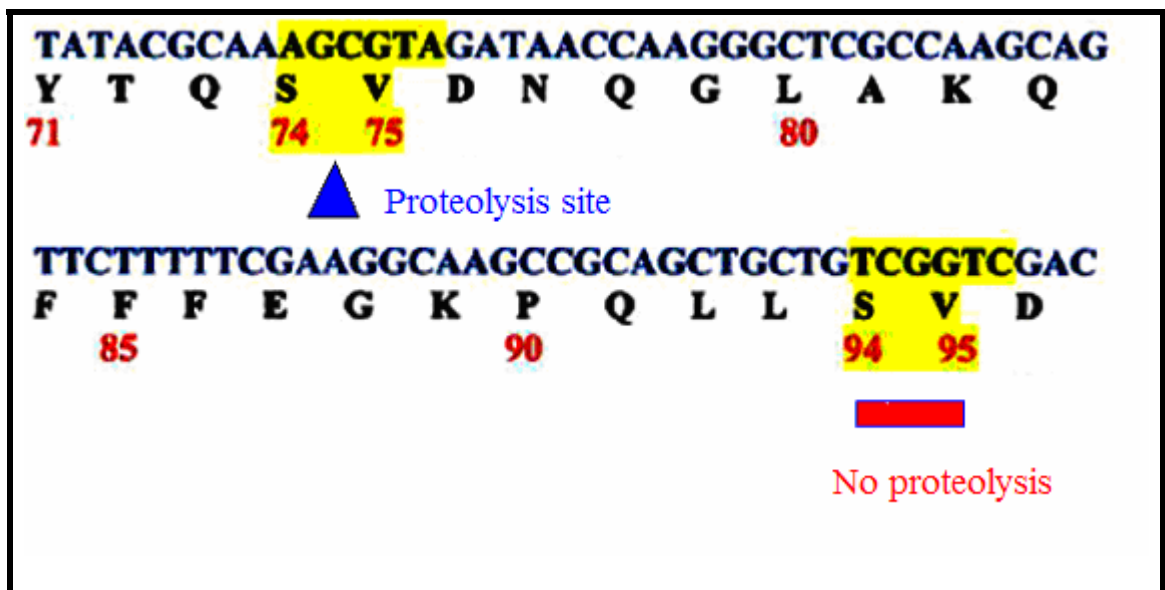


Fig 31a. Proteolysis site between Ser74 and Val75

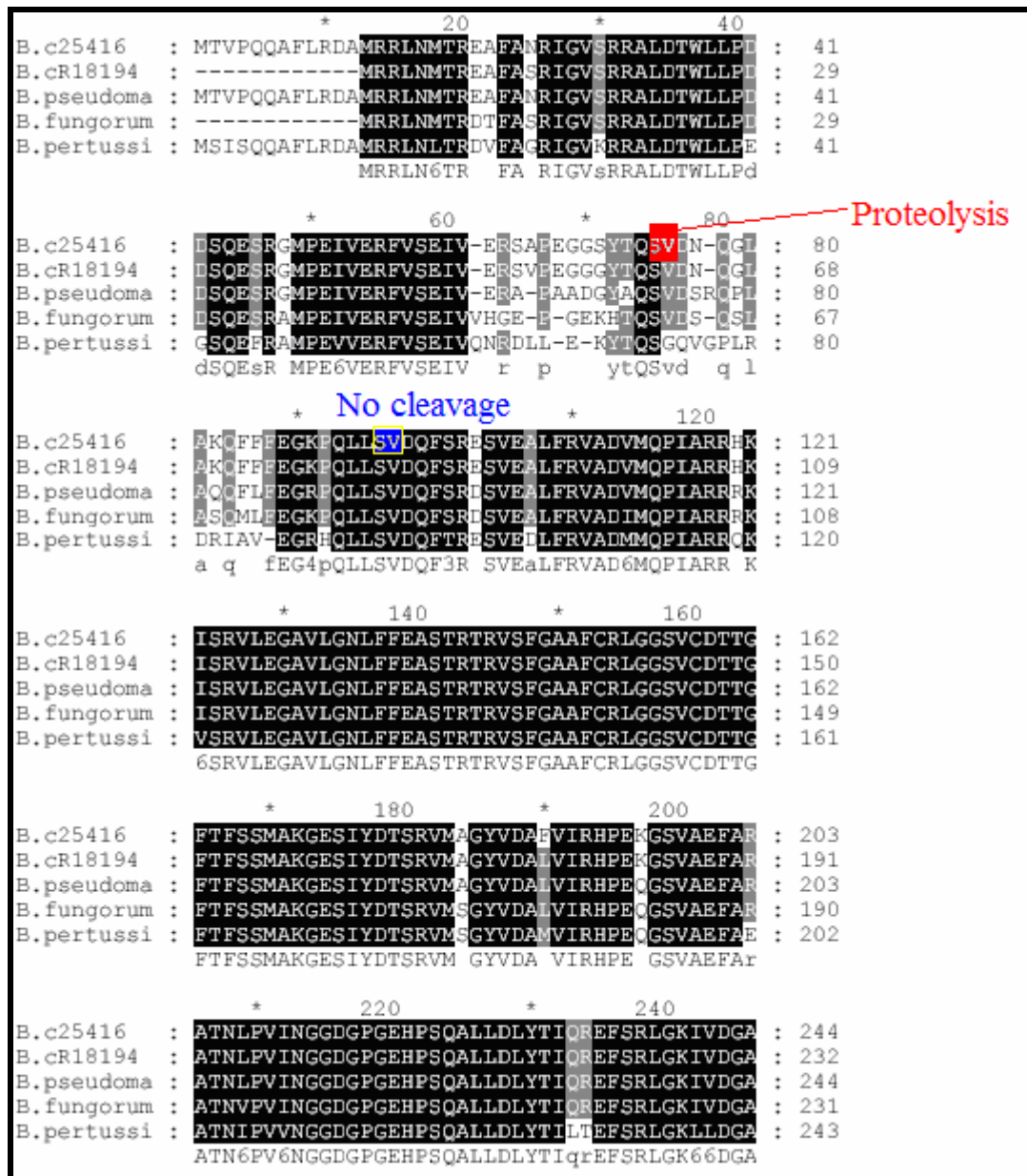


Fig 31b. Proteolysis site in amino acid sequences of PyrB subunit

A. Met	Tyr	Pro	Arg ↓	Gly	Asn
B. Ile	Arg	Pro	Lys ↓	Leu	Lys
C. Leu	Arg	Pro	Arg ↓	Gly	Ser
D. Ala	Arg ↓	Gly			
E. Gly	Lys ↓	Ala			

Table 3. Thrombin recognition site in PyrB subunit

Enzyme Kinetics of Proteolyzed ATCase

To investigate the nature of purified ATCases, ATCase assays were performed to determine the K_M for the uncleaved ATCase and the proteolytic ATCase (Fig 32, 33). Both purified ATCases were assayed for ATCase activity by measuring the amount of CAA produced at 37°C for 20 minutes using the colorimetric method described by Prescott & Jones 1969. The assay was conducted in a microtiter plate and the absorbance was read at 450 nm in a kinetic microplate reader.

The K_M for aspartate was calculated to be 1.5 mM for the uncleaved ATCase and 1.2 mM for the proteolytic ATCase. From this result, it was shown that the auto-proteolytic ATCase had a higher affinity for aspartate than did the uncleaved ATCase. Both the uncleaved ATCase (47 kDa) and the cleaved ATCae (40 kDa) make active trimers but it is not yet established which trimer is present as a dodecameric holoenzyme complex.

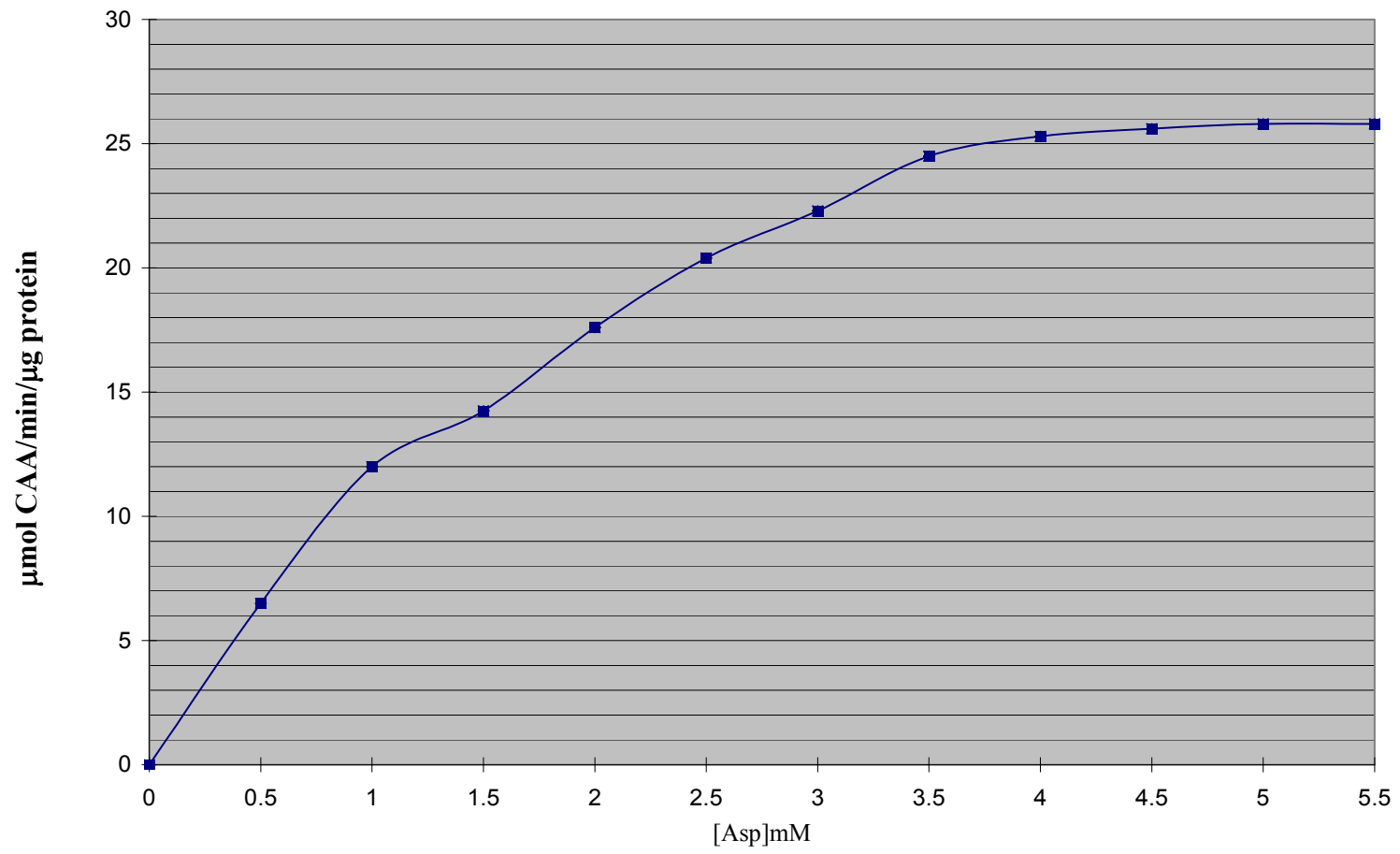


Fig 32. Michaelis-Menten plot for purified proteolytic ATCase between Ser74/Val75 from *B. cepacia*

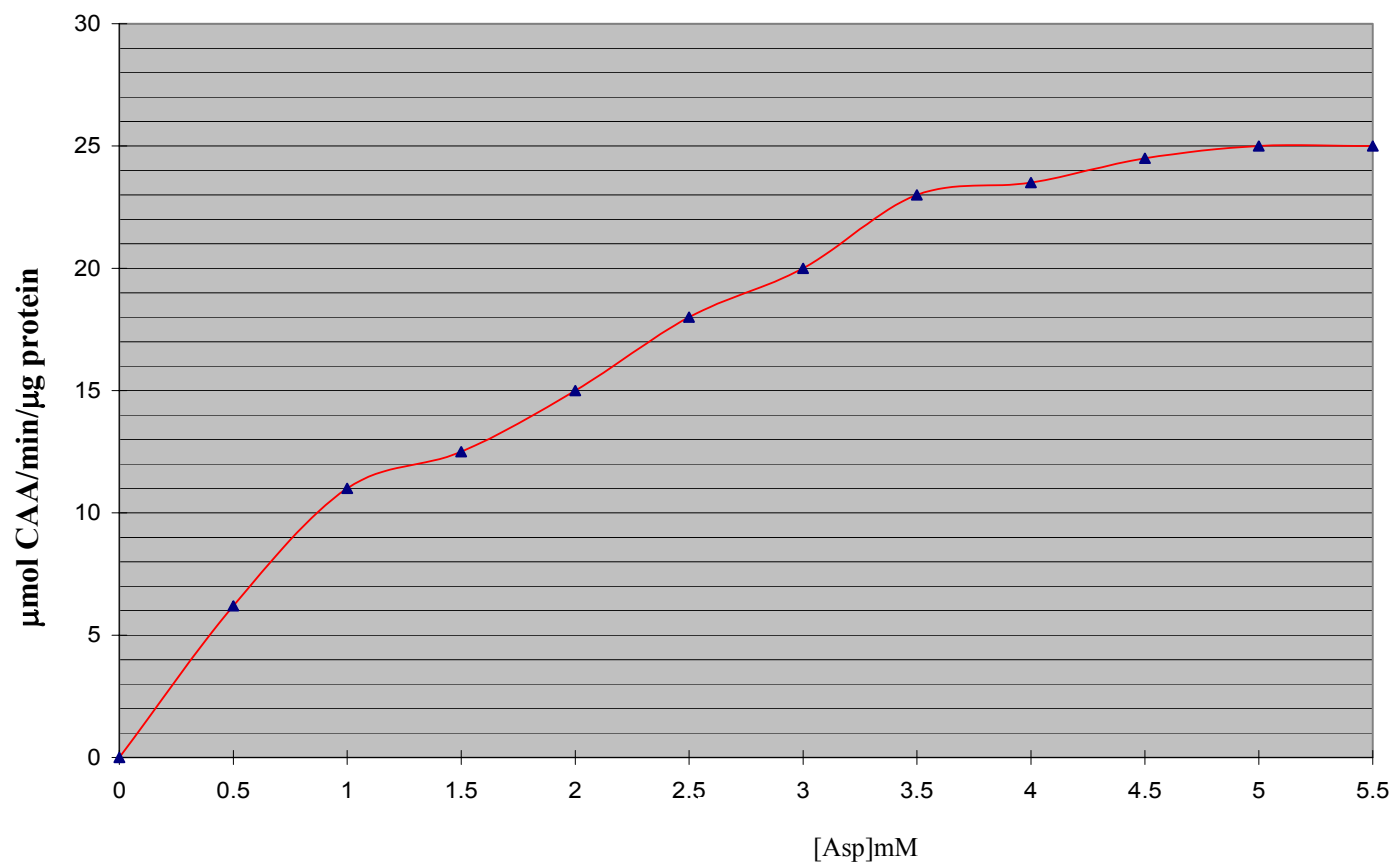


Fig 33. Michaelis-Menten plot for purified uncleaved ATCase from *B. cepacia*

Mutagenesis at Proteolysis Site

To confirm the atypical site-specific proteolysis between Ser74 and Val75 residues, site-directed mutagenesis by overlap extension was carried out. Two mutagenesis were established; Ser74 to Arg74 and Ser74 to Arg74. Two step PCR was performed to establish the missense mutation of the *pyrB* gene at Ser74 position. From the first step PCR, two sizes of amplified DNA were produced; 220 bp and 1.28 kb as expected (Fig 34, lane 1, 2, 3). From the second PCR, complete *pyrB* gene with site-directed mutagenesis was amplified (Fig 34, lane 4, 5, 6). A pSKBB18N plasmid was constructed from the ligation of site-directed mutagenesis *pyrB* gene to pSKBB18 plasmid by restriction with *EcoRI* and *BamHI*. A pSK2TN was constructed for protein purification from pSKBB18N (Fig 35). Using the same procedure, pSKBB18A and pSK2TA were also constructed.

The pSK2T containing Ser74, the pSK2TN containing Arg74 did not produce the proteolyzed 40 kDa fragment on SDS-PAGE during enzyme purification (Fig 36, lane 1, 2, 3). This mutagenized ATCase also did not show any active fragment in ATCase activity gel (Fig 38, lane 6). ATCase assay confirmed that no enzyme activity was presented (Fig 40). The amount of purified protein was less than that of wild type ATCase. The conformational disruption by positively charged Arg might diminish protein production. A pSK2TA containing Ala74 also did not produce the proteolyzed 40 kDa fragment on SDS-PAGE during enzyme purification (Fig 37, lane 1, 3). However, ATCase from this plasmid still demonstrated high activity in the ATCase activity gel (Fig 38, lane 7) and ATCase (Fig 40). In comparing each purified ATCase, there was no

significant difference in enzyme specific activity between the wild type (3 X 47 kDa)-cloned ATCase, proteolyzed (3 X 40 kDa)- cloned ATCase, and mutagenized ATCase (Ala74, 3 X 47 kDa) ATCase (Fig 40). From these results, replacing Ser residue in the polar domain with an Arg is likely to disrupt the enzyme folding. Replacing Ser with an Ala may not affect enzyme folding. This is a similar result to that of Stevens, R.C. group's proposal.

Earlier studies in our laboratory suggested that the *B. cepacia* ATCase had a molecular mass of about 550 kDa. It was composed of 47 kDa PyrB and 38 kDa PyrC polypeptides, and it was active as a holoenzyme and as a trimer of ~150kDa (47kDa X 3). Now we find that in addition to the 47 kDa PyrB polypeptide, there is also 40 kDa PyrB polypeptide (proteolyzed) that is active in both the trimeric form and in the holoenzyme. This might constitute a new class of ATCase, namely Class D, to accommodate the unique *Burkholderia cepacia* and *Burkholderia cepacia-like* ATCase (Fig 41).

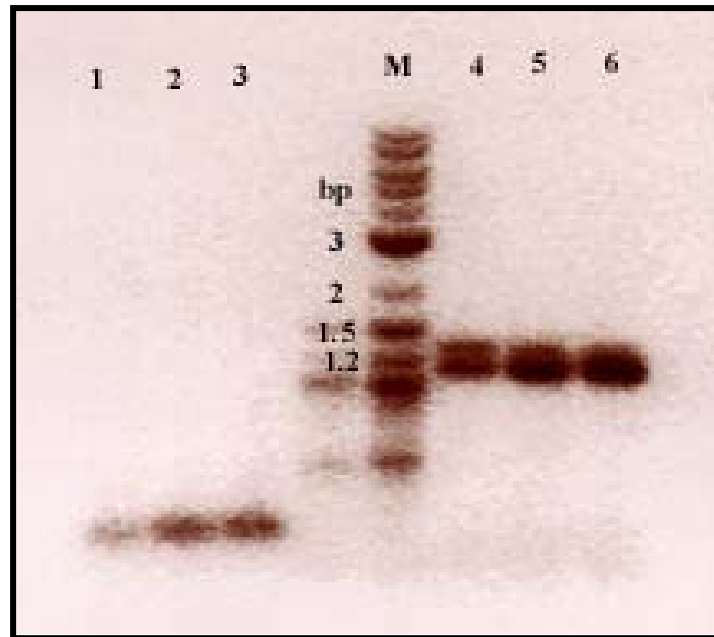


Fig 34. First PCR from site-directed mutagenesis by overlap extension. Each sample was loaded on 1 % agarose gel.

1, 2, 3: Amplified DNA from 5' to mutation site (220 bp)

1. For converting Ser74 to Arg74

2, 3. For converting Ser74 to Ala74

4, 5, 6: Amplified DNA from mutation site to 3' (1.28 kb)

4. For converting Ser74 to Arg74

5, 6. For converting Ser74 to Ala74

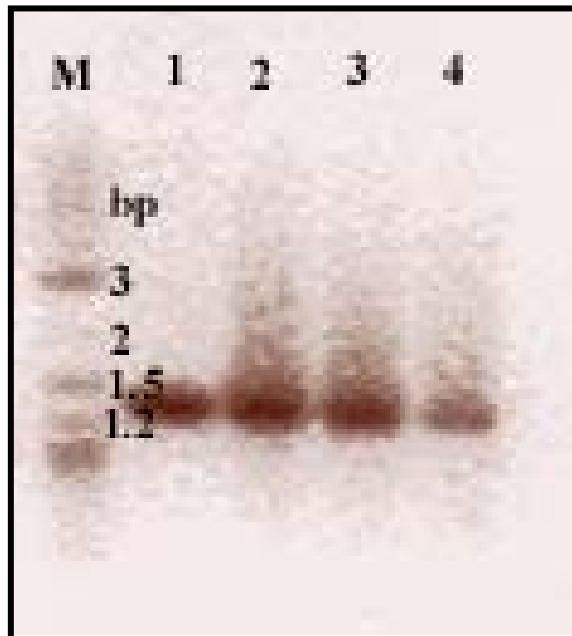


Fig 35. Second PCR for complete mutagenesis from site-directed mutagenesis by overlap extension.

Each sample was loaded on 1 % agarose gel.

1, 2. For converting Ser74 to Ala74 (1.3 kb)

3, 4. For converting Ser74 to Ala74 (1.3 kb)

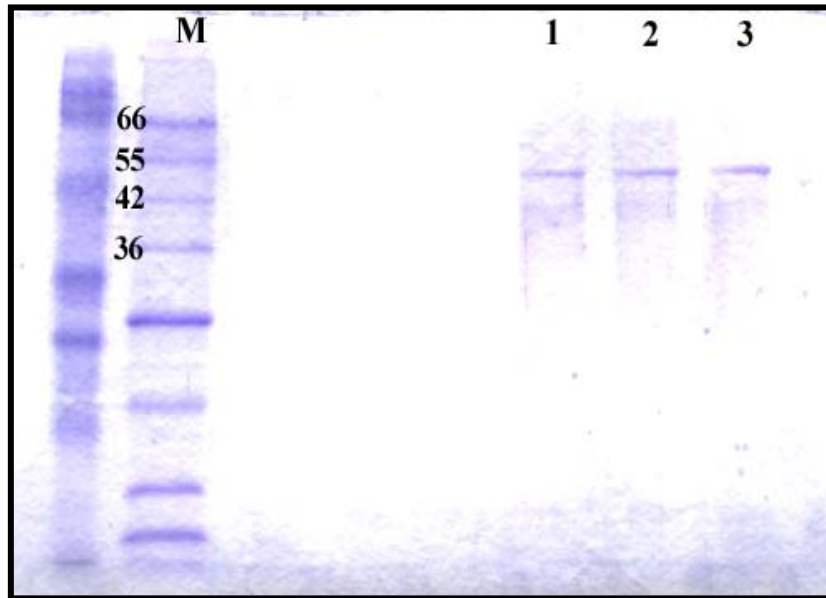


Fig 36. Expression of purified ATCase (Ser74 converted to Arg74) in 10 % SDS-PAGE. These proteins were eluted after thrombin treatment directly.

M. Molecular weight marker, 1. E1, 2. E2, 3. E3

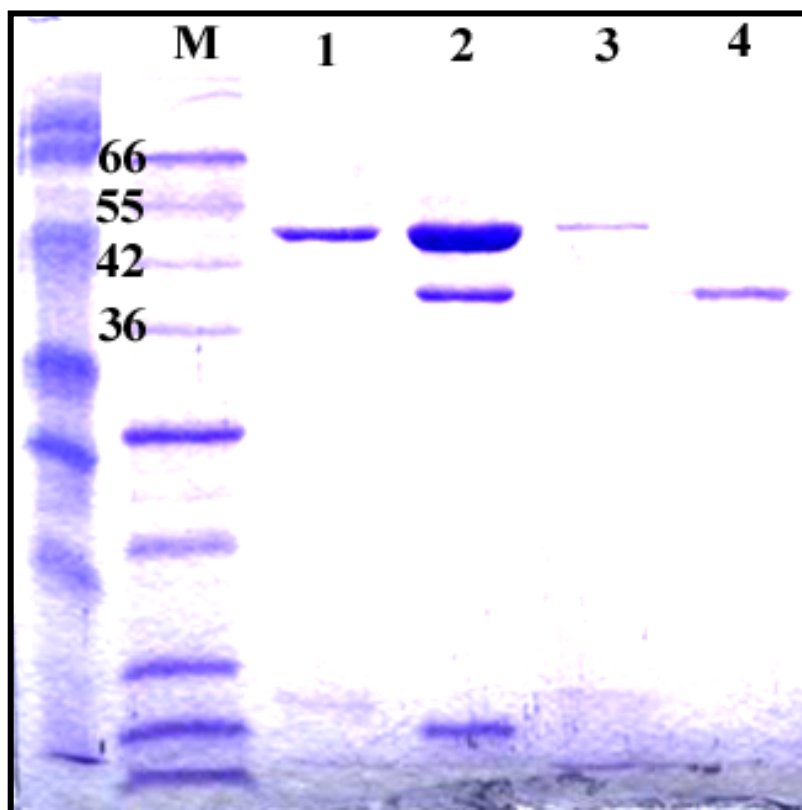


Fig 37. Expression of purified ATCase (Ser74 converted to Ala74) in 10 % SDS-PAGE. These proteins were eluted after thrombin treatment directly.

M. Molecular weight marker

1, 3. E1 and E2, of ATCase (Ser74 converted to Ala74)

2, 4. E1 and E2 of wild type ATCase

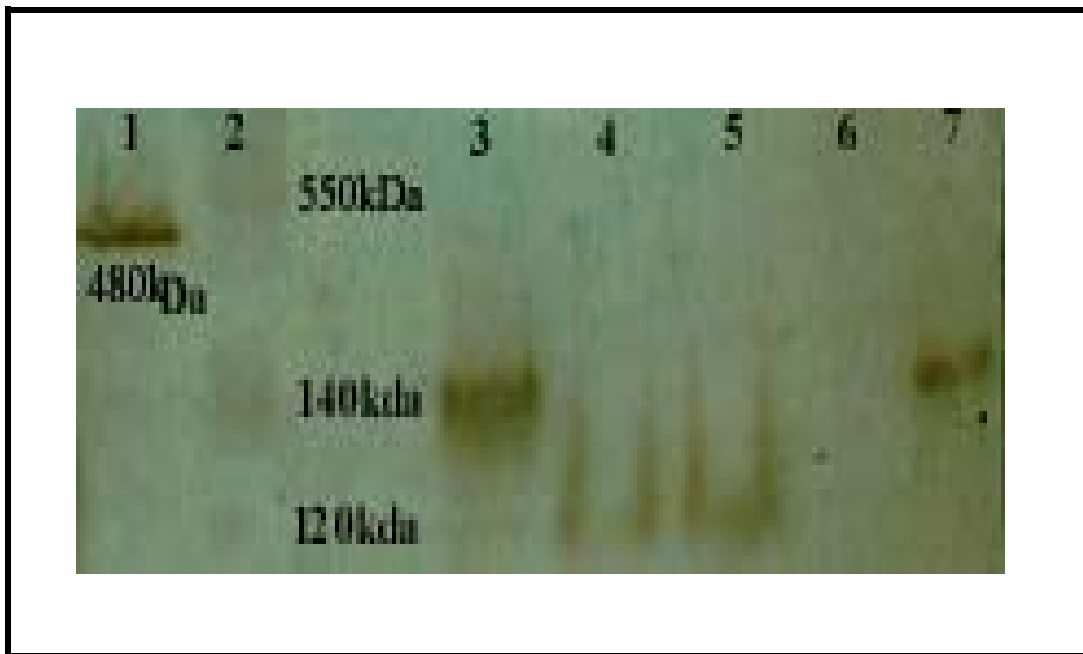


Fig 38. ATCase activity gel in 8 % N-SDS-PAGE

1: *P. aeruginosa* cell extract 2: *B. cepacia* cell extract

3: Purified ATCase (uncleaved ATCase)

4, 5: Purified proteolytic ATCase

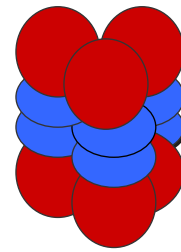
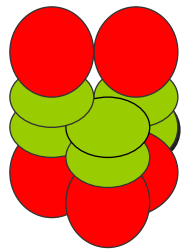
6: Purified mutagenized ATCase (Ser converted to Arg)

7: Purified mutagenized ATCase (Ser converted to Ala)

Class A(480 kDa): *P. aeruginosa*

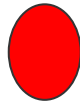
Class D (550 kDa): *B. cepacia*

Structure



Subunit

PyrB catalytic 34kDa



PyrB catalytic 47kDa



Proteolytic PyrB 40kDa



PyrC' active or inactive 45 kDa



PyrC' active 45 kDa



Fig 39. Proposed new class of ATCase, Class D

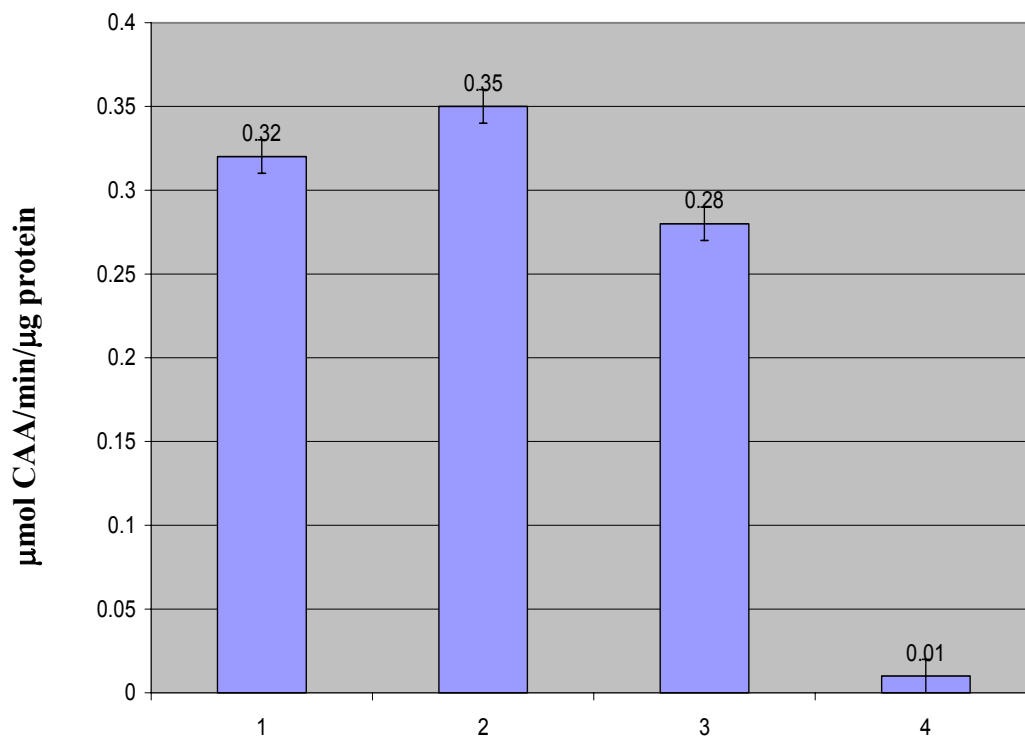


Fig 40. ATCase specific activity.

1. Purified ATCase (Uncleaved)
2. Purified proteolytic ATCase(Ser74/Val75),
3. Purified mutagenized ATCase (Ser74 converted to Ala74),
4. Purified mutagenized ATCase (Ser74 converted to Arg74)

Expression of Second ATCase in *B. cepacia*

From previous research, there were likely to be two ATCases in *B. cepacia*. To learn more about the *B. cepacia* ATCase, we constructed a *pyrB* knockout strain using a mini-transposome kit. The *B. cepacia pyrB* gene was cloned into pUC18. The transposon was then inserted about 400 bp downstream of the *pyrB* start. This was confirmed by sequencing. This mutagenic construction was then mated into wild type *B. cepacia* using triparental mating. *B. cepacia* is naturally very resistant to a range of antibiotics. In the case of gentamicin, the Minimum Bactericidal Concentration (MBC) was 3 mg/mL (data not shown) and kanamycin was 0.5 mg/mL. Therefore the recombinant *B. cepacia* was screened by plating on Psmm containing kanamycin (0.5 mg/mL) with uracil supplied. The recombinant was confirmed by gel band shift in the up direction (Fig 41, lane 1, 2). The *pyrB* knock-out strains grew very slowly in minimal medium at 30°C but after fully growing then the growth rate was comparable to that of wild type *B. cepacia*. Moreover, this strain became prototrophic and grew in Psmm without uracil supplement. In the knock out strain, the 550 kDa holoenzyme, the 140 kDa and 120 kDa trimers disappeared. They were replaced by a previously unseen 480 kDa holoenzyme, which is similar in size to *Pseudomonas* ATCase (Fig 42). The ATCase specific activity of the new 480 kDa ATCase was 0.26 μmol/min/μg, which was 80% of the 550 kDa holoenzyme (0.32 μmol/min/μg). This suggests that there are two *pyrB* genes in *B. cepacia* with the second *pyrB* (designated *pyrB2*) only when the first *pyrB* (designated *pyrB1*) is inactivated. The further characteristic of the strains is noted: *B. cepacia* wild type (*pyrB1*⁺*pyrB2*⁻) secretes a unique yellow pigment while *pyrB1*⁻

pyrB2⁺ *B. cepacia* does not produce yellow pigments any more (Fig 43). It is likely the yellow pigments are produced from the metabolic pathway related to expression of *pyrB1* gene.

To investigate the expression of ATCase further, wild type *B. cepacia* (*pyrB1⁻*) was cultured at 25°C for 3 to 5 days. The wild type cell expressed the 480kDa ATCase in addition to 550 kDa ATCase holoenzyme after 5 days incubation at 25°C (Fig 44, lane 6). The 140 kDa and 120 kDa were also disappearing (Fig 44, lane 4, 5, 6). This suggests that *B. cepacia* has second or another pathway for ATCase metabolism in order to adapt in unfavorable condition.

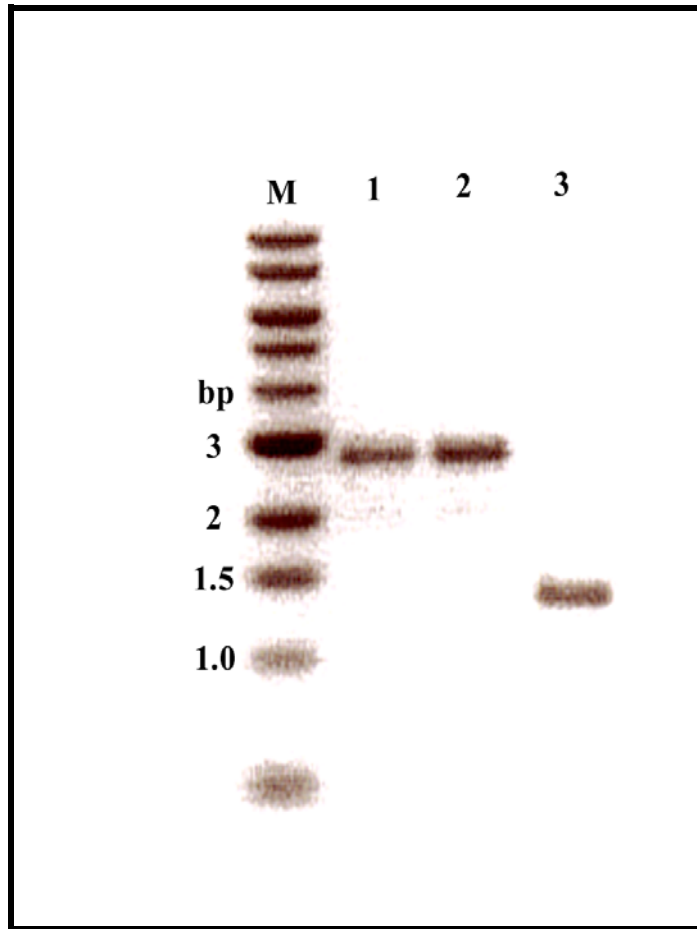


Fig 41. Verification of transposon insertion in the *pyrB* gene. PCR products were run on 1 % agarose gel. A forward and a reverse primer for *B. cepacia pyrB* gene were used.

M. 1 kb ladder,

1, 2. PCR using chromosomal DNA of *pyrB⁻ B. cepacia* as template

3. PCR using the chromosomal DNA of wild type *B. cepacia* as template

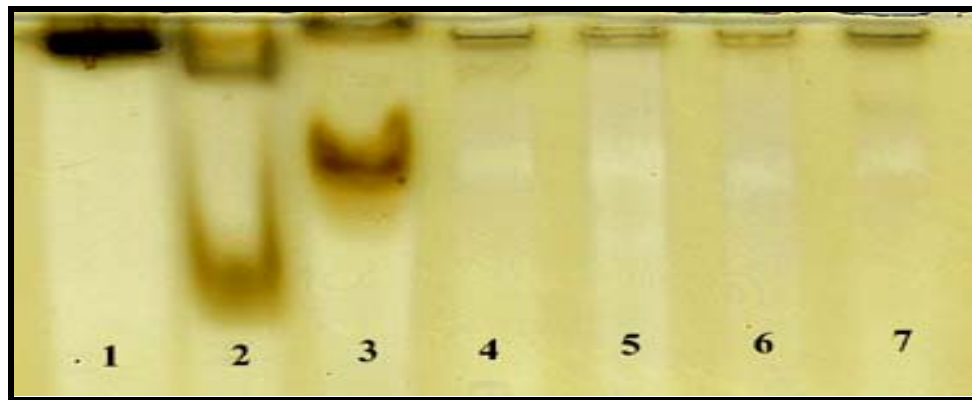


Fig 42. Expression of second ATCase in activity gel. Samples were run on 8 % N-SDS-PAGE and stained by 3 % sodium sulfide. .

1. *P. aeruginosa* (480 kDa) 2. *E.coli* (300 kDa, and 100 kDa)

3. *B. cepacia* (600 kDa, 140 kDa, and 120 kDa)

4, 5, 6, 7. *pyrB1⁻pyrB2⁺* *B. cepacia* (480 kDa)

1

2



Fig 43. The pigment comparison of wild type and *pyrB*⁻ *B. cepacia* in PIA plate without uracil

1. *pyrB*⁻ *B. cepacia* 2. Wild type *B. cepacia*

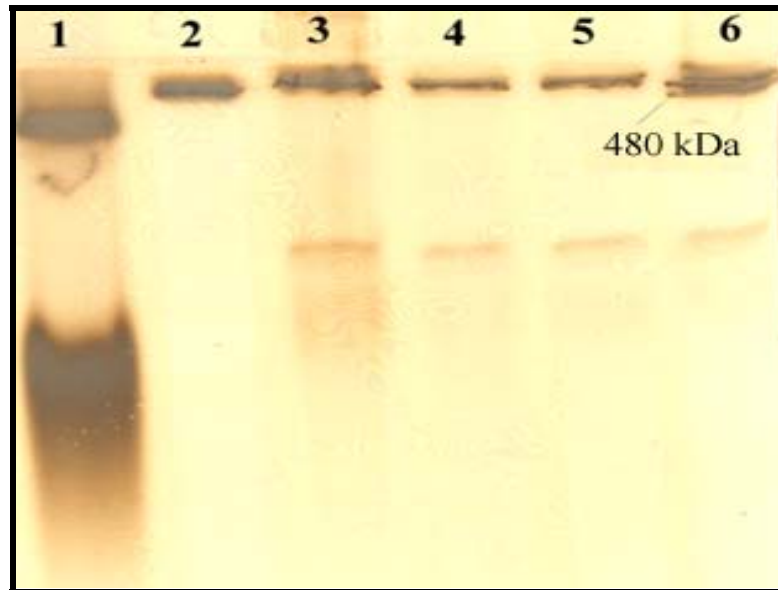


Fig 44. Expression of second ATCase on ATCase activity gel

1. *E. coli* cell extracts
2. *P. aeruginosa* cell extracts (480 kDa)
3. *B. cepacia* cell extracts incubated at 30°C overnight
4. *B. cepacia* cell extracts incubated at 25°C 3 days
5. *B. cepacia* cell extracts incubated at 25°C 4 days
6. *B. cepacia* cell extracts incubated at 25°C 5 days

Virulent Test of *pyrBI*⁻ *B. cepacia*

Darby et al. (1999) reported that wild type *P. aeruginosa* PAO1 is able to kill *Caenorhabditis. elegans* while a *pyrC* auxotroph does not. Maksimovas et al. (1993) also reported that in a dihydroorotase (DHOase) mutant strain of *P. putida* failed to produce the siderophore pyoverdin, which is one of its virulence factors. The *P. aeruginosa* DHOase mutant was also found to produce significantly less pyoverdin than did the wild type. In addition, it was observed that the mutant produced only 40% of the phenazine antibiotic pyocyanin produced by wild type. Brichta (2003) has shown that the two genes that encode dihydroorotase (DHO), *pyrC* and *pyrC2* of *Pseudomonas aeruginosa* are involved in the production of the siderophores; pyoverdin and pyocyanin, which are virulence factors. Therefore, it was important to see if the same relationship held for *B. cepacia*. The model organism *C. elegans* was used to compare wild type *B. cepacia* and a *pyrB* prototroph in their killing capacity of *C. elegans*. This part of the research was performed by Sara Anvari.

The growth curve of wild type (*pyrBI*⁺) and *pyrBI*⁻ *B. cepacia* clearly showed the prototrophic life of *pyrBI*⁻ *B. cepacia* (Fig 45, 46). Growth curves for wild type and *pyrBI*⁻ strain are nearly identical in the presence and absence of uracil. The *pyrBI* knockout *B. cepacia* is clearly a prototroph.

To investigate the virulence effect of *pyrB1* and *pyrB2* genes, wild type *B. cepacia* and *pyrBI*⁻ *B. cepacia* were tested for virulence by using *C. elegans* model system, which is alternative pathogenic test for mammals. It has been reported that the virulent factors of *P. aeruginosa* killed the *C. elegans* by paralyzing the pharyngeal

muscles. In this research, wild type *B. cepacia* paralyzed the pharyngeal muscles but *pyrBI⁻ B. cepacia* did not kill the nematodes (Fig 47, 48) (Anvari, 2004). In the standard paralysis assay, it was clear that *pyrBI⁻ B. cepacia* didn't produce virulent factors because while wild type *B. cepacia* reduced the viability of nematodes 80 % after 8 hours, *pyrBI⁻ B. cepacia* reduced viability 20 % only in the same time (Fig 49).

B. cepacia and *pyrBI*⁻ *B. cepacia*

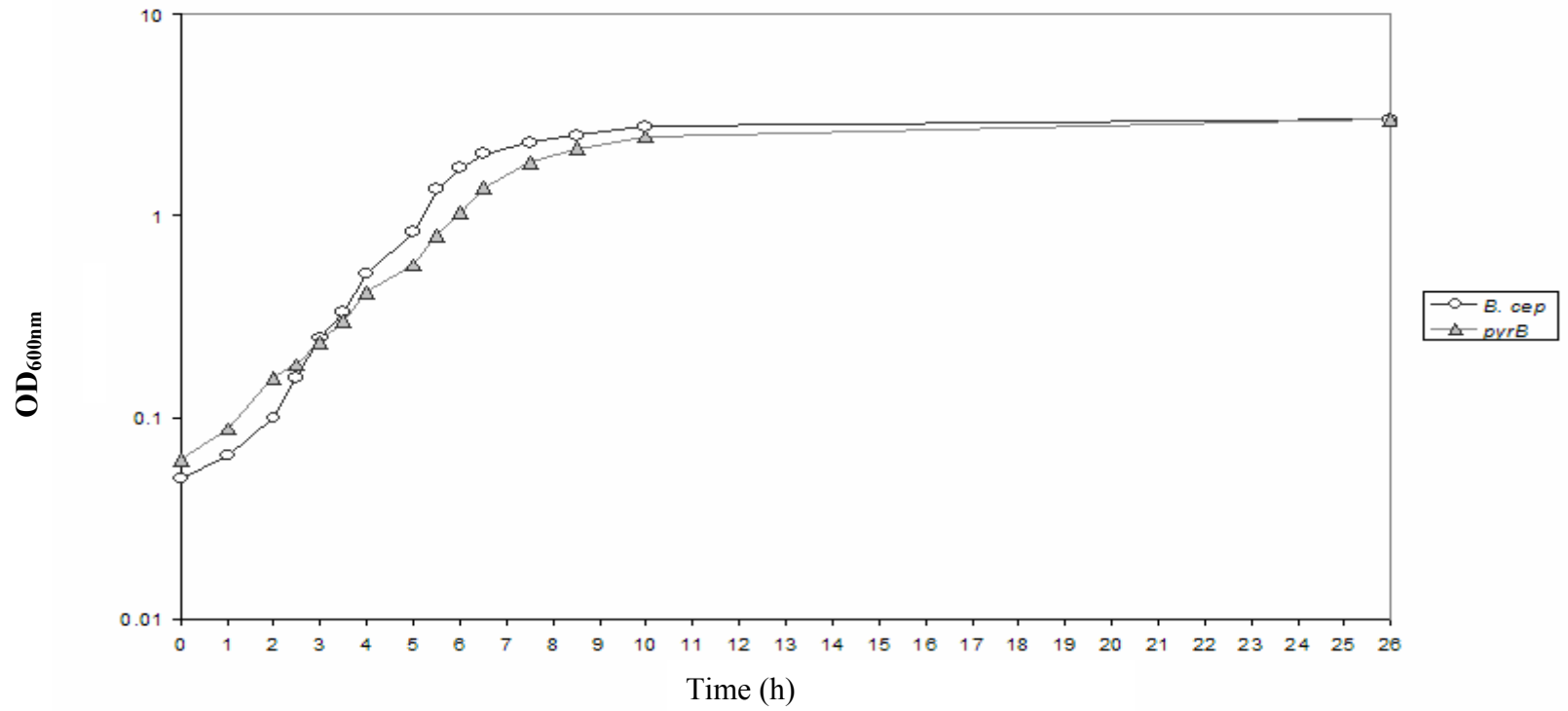


Fig 45. Growth curve of wild type *B. cepacia* and *pyrBI*⁻ *B. cepacia*

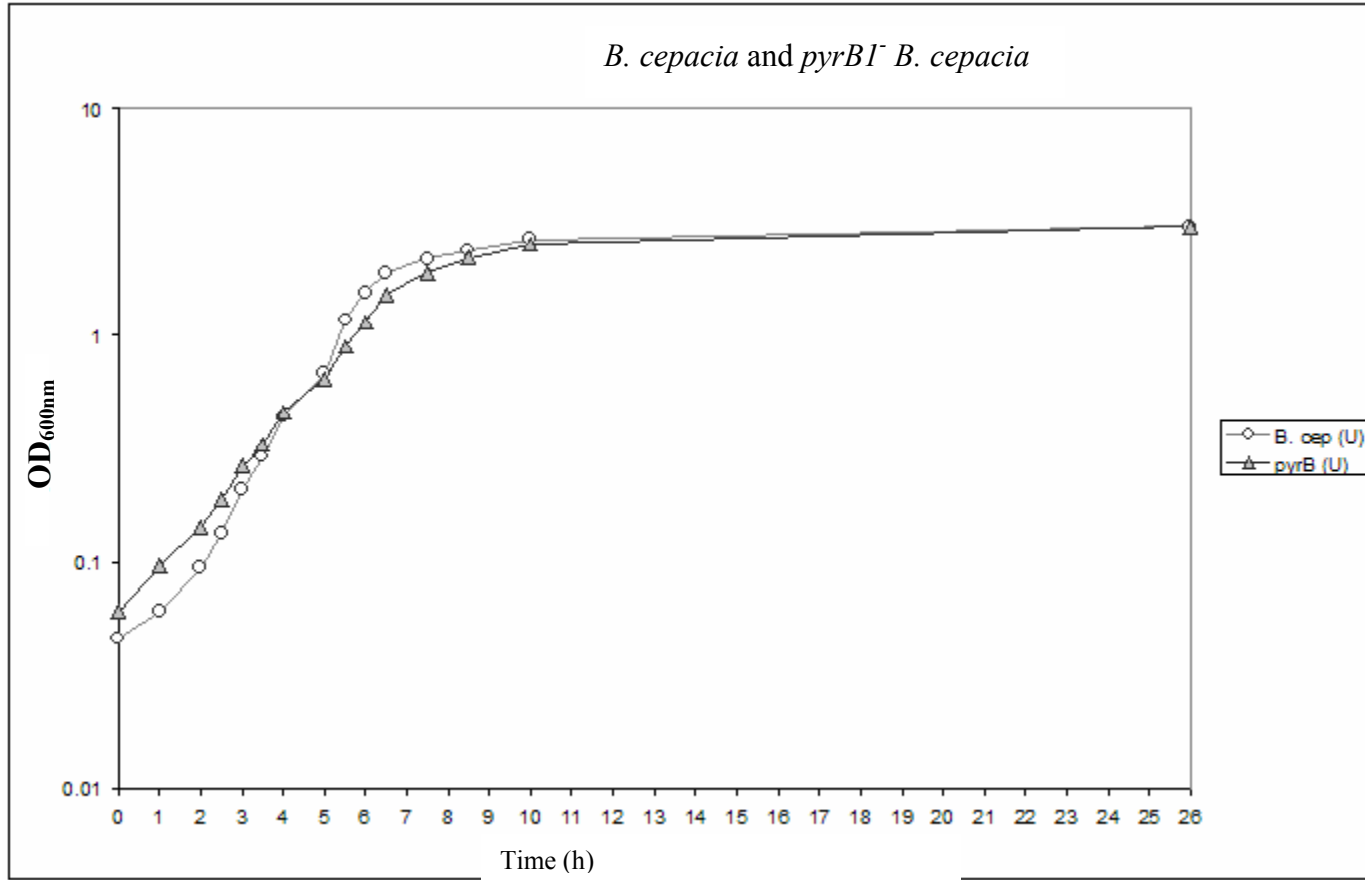


Fig 46. Growth curve of wild type *B. cepacia* and *pyrBI*⁻ *B. cepacia* with uracil

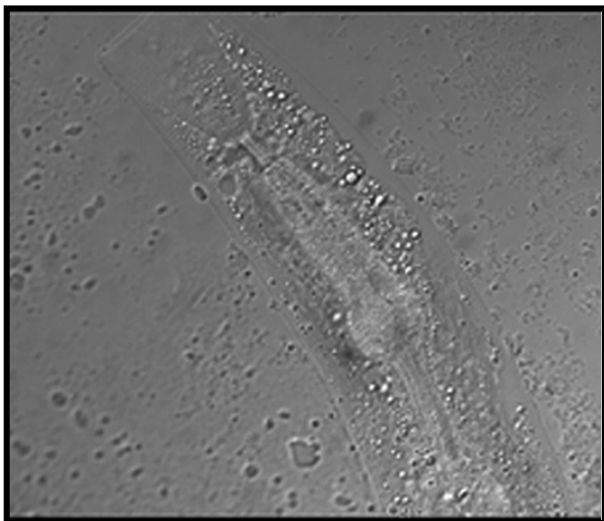


Fig 47. Wild type *B. cepacia* paralyzed the pharyngeal muscles and killed the nematodes



Fig 48. *pyrBI*⁻*B. cepacia* did not kill the nematodes

Standard Paralysis Assay

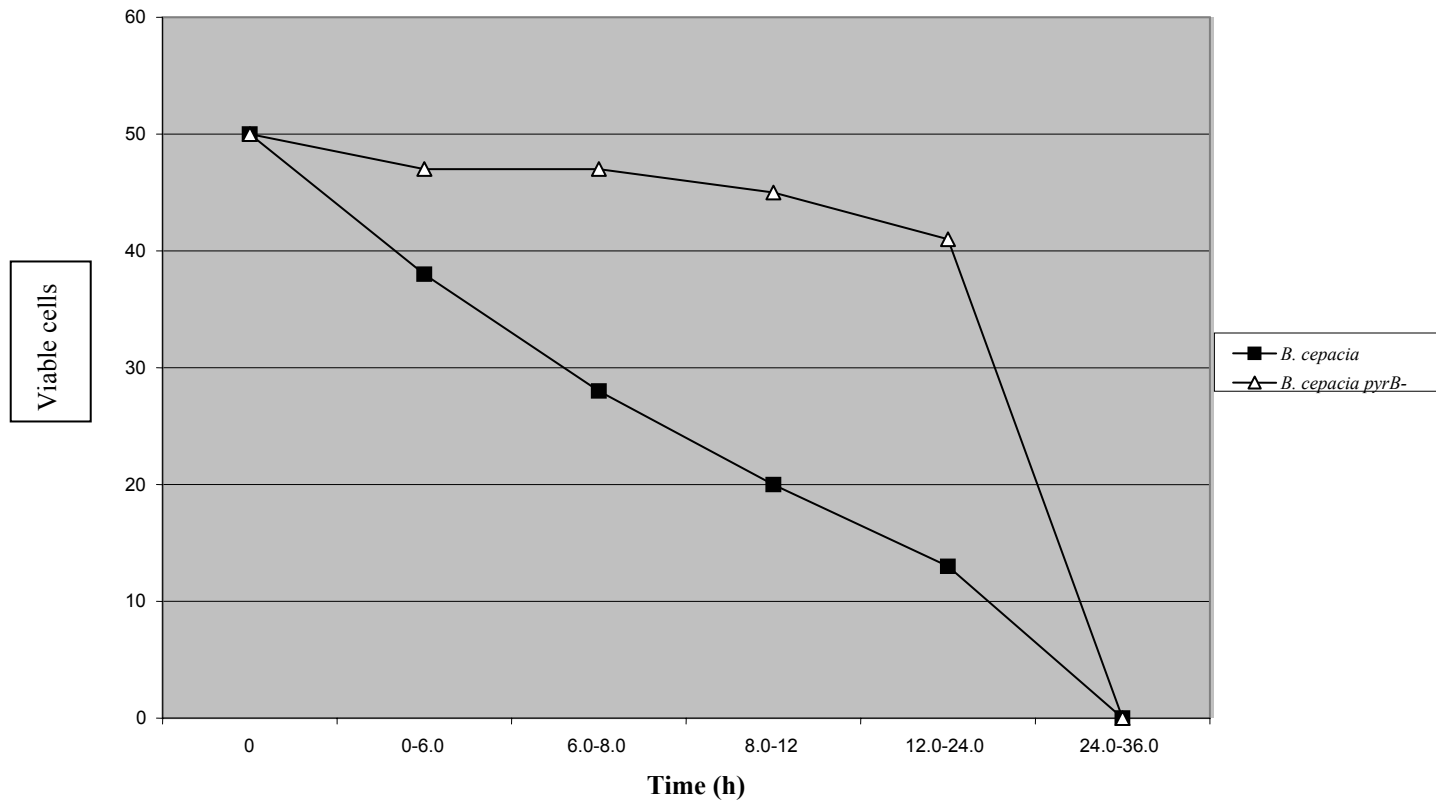


Fig 49. Standard paralysis assay of wild type *B. cepacia* and *pyrB* *B. cepacia*

CONCLUSIONS

From the results in this research, we can conclude that ATC1 encoded by *pyrB1*⁺ of *B. cepacia* ATCase is proteolytic ATCase (40 kDa as monomer) and constitutive while *pyrB2*⁺ encodes ATC2 (480 kDa), which is a *P. aeruginosa* type ATCase and is expressed only in the absence of ATC1 activity. ATC1 has a proteolysis between Ser74 and Val75. ATC1 also presents as uncleaved form (47 kDa as monomer). Both uncleaved and proteolytic ATCase make active trimers. Moreover, ATC1 may be involved in the production of virulent factors in *B. cepacia* and ATC2 is not, while ATC2 is expressed only under condition of stress, or in a *pyrB*⁻ background. The regulation of ATC1 and ATC2 will be compared afterward.

REFERENCES

Abdelal, A., E. Griego, and J. L. Ingraham. 1976. Arginine-sensitive phenotype of mutations in *pyrA* of *Salmonella typhimurium*: role of ornithine carbamoyltransferase in the assembly of mutant carbamoyl phosphate synthetase. *J. Bacteriol.* **128**:105-113

Aiyar. 2001. Molecular cloning: a laboratory manual, Cold Spring Harbor Laboratory, Cold Spring Harbor, N. Y.

Anderson, P. M. 1983. CTP synthetase from *Escherichia coli*: an improved purification procedure and characterization of hysteric and enzyme concentration effects on kinetic properties. *Biochemistry* **22**:3285-3292

Anderson, P. M., and A. Meister. 1965. Evidence for an activated form of carbon dioxide in the reaction catalyzed by *Escherichia coli* carbamoyl phosphate synthetase. *Biochemistry* **4**:2803-2809

Anderson, P. S., Smith, J. M. & Mygind, B. 1992. Characterization of the *upp* gene encoding uracil phosphoribosyltransferase of *Escherichia coli* K12. *Eur. J. Biochem.* **204**: 51-56

Ashley, G. W. & Bartlett, P. A. 1984. Purification and properties of cytidine deaminase from *Escherichia coli*. *J. Biol. Chem.* **259**: 13615-13620

Ballard, R.W., M. Doudoroff, and M. Mandel. 1970. Taxonomy of the aerobic pseudomonads: *Pseudomonas cepacia*, *P. marginata*, *P. allicola*, and *P. caryophylli*. *J. Gen. Microbiol.* **60**:199-214

Barilla, K. C., R. A. Kelln. 1992. Regulation and expression of the *pyrBI* operon of *Salmonella typhimurium* LT2. *Mol. Biol.* **11**:169-177

Beacham, I. R., D. Haas, and E. Yagil. 1977. Mutant of *Escherichia coli* "cryptic" for certain periplasmic enzymes: evidence for an alteration of the outer membrane. *J. Bacteriol.* **129**:1034-1044

Beck, D. A. 1995. Pyrimidine salvage enzymes in microorganisms: Labyrinths of enzymatic diversity. Ph.D.dissertation (Biology) University of North Texas.

Beck, D. F. and J. L. Ingraham. 1971. Location on the chromosome of *Salmonella typhimurium* of genes governing pyrimidine metabolism. *Mol. Gen. Genet.* **111**:303-316

Beckwith, J. R., Pardee, A. B., Austrain, R. & Jacob, F. 1962. Coordination of the synthesis of the enzymes in the pyrimidine pathway of *E. coli*. *J. Mol. Biol.* **5**:618-634

Berns, K. L. & Thomas, C. A. Jr. 1965. Isolation of high molecular weight DNA from *Haemophilus influenza*. *J. Mol. Biol.* **11**:476-490

Bethell, M. R., and Jones, M. E. 1969. Molecular size and feedback-regulation characteristics of bacterial aspartate transcarbamoylases. *Arch. Biochem. Biophys.*, **134**:352-365

Bhatia, M. B., and C. Grubmeyer. 1993. The role of divalent magnesium in activating the reaction catalyzed by orotate phosphoribosyltransferase. *Arch. Biochem. Biophys.* **303**:321-325

Bothwell, M. 1975. Ph.D. thesis. University of California, Berkeley, California

Bothwell, M., and H. K. Schachman. 1980. A model for the assembly of aspartate transcarbamoylase from catalytic and regulatory subunits. *J. Biol. Chem.* **255**:1971-1977

Bouvier, J., J. C. Patte, and P. Stragier. 1984. Multiple regulatory signals in the control region of the *Escherich coli carAB* operon. *Proc. Natl. Acad. Sci. USA* **81**:4139-4143

Brabson, J. S., and Switzer, R. L. 1975. Purification and property of *Bacillus subtilis* aspartate transcarbamoylase. *J. Biol. Chem.* **250**:8664-8669

Huber, B., K. Riedel, M. Hentzer, A. Gotschlich, M. Givskov, S. Molin, and L. Eberl. 2001. The *cep* quorum-sensing system of *Burkholderia cepacia* H111 controls biofilm formation and swarming motility. *Microbiol.* **147**: 2517-2528.

Charlier, D., G. Weyens, M. Roovers, J. Piette, C. Bocquet, A. Pierar, and N. Glansdroff. 1988. Molecular interactions in the control region of the *carAB* operon encoding *Escherichia coli* carbamoylphosphate synthetase. *J. Mol. Biol.* **204**:867-877

Cheng, H. P., and T. G. Lessie. 1994. Multiple replicons constituting the genome of *Pseudomonas cepacia* 17616. *J. Bacteriol.* **176**:4034-4042

Choi, K. Y., and H. Zalkin. 1990. Regulation of *Escherichia coli pyrC* by the purine regulon repressor protein. *J. Bacteriol.* **172**:3201-3207

Clemmensen, K., F. Bonnekamp, O. Karlstrom, and K. F. Jensen. 1985. Role of translation in the UTP-modulated attenuation at the *pyrBI* operon of *Escherichia coli*. *Mol. Gen. Genet.* **201**:247-251

Cole, S. T., and I. Saint-Girons. 1994. Bacterial genomics. *FEMS Microbio. Rev.* **14**:139-160

De Lorenzo, V. & Timmis, K. N. 1994. Analysis and construction of stable phenotypes in Gram negative bacteria with Tn5 and Tn10-derived transposons. *Meth. Enzymol.* **235**:386-405

Denning, G. M., Railsback, M. A., Rasmussen, G. T., Cox, C.,D., and Britigan, B. E. 1998. *Pseudomonas* pyocyanin alters calcium signaling in human airway epithelial cells. *J. Biol. Chem.* **274**:893-900

Di Cello, F., Bevivino A., Chiarini L., Fani R., Paffetti D., Tabacchioni S., and Dalmastri C. 1995. Biodiversity of a *Burkholderia cepacia* population isolated from the maize rhizosphere at different plant growth stages. *Appl. Environ. Microbiol.* Nov; **63**(11):4485-93

Donahue, J. P., and C. L. Turnbough. 1990. Characterization of transcriptional initiation from promoters P1 and P2 of the *pyrBI* operon of *Escherichia coli* K-12. *J. Biol. Chem.* **266**:19091-19099

Bonnekamp, F., Clemmensen, K., O. Karlstrom, and K. F. Jensen. 1984. Mechanism of in the UTP-modulated attenuation at the *pyrE* gene of *Escherichia coli*: an example of operon polarity control through the coupling of transcription and translation. *EMBO J.* **3**:2857-2861

Gerhart, J. c., and Pardee A. B. 1962. The enzymology of control by feedback inhibition. *J. Biol. Chem.* **237**:891-896

Gilardi, G. 1985, Manual of clinical microbiology, 4th ed. American Society for Microbiology. Washington, D. C.

Gilligan, P. H., and D. V. Schidlow. 1984. Role of *Pseudomonas cepacia* in pulmonary disease of cystic fibrosis patients. *Clin. Microbiol. Newslett.* **6**:42-44

Gilligan, P. H., P. A. Gage, L. M. Bradshaw and B. T. Decicco. 1985. Isolation medium for the discovery of *Pseudomonas cepacia* from respiratory secretions of patients with cystic fibrosis. *J. Clin. Microbio.* **22**:5-8

Govan, J. R., and Vandamme, P. 1998. Agricultural and medical microbiology: a time for bridging gaps. *Microbiol.* **144**: 2373-2375

Govan, J. R., Hughes, J. E., and Vandamme, P. 1996. *Burkholderia cepacia*: medical, taxonomic and ecological issues. *J. Med. Microbiol.* **45**:395-407

Hammer-Jespersen, K., and Munch-Peterson. 1973. Mutants of *Escherichia coli* unable to metabolize cytidine: isolation and characterization. *Mol. Gen. Genet.* **126**:177-186

Hassett, D. J., Cuppoletti, J., Trapnell, B., Lymar, S. V., Rowe, J. J., Sun Yoon, S., Hilliard, G. M., Hwang, S. H., and Ochsner, U. A. 2002. Anaerobic metabolism and quorum sensing by *Pseudomonas aeruginosa* biofilms in chronically infected cystic fibrosis airways: rethinking antibiotic treatment strategies and drug targets. *J. Biol. Chem.* **54**:1425-1443

Holmes, A., Govan, J. R., and Goldstein R. 1998. Could the agricultural use of *Burkholderia cepacia* pose a threat to human health? *Emerg. Infect. Dis.* **4**:221-227

Hove-Jensen, B., K. W. Harlow, C. J. King, and R. L. Switzer. 1986. Phosphoribosylpyrophosphate synthetase of *Escherichia coli*. Properties of the purified enzyme and primary structure of the *prs* gene. *J. Biol. Chem.* **261**:6765-6771

Huff, J. P., Grant, B. J., Penning, C. A. and Sullivan, K. F. 1990. Optimization of transformation of *Escherichia coli* with plasmid DNA. *Biotechniques* **9**: 570-577

Ingraham, J. L., and J. Neuhard. 1972. Cold-sensitive mutants of *salmonella typhimurium* defective in uridine monophosphate kinase (*pyrH*). *J. Biol. Chem.* **247**:6259-6265

Jensen, K. F. 1979. Apparent involvement of purines in the control of expression of *Salmonella typhimurium pyr* genes: analysis of a leaky *guaB* mutant resistant to pyrimidine analogs. *J. bacteriol.* **138**:731-738

Jensen, K. F. 1989. Regulation of *Salmonella typhimurium pyr* gene expression: effects of changing both purine and pyrimidine nucleotides pool. *J. Gen. Microbiol.* **135**:805-815

Jordan, A. I. Gibert, and J. Barbe. 1994. Cloning and sequencing of the genes from *Salmonella typhimurium* encoding a new bacterial ribonucleotide reductase. *J. Bacteriol.* **176**:3420-3427

Karibian, D. 1978. Dihydroorotate dehydrogenase (*Escherichia coli*). *Methods Enzymol.* **51**:150-153

Kedzie, K. M. 1987. Ph.D. thesis. Texas A&M University, College Station, Texas.

Kimsey, H. H., and D. Kaiser. 1992. The orotidine-5'-monophosphate decarboxylase gene of *Myxococcus xanthus*. Comparison of the OMP decarboxylase gene family. *J. Biol. Chem.* **267**:819824

Lessie, T. G., M. S. Woods, and A. Ferrante. 1990. Transposable gene-activating elements in *Pseudomonas cepacia*. P. 279-291. *Pseudomonas: Biotransformation, pathogenesis, and evolving biotechnology.* American Society for Microbiology. Washington, D. C.

Lam, J. S., de Kievit, T. R. & Currie, H. L. 1996. Genes involved in the biosynthesis of *Pseudomonas aeruginosa* lipopolysaccharide. In: *Molecular biology of Pseudomonads.* Nakazawa, T., Furukawa, K., Haas, D. & Silver, S. (Eds). 451-461. American Society for Microbiology, Washington, D.C.

Levitzki, A., and Koshland Jr, D. E. 1970. Cytidine triphosphate synthetase. Covalent intermediates and mechanisms of action. *Biochem.* **18**:3365-3370

Lichtenstein, J., H. D. Barner, and S. S. Cohen. 1960. The metabolism of exogeneously supplied nucleotides by *Escherichia coli* K-12. *J. Biol. Chem.* **235**:457-465

Long, C. W., Levitzki, A., and Koshland Jr, D. E. 1970. The subunit structure and subunit interactions of cytidine triphosphate synthetase. *J. Biol. Chem.* **245**:80-87

Lu, C. D., and A. T. Abdelal. 1992. Characterization of the Arginine repressor of *Salmonella typhimurium* and its interaction with the *carAB* operator. *J. Mol. Biol.* **225**:11-24

Machida, H., and A. Kuninaka. 1969. Studies on the accumulation of orotic acid by *Escherichia coli* K12. *Agric. Biol. Chem.* **33**:868-875

Mahony, T. J., & Miller, D. J. 1998. Linkage of genes encoding enolase (*eno*) and CTP synthase (*pyrG*) in the beta-subdivision proteobacterium *Nitrosomonas europaea*. *Fems. Microbiol. Lett.* Aug 1; **165** (1):153-157

Matthews, D. A., J. E. Villafranca, C. A. Jason, W. W. Smith, K. Welsh, and S. Freer. 1990. Stereochemical mechanism of action for thymidylate synthase based on the X-ray structure of the covalent inhibitory ternary complex with 5-fluoro-2' deoxyuridylate and 5, 10-methylenetetrahydrofolate. *J. Mol. Biol.* **214**:937-948

Meyer, J. M., Neely, A., Stintzi, A., Georges, C., and Holder, I. A. 1996. Pyoverdinin is essential for virulence of *Pseudomonas aeruginosa*. *J. Biol. Chem.* **271**:518-523

Michaels, G., R. A. Kelln, and F. E. Nargang. 1987. Cloning nucleotide sequence and expression of the *pyrBI* operon of *Salmonella typhimurium*. *Eur. J. Biochem.* **166**:55-61

Miller, J. H. 1992. Experiments in molecular genetics, P. 432. Cold Spring Harbor Laboratory, Cold Spring Harbor, NY.

Nagy, M., F. Lacroute, and D. Thomas. 1992. Divergent evolution of pyrimidine biosynthesis between anaerobic and aerobic yeasts. *Proc. Natl. Acad. Sci. USA* **89**:8966-8970

Neuhard, J. & Nygaard, P. 1987. Purines and pyrimidines, P. 458-464. In *Echerichia coli* and *Salmonella typhimurium* cellular and molecular biology. Edited by F. C. Neidhardt. American Society for Microbiology. Washington DC

Neuhard, J. 1983. Utilization of preformed pyrimidine bases and nucleosides, P.95-148. Academic Press Inc, Ltd., London

Neuhard, J. and Nygaard, P. 1985. Cloning and characterization of the *Salmonella typhimurium pyrC* gene encoding dihydroorotase. *Eur. J. Biochem.* **157**:335-342

Neuhard, J. and R. A. Kelln. 1988. A chromosomal mutation mediating increased expression of *pyrE* in *Salmonella typhimurium* is located within the proposed attenuator. *Can. J. Microbiol.* **34**:686-687

O' Donovan, G. A., Herlick, S., Beck, D. E., Dutta, P. K. 1989. UTP/CTP ratio, an important regulatory parameter for ATCase expression. *Arch. Microbiol.* **153**:19-25

O' Donovan, G. A. & Shanley, M. S. 1995. Pyrimidine metabolism in *Pseudomonas*. Paths to pyrimidines, An International News Letter. **3**:49-60

O' Donovan, G. A. 1978. Thymidine metabolism in bacteria, "How, or how not, to label DNA". P. 219-253. In *DNA Synthesis: Present and Future*, Edited by I. Molineaux and M. Kohiyama. Plenum Publishing Corp.

Ornston, L. N. & Stanier, R. Y. 1966. The conversion of catechol and protocatechuate to β -ketoadipate by *Pseudomonas putida*. *J. Biol. Chem* **16**: 3776-3786

Ozier-Kalogeropoulos, O., Fasiolo, F., Adeline, M. -T., Collin, J., & Lacroute, F., 1991. Cloning sequencing and characterization of the *Saccharomyces cerevisiae* URA7 gene encoding CTP synthetase. *Mol. Gen. Genet.* **231**: 7-16

Pakula, A., Bieszkiewicz, E., Boszczyk-Maleszak H., and Mycielski R. 1999. Biodegradation of phenol by bacterial strains from petroleum-refining wastewater purification plant. *Acta Microbiol Pol.* **48**(4):373-80

Prescott, L. M., and Jones, M. E. 1969. Modified methods for the detection of carbamyl aspartate. *Anal. Biochem.* **32**:408-419

Ratledge, C., and Dover, L. G. 2000. Iron metabolism in pathogenic bacteria. *J. Biol. Chem.* **54**:881-941

Rodley, P. D., U. Romling, and B. Tummeler. 1995. A physical genome map of the *Burkholderia cepacia* type strain. *Mol. Microbiol.* **17**:57-67

Roland, K. L., C. Liu, and C. L. Turnbough. 1988. Role of the ribosome in suppressing transcriptional termination at the *pyrBI* attenuator of *Escherichia coli* K-12. *Proc. Natl. Acad. Sci. USA.* **85**:7149-7153

Saiki, R. K., Gelfland, D. H., Stoffel, S., Scharf, S. J., Higuchi, R., Harn, G. T., Mullis, K. B. and Erlich, H. A. 1986. Primer-directed enzymatic amplification of DNA with a thermostable DNA polymerase. *Science* **239**:487-491.

Sambrook, J., Fritsch, E. F. and Maniatis, T. 1989. Molecular cloning: a laboratory manual, 2nd ed. Cold Spring Harbor Laboratory, N. Y.

Schwartz, M., & Neuhard, J.. 1975. Control of expression of the *pyr* genes in *Salmonella typhimurium*: Effects of variation in uridine and cytidine nucleotide pools. *J. Bac.* **121** No:3, 814-822.

Serina, L., C. Blondin, E. Krin, O. Sismeiro, A. Danchin, H. Sakamoto, A. M. Gilles, and Barzu, A. 1995. *Escherichia coli* UMC kinase, a member of aspartokinase family, is a hexamer regulated by guanine nucleotides and UTP. *Biochemistry* **34**:5066-5074

Smith, J. M., Kelln, R. A., & O' Donovan, G. A., 1980. Repression and Derepression of the enzymes of the pyrimidine pathway in *Salmonella typhimurium*. *J. Gen. mic.* **121**: 27-38

Stover, C. K., X. Q. Pham., Erwin, A. L., Mizaoguchi, S. D., Warrenner, P., Hickey, M. J., Brinkman, F. S. L., Hufnagle, W. O., Kowalk, D. J., Lagrou, M., Garber, R. L., Goltry, L., Tolentino, E., Westbrook-Wadman, S., Yuan, Y., Brody, L. L., Coulter, S. N., Folger, K. R., Kas, A., Larbig, K., Lim, R., Smith, K., Spencer, D., Wong, G. K-S., Wu, Z., Paulsen, I. T., Reizer, J., Saier, M. H., Hancock, R. E. W., Lory, S., & Olson, M. V. 2000. Complete genome sequence of *Pseudomonas aeruginosa* PAO1, an opportunistic pathogen. *Nature* **406**: 959-964

Terada, M., Tatibana, M. & Hayashi, O. 1967. Purification and properties of nucleoside hydrolase from *Pseudomonas fluorescens*. *J. Biol. Chem.* **242**:5578-5585

Usher, L. R., Lawson, R. A., Geary, L., Taylor, C. J., Bingle, C. D., Taylor, G. W., and Whyte, M. K. 2002. Induction of neutrophil apoptosis by the *Pseudomonas aeruginosa* exotoxin pyocyanin: potential mechanism of persistent infection. *J. Biol. Chem.* **168**:1861-1868

Van der Saal, W., P. M. Anderson, and J. J. Villafranca. 1985. Mechanistic investigations of *Escherichia coli* cytidine-5'-triphosphate synthetase. Detection of intermediate by positional isotope exchange experiments. *J. Biol. Chem.* **260**:14993-14997

Vickery, J.F. 1993. Ph.D. thesis. University of North Texas, Denton, Texas.

Washabaugh, M., and K. D. Collin. 1984. Dihydroorotase from *Escherichia coli*. Purification and characterization. *J. Biol. Chem.* **259**:3293-3298

Washabaugh, M., and K. D. Collin. 1986. Dihydroorotase from *Escherichia coli*. Sulfhydryl group-metal ion interaction. *J. Biol. Chem.* **261**:5920-5929

West, T. P., M. S. Shanley, and G. A. O'Donovan. 1982. Purification and some properties of cytosine deaminase from *Salmonellas typhimurium*. *Biochem. Biophys. Acta.* **719**:251-258

Wild, J. R., Foltermann, K. F., and O'Donovan, G. A. 1980. Regulatory divergence of aspartate transcarbamoylase within the *Enterobacteriaceae*. *Arch. Biochem. Biophys.* **201**:506-517

Yabuuchi, E., Y. Kossaco, H. Oyaizu, and M. Arakawa. 1981. Proposal of *Burkholderia* gen. nov. and transfer of seven species of the genus *Pseudomonas* homology group II to the new genus, with the type species *Burkholderia cepacia* comb. Nov. *Microbiol. Immunol.* **36**:1251-1275